

รายงานวิจัยฉบับสมบูรณ์

ทุนส่งเสริมกลุ่มวิจัย สกว.

ชื่อโครงการ

การประยุกต์ใช้โปรตีโอมิกส์ในการศึกษาโรคที่พบบ่อยในเมืองไทย DISEASE PROTEOMICS: APPLICATIONS TO COMMON DISEASES IN THAILAND

โดย

ศาสตราจารย์นายแพทย์ วิศิษฎ์ ทองบุญเกิด

หน่วยโปรตีโอมิกส์การแพทย์ สถานส่งเสริมการวิจัย คณะแพทยศาสตร์ศิริราชพยาบาล มหาวิทยาลัยมหิดล

เสร็จสิ้นโครงการเมื่อ เดือนสิงหาคม พ.ศ. 2556 (ระยะเวลาดำเนินการตั้งแต่วันที่ 1 กันยายน 2553 ถึงวันที่ 31 สิงหาคม 2556)

รายงานวิจัยฉบับสมบูรณ์

ทุนส่งเสริมกลุ่มวิจัย สกว.

ชื่อโครงการ

การประยุกต์ใช้โปรตีโอมิกส์ในการศึกษาโรคที่พบบ่อยในเมืองไทย DISEASE PROTEOMICS: APPLICATIONS TO COMMON DISEASES IN THAILAND

โดย

ศาสตราจารย์นายแพทย์ วิศิษฎ์ ทองบุญเกิด

หน่วยโปรตีโอมิกส์การแพทย์ สถานส่งเสริมการวิจัย คณะแพทยศาสตร์ศิริราชพยาบาล มหาวิทยาลัยมหิดล

สหับสนุนโดยสำนักงานกองทุนสนับสนุนการวิจัย

(ความเห็นในรายงานนี้เป็นความเห็นของผู้วิจัย สกว. ไม่จำเป็นต้องเห็นด้วยเสมอไป)

สารบัญ

	หน้า	
บทคัดย่อ	1	
Abstract	1	
หน้าสรุปโครงการ (Executive Summary)		
ชื่อโครงการ	2	
ทีมวิจัย	2	
ความสำคัญและที่มาของปัญหา	3	
วัตถุประสงค์หลัก	3	
โครงการย่อย	3	
สรุปผลการดำเหินงานวิจัยในแต่ละช่วง 6 เดือนตลอดระยะเวลาโครงการ 3 ปี	5	
ผลผลิต/ผลลัพธ์ (Output/Outcome) ที่ได้จากโครงการ	7	
เนื้อหางานวิจัย	9	
Materials and Instruments	9	
Common Methods for All Subprojects	9	
Specific Methods for Individual Subprojects	11	
ผลผลิต/ผลลัพธ์ (Output/Outcome) ที่ได้จากโครงการ		
ผลงานตีพิมพ์ (Publications)	18	
เครือข่ายวิจัย (Networking)	24	
การผลิตนักวิจัยรุ่นใหม่ (Training)	25	
การนำผลงานไปใช้ประโยชน์ในเชิงพาณิชย์ เชิงสาธารณะ หรือเชิงนโยบาย	25	
วิทยากรรับเชิญในการประชุมที่สำคัญระดับชาติและระดับนานาชาติ	26	
รางวัลที่ได้รับระหว่างรับทุนส่งเสริมกลุ่มวิจัย	31	
นักวิจัยในโครงการที่ได้รับรางวัลหรือได้รับทุนวิจัยอื่นในระหว่างที่รับทุนส่งเสริมกลุ่มวิจัย	32	
รายชื่อกลุ่มวิจัยและสถานภาพปัจจุบัน	35	
ภาคผนวก	40	
ผลงานตีพิมพ์ในวารสารวิชาการระดับนานาชาติและหนังสือ	40	

บทคัดย่อ

โปรตีโอมิกส์ (การวิเคราะห์ชนิด ปริมาณ และหน้าที่ของโปรตีนหลายชนิดพร้อมกันอย่างเป็นระบบ) เป็น วิทยาศาสตร์แขนงใหม่ที่สำคัญและแพร่หลายอย่างรวดเร็วในยุคหลังจีโนมในการนำไปศึกษาถึงปั้ญหาที่สำคัญทาง ชีววิทยาและทางการแพทย์ เป้าหมายสูงสุดของการประยุกต์ใช้โปรตีโอมิกส์ คือ 1) เพื่อเข้าใจถึงชีววิทยาและสรีรวิทยา ของเซลล์ เนื้อเยื่อ และอวัยวะต่างๆ ในภาวะปกติ 2) เพื่อเข้าใจถึงกลไกการเกิดและพยาธิสรีรวิทยาของโรคต่างๆ 3) เพื่อค้นหาตัวบ่งชี้โรคและเป้าการรักษาใหม่ และ 4) เพื่อค้นหายาและวัคซีนชนิดใหม่ โครงการนี้จึงประยุกต์เอา เทคโนโลยีทางด้านโปรตีโอมิกส์มาศึกษาโรคที่พบบ่อยในประเทศไทย ได้แก่ โรคนิ่วในไต เบาหวาน ธาลัสซีเมีย และไต อักเสบลูปัสในคน รวมทั้งโรคหัวเหลืองในกุ้งซึ่งเป็นสัตว์เศรษฐกิจที่สำคัญของไทย ข้อมูลและองค์ความรู้ที่ได้จาก โครงการนี้อาจนำมาสู่ความรู้ความเข้าใจโรคที่ดีขึ้น การดูแลรักษาและป้องกันโรคที่มีประสิทธิภาพมากขึ้น โครงการนี้ ยังได้ริเริ่มการสร้างเครือข่ายวิจัยทางด้านโปรตีโอมิกส์ภายในประเทศอีกด้วย นอกจากนี้โครงการ/เครือข่ายวิจัยนี้ยังได้ สร้าง/ผลิตนักวิจัยรุ่นใหม่จำนวนหนึ่งที่มีศักยภาพในด้านการวิเคราะห์เชิงโปรตีโอมิกส์อีกด้วย

<u>คำหลัก</u>

1) โปรตีโอมิกส์ 2) โปรตีน 3) กลไกการเกิดโรค 4) ตัวบ่งชี้ 5) โรคนิ่วในไต 6) เบาหวาน 7) ธาลัสซีเมีย 8) ลูปัส 9) โรคหัวเหลือง

Abstract

Proteomics (systematic analysis of proteins for their identities, quantities and functions) has recently become an important field of modern sciences in the post-genomic era. It has been widely used to address many biological and medical problems. Applications of proteomics will ultimately lead to: 1) better understanding of biology and physiology of normal cells, tissues or organs; 2) unraveling the complexity of pathogenic mechanisms and pathophysiology of diseases; 3) identification of novel biomarkers and new therapeutic targets; and finally 4) drug and vaccine discovery. This project has applied proteomics to investigate common diseases in Thailand including kidney stone disease, diabetes mellitus, thalassemia and lupus nephritis in humans, as well as yellowhead disease in shrimps. The data and knowledge obtained from this project may lead to better understanding, proper management, and effective prevention of these common diseases. In addition, this project has initiated collaborative efforts and networking among scientists and clinicians in Thailand who are interested in proteomics. Moreover, this project/network has generated a number of young Thai scientists who are skillful in proteomic analysis.

Keywords

- 1) Proteomics 2) Proteins 3) Disease mechanisms 4) Biomarkers 5) Kidney stone 6) Diabetes
- 7) Thalassemia 8) Lupus 9) Yellowhead disease

หน้าสรุปโครงการ (Executive Summary)

1. ชื่อโครงการ (ภาษาไทย) การประยุกต์ใช้โปรตีโอมิกส์ในการศึกษาโรคที่พบบ่อยในเมืองไทย (ภาษาอังกฤษ) Disease Proteomics: Applications to Common Diseases in Thailand 2. ทีมวิจัย 2.1. ที่ปรึกษาโครงการ ศ.ดร.มรว. ชิษณุสรร สวัสดิวัตน์ (Prof.MR. Jisnuson Svasti, PhD) (คณะวิทยาศาสตร์ มหาวิทยาลัยมหิดล และสถาบันวิจัยจุฬาภรณ์) 2.2. หัวหน้าโครงการ นพ. วิศิษฎ์ ทองบุญเกิด (Visith Thongboonkerd, MD) (สถานส่งเสริมการวิจัย คณะแพทยศาสตร์ศิริราชพยาบาล มหาวิทยาลัยมหิดล) 2.3. ผู้ร่วมโครงการ 2.3.1. รศ.ดร. รัชนีกร กัลล์ประวิทธ์ (Assoc.Prof. Ruchaneekorn Kalpravidh, PhD) (ภาควิชาชีวเคมี คณะแพทยศาสตร์ศิริราชพยาบาล มหาวิทยาลัยมหิดล) 2.3.2. รศ.นพ. ยิ่งยศ อวิหิงสานนท์ (Assoc.Prof. Yingyos Avihingsanon, MD) (ภาควิชาอายุรศาสตร์ คณะแพทยศาสตร์ จุฬาลงกรณ์มหาวิทยาลัย) 2.3.3. รศ.ดร.พญ. ณัฏฐิยา หิรัญกาญจน์ (Assoc.Prof. Nattiya Hirankarn, MD, PhD) (ภาควิชาจุลชีววิทยา คณะแพทยศาสตร์ จุฬาลงกรณ์มหาวิทยาลัย) 2.3.4. รศ.นพ. วิทูรย์ ประสงค์วัฒนา (Assoc.Prof. Vitoon Prasongwatana, MD) (ภาควิชาชีวเคมี คณะแพทยศาสตร์ มหาวิทยาลัยขอนแก่น) 2.3.5. รศ.ดร. ชาติชาย กฤตนัย (Assoc.Prof. Chartchai Krittanai, PhD) (สถาบันชีววิทยาศาสตร์โมเลกุล มหาวิทยาลัยมหิดล) 2.3.6. ผศ.ดร.นพ. ชัชวาลย์ ศรีสวัสดิ์ (Assist.Prof. Chatchawan Srisawat, MD, PhD) (ภาควิชาชีวเคมี คณะแพทยศาสตร์ศิริราชพยาบาล มหาวิทยาลัยมหิดล) 2.3.7. นพ.ดร. สมชาย ชุติพงศ์ธเนศ (Somchai Chutipongtanate, MD, PhD) (สถานส่งเสริมการวิจัย คณะแพทยศาสตร์ศิริราชพยาบาล มหาวิทยาลัยมหิดล) 2.3.8. ดร. รัตติยาภรณ์ กัลยา (Rattiyaporn Kanlaya, PhD) (สถานส่งเสริมการวิจัย คณะแพทยศาสตร์ศิริราชพยาบาล มหาวิทยาลัยมหิดล) 2.3.9. ดร.พญ. จารุภา สูงสถิตานนท์ (Jarupa Soongsathitanon, MD, PhD) (ภาควิชาวิทยาภูมิคุ้มกัน คณะแพทยศาสตร์ศิริราชพยาบาล มหาวิทยาลัยมหิดล) 2.3.10. ดร. ราตรี ทวิชากรตระกูล (Ratree Tavichakorntrakool, PhD) (คณะเทคนิคการแพทย์ มหาวิทยาลัยขอนแก่น) 2.3.11. นาย ศักดิเทพ ไชยฤทธิ์ (Sakdithep Chaiyarit, PhD Candidate)

(สถานส่งเสริมการวิจัย คณะแพทยศาสตร์ศิริราชพยาบาล มหาวิทยาลัยมหิดล)

3. ความสำคัญและที่มาของปัญหา

After the completion of the Human Genome Project, there was an immediate flooding of human genome information obtained from the high-throughput genomic approach. This big leap has led to the development and/or improvement of several biotechnologies to utilize the genomic information to explain biology and (patho)physiology of cells, tissue or organs during normal and abnormal (diseased) states. One of such post-genomic studies is proteomics, which can simultaneously examine a large number (or a set) of proteins encoded by the genome (proteome). Proteomics has been recently defined as "the systemic analysis of proteins for their identity, quantity and function". With its high-throughput capability and other advantages that overcome limitations in conventional methods, proteomics has become one of the most powerful tools for biomedical research. The ultimate goals of a classical proteomics study include: 1) better understanding of biology and physiology of normal cells, tissues or organs; 2) unraveling the complexity of pathogenic mechanisms and pathophysiology of diseases; 3) identification of novel biomarkers and new therapeutic targets; and finally 4) drug and vaccine discovery. This project applied proteomics to investigate common diseases in Thailand including kidney stone disease, diabetes mellitus, thalassemia and lupus nephritis in humans, as well as yellowhead disease in shrimps that causes a remarkable loss of production and export value for our country.

4. วัตถุประสงค์หลัก

- 4.1. To establish a proteomics network in Thailand.
- 4.2. To apply proteomic technologies to the study of common diseases in Thailand including kidney stone disease, diabetes mellitus, thalassemia and lupus nephritis in humans, as well as yellowhead disease in shrimps.
- 4.3. To offer training opportunities on proteomic analysis for PhD and MSc students.

5. โครงการย่อย

5.1. Proteomic analysis of changes in mitochondrial proteome in distal renal tubular cells induced by COM crystal adhesion

(PI: Dr. Visith Thongboonkerd)

Specific Aim(s):

- To examine alterations in mitochondrial proteome in renal tubular cells induced by CaOx crystal adhesion.
- 5.2. Proteomic identification of COM crystal-binding proteins on apical membranes of distal renal tubular cells

(PI: Dr. Visith Thongboonkerd)

Specific Aim(s):

- To globally identify COM crystal-binding proteins on apical membranes of distal renal tubular cells.
- 5.3. Characterizations of secretome from distal renal tubular cells and its COM-crystal binding components

(PI: Dr. Somchai Chutipongtanate)

Specific Aim(s):

- To globally identify secretome from distal renal tubular cells and its COM-crystal binding components.

5.4. Insights into preventive mechanisms of green tea extract against oxalate-induced renal fibrosis: a proteomics approach

(PI: Dr. Rattiyaporn Kanlaya)

Specific Aim(s):

- To characterize changes in distal renal tubular cells induced by oxalate that could be reversible by green tea catechin treatment.

5.5. Evaluation of altered proteome in macrophages in response to basolateral secretion of renal tubular epithelial cells treated with COM crystals

(PI: Sakdithep Chaiyarit)

Specific Aim(s):

- To define altered proteome profile of monocytes and macrophages in response to basolateral secretion of COM crystal treated renal tubular epithelial cells.

5.6. Proteomic analysis of Trimethoprim/Sulfamethoxazole-resistance *Escherichia coli* isolated from kidney stone

(PI: Dr. Ratree Tavichakorntrakool & Dr. Vitoon Prasongwatana)

Specific Aim(s):

- To identify differentially expressed proteins in Trimethoprim/Sulfamethoxazole-resistance vs.

Trimethoprim/Sulfamethoxazole-susceptible *Escherichia coli* isolated from kidney stone.

5.7. Biology of interactions between natural killer (NK) cells and dendritic cells in the pathogenesis of atherosclerosis in diabetes

(PI: Dr. Jarupa Soongsathitanon)

Specific Aim(s):

- To determine alterations of dendritic cell and NK cellular proteomes in high glucose environment.

5.8. Proteomics of lupus nephritis: A biomarker validation project

(PI: Dr. Yingyos Avihingsanon & Dr. Nattiya Hirankarn)

Specific Aim(s):

- To validate selected biomarkers in a well-designed clinical trial. The selected proteins discovered from our previous study will be validated in an independent set of samples. There will be two groups of patients including responders and non-responders to the treatment. All these patients were from a randomized-controlled multi-center clinical trial in Thailand.
- To define a protein map of filtered plasma from severe lupus patients. A preliminary protocol will be developed from 2-D PAGE followed by MS/MS approach.

5.9. Changes in plasma proteome of β -thalassemia/HbE patients treated with anti-oxidant cocktail

(PI: Dr. Ruchaneekorn Kalpravidh & Dr. Chatchawan Srisawat)

Specific Aim(s):

- To identify altered plasma proteins in β -thalassemia/HbE patients after anti-oxidant cocktail treatment.

5.10. Development of 2-D Blue Native PAGE for protein interaction analysis in viral infected shrimp hemocytes

(PI: Dr. Chartchai Krittanai)

Specific Aim(s):

- To develop 2-D Blue Native PAGE for an analysis of protein interaction in shrimp semi-granular cells during yellowhead disease.

6. สรุปผลการดำเนินงานวิจัยในแต่ละช่วง 6 เดือนตลอดระยะเวลาโครงการ 3 ปี

Period	Research activities	Outputs
Month	- Clinical sample collection and preparation.	- Kidney stones, urine, and blood were collected
1-6	- Cultivation of various cells.	from patients.
	- Cell intervention/treatment.	- Various cells were maintained and ready for
	- Isolation of apical membranes.	subsequent experiments.
	- Isolation of mitochondria.	- The cells were treated with various conditions
		for subsequent analyses.
		- Apical membranes were successfully isolated
		from the cells.
		- Mitochondria were successfully isolated from
		the cells.
Month	- Validation of the experimental models.	- Various experimental models were successfully
7-12	- Isolation of <i>E. coli</i> from kidney stones.	validated and ready for proteomic analysis.
	- TMP/SMX susceptibility test.	- E. coli isolates were identified and ready for
	- 2-D PAGE.	subsequent tests.
	- Spot matching and intensity analysis.	- TMP/SMX susceptibility was complete.
	- Preparation and submission of 1-2	- Some 2-D gel images were obtained and
	manuscripts.	analyzed.
	- First annual meeting.	- Spot matching and intensity analysis were done
		on some samples or entirely in a couple of
		subprojects.
		- A number of manuscripts were submitted and
		published in international journals with Impact
		Factor.
		- The first annual meeting was organized.
Month	- 2-D PAGE (cont.).	- More 2-D gel images were obtained and
13-18	- Spot matching and intensity analysis (cont.).	analyzed.

	- Optimization of 2-D Blue Native PAGE.	- Spot matching and intensity analysis were done
	- Mass spectrometric analyses.	on more samples or entirely in more subprojects.
	- Preparation and submission of 1-2 more	- 2-D Blue Native PAGE was tried.
	manuscripts.	- Some protein spots/bands were successfully
		identified.
		- A number of manuscripts were submitted and
		published in international journals with Impact
		Factor.
Month	- 2-D PAGE (cont.).	- All 2-D gel images were obtained and analyzed.
19-24	- Spot matching and intensity analysis (cont.).	- Spot matching and intensity analysis were done
15 = 1	- Optimization of 2-D Blue Native PAGE (cont.).	on all samples and entirely in all subprojects.
	- Mass spectrometric analyses (cont.).	- 2-D Blue Native PAGE were optimized.
	- Validation of proteomic data by Western blot	- More protein spots/bands were successfully
	analysis or ELISA.	identified.
	- Preparation and submission of 1-3 more	- Some proteomic data were successfully
	manuscripts.	confirmed by Western blot analysis or ELISA.
	- Second annual meeting.	- A number of manuscripts were submitted and
	_	published in international journals with Impact
		Factor.
		- The second annual meeting was organized.
Month	- Mass spectrometric analyses (cont.).	- More protein spots/bands were successfully
25-30	- Validation of proteomic data by Western blot	identified.
	analysis or ELISA (cont.).	- More proteomic data were successfully
	- Analysis of protein interactions or networks	confirmed by Western blot analysis or ELISA.
	based on the identified proteins.	- Networks of protein interactions based on the
	- Preparation and submission of 1-3 more	identified proteins were obtained.
	manuscripts.	- A number of manuscripts were submitted and
		published in international journals with Impact
		Factor.
Month	- Validation of urinary biomarker candidates in	- Urinary biomarkers for LN were validated.
31-36	LN patients in a large number of independent	- All the data were summarized.
	samples.	- A number of manuscripts were submitted and
	- Summary of all data.	published in international journals with Impact
	- Preparation and submission of 2-4 more	Factor.
	manuscripts	- The third annual meeting was organized.
	- Third annual meeting	

7. ผลผลิต/ผลลัพธ์ (Output/Outcome) ที่ได้จากโครงการ

7.1. Publications

A total of 30 research articles and 1 book chapter were published in high-impact international journals/book after the completion of the project. These include:

- 5 articles in Journal of Proteome Research (2011 IF = 5.113) (2012 IF = 5.056) (2013 IF = 5.001)
- 4 articles in Journal of Proteomics (2011 IF = 4.878) (2012 IF = 4.088) (2013 IF = 3.929)
- 3 articles in Proteomics Clinical Applications (2011 IF = 1.970) (2012 IF = 2.926)
- 2 articles in Molecular BioSystems (2011 IF = 3.534) (2012 IF = 3.350)
- 2 articles in Talanta (2012 IF = 3.498)
- 2 articles in Biochemical and Biophysical Research Communications (2011 IF = 2.484) (2012 IF = 2.406)
- 1 article in Scientific Reports (2013 IF = 5.078)
- 1 article in Clinical Science (2013 IF = 4.859)
- 1 article in Nephrology Dialysis Transplantation (2012 IF = 3.371)
- 1 article in European Journal of Clinical Investigation (2012 IF = 3.365)
- 1 article in Journal of Biological Inorganic Chemistry (2013 IF = 3.164)
- 1 article in Clinical Chemistry and Laboratory Medicine (2012 IF = 3.009)
- 1 article in European Journal of Pharmacology (2012 IF = 2.592)
- 1 article in World Journal of Gastroenterology (2013 IF = 2.433)
- 1 article in Annals of Hematology (2013 IF = 2.396)
- 1 article in Microbial Pathogenesis (2011 IF = 1.938)
- 1 article in Monoclonal Antibodies in Immunodiagnosis and Immunotherapy (2013 IF = 0.244)
- 1 article in Journal of Analytical Science and Technology (ยังไม่มี IF)
- 1 chapter in an international book series, Contributions to Nephrology

7.2. Proteomics Network in Thailand

This project is a great opportunity to create a proteomics network in Thailand. This network has been joined by several scientists and clinicians, as well as their associates and students who are interested in proteome science. This network offers collaboration, consultation and discussion on trouble shootings in proteomics to enhance the rapid progress of proteomics in Thailand. In practical, this network has regular activities, at least as an annual meeting, as part of the annual meeting of the Protein Society of Thailand.

7.3. International Proteomics Networks

7.3.1. Human Kidney and Urine Proteome Project (HKUPP), Human Proteome Organisation (HUPO)

HKUPP is an international collaborative network officially approved by the HUPO as one of its initiatives. The mission of HKUPP is to encourage and facilitate applications of proteomics to better understand renal (patho)physiology and to define urinary biomarkers for kidney diseases and related

disorders. Dr. Visith is a key member of HKUPP responsible for several projects, especially determination of standards and guidelines for kidney and urine proteome analyses.

7.3.2. European Network for Kidney and Urine Proteomics (EuroKUP)

EuroKUP has been established after HKUPP and focuses its activities within European countries. From approximately 50 participating PIs from almost all European countries, Dr. Visith is one among four members from outside Europe and has joined many EuroKUP projects. He is also responsible for determination of standards and guidelines for kidney and urine proteome analyses.

7.3.3. Institute of Biological Chemistry and Genomic Research Center, Academia Sinica, Taipei,
Taiwan (Prof. Shui-Tein Chen, PhD)

With a long-term collaboration, Prof. Chen is one of the key members in our network that are always helpful. Not only us, Prof. Chen has collaborated with many Thai scientists from various institutions.

- 7.3.4. Department of Medicine I, Charles University Medical School, Pilsen, Czech Republic
- 7.3.5. The University of Hong Kong, Hong Kong
- 7.3.6. Mosaiques Diagnostics and Therapeutics AG, Hannover, Germany
- 7.3.7. Nephrology and Rheumatology UMG, Georg-August University Goettingen, Germany
- 7.3.8. Biomedical Research Foundation Academy of Athens, Greece
- 7.3.9. Institute of Nephrology, Niigata University Graduate School of Medical and Dental Sciences, Niigata, Japan
- 7.3.10. Institut National de la Santé et de la Recherche Médicale (INSERM), U858, Toulouse, France and Université Toulouse III Paul-Sabatier, Institut de Médecine Moléculaire de Ranqueil, Equipe n°5, IFR150, Toulouse, France
- 7.3.11. University of Alabama at Birmingham, Birmingham, Alabama, USA

7.4. Training

This study has offered training opportunities on proteomic analysis for a total of 2 post-docs, 7 research associates, 11 PhD students, and 8 MSc students. For all of the students, their thesis works were related to disease proteomics. They have obtained basic knowledge of methodologies in quantitative and qualitative proteomics and biochemical techniques to examine pathogenic mechanisms of diseases. Specifically, they are able to perform cell culture, cellular fractionation, sample preparation for proteomic analysis, 2-D PAGE, spot matching, quantitative intensity analysis, protein identification by mass spectrometry, and 1-D/2-D Western blotting. These knowledge and skills will make them be able to perform other proteomic studies independently. These really are opportunities to make this new biotechnology more widely used and applied in other areas with a high efficacy.

เนื้อหางานวิจัย

1. Materials and Instruments

- MDCK (Madin-Darbin Canine Kidney) cells, which represent renal tubular epithelial cells of distal nephron, human monocytes (U937), and macrophage cells (PMA-activated U937 cells)
- Permeable polycarbonate membrane inserts
- Scanning electron microscope
- Transmission electron microscope
- Flow cytometer
- Laser scanning confocal/fluorescence microscope
- 2-D PAGE apparati
- Typhoon laser scanner
- 2-D image analysis software
- Q-TOF mass spectrometer

2. Common Methods for All Subprojects

2.1. Protein extraction

For cellular proteome analysis, the cells were harvested and washed three times with PBS. Cell pellets were resuspended in a 2-D lysis buffer containing 7 M urea, 2 M thiourea, 4% 3-[(3-cholamidopropyl) dimethyl-ammonio]-1-propanesulfonate (CHAPS), 120 mM dithiothreitol (DTT), 2% ampholytes (pH 3-10) and 40 mM Tris-HCl, and further incubated at 4°C for 30 min. Unsolubilized nuclei, cell debris, and particulate matters were removed by centrifugation at 12,000 rpm for 2 min. Protein concentrations were determined using the Bradford method.

For urine and secretome analysis, proteins in the urine and culture supernatants were subjected to precipitation using organic solvents. The recovered pellets were then resuspended in 2-D lysis buffer as aforementioned. Protein concentrations were determined using the Bradford method.

2.2. 2-D PAGE

Immobilized pH gradient (IPG) strips, nonlinear pH 3-10 (GE Healthcare), were rehydrated overnight with 100-200 μg proteins using rehydration buffer containing 8 M urea, 2% CHAPS, 0.01 M DTT, 2% ampholytes and bromophenol blue. The first dimensional separation (IEF) were then performed in Ettan IPGphor II Isoelectric Focusing Unit (GE Healthcare) at 20°C, using stepwise mode to reach 9,083 volt.hours. After completion of the IEF, the samples were equilibrated with a buffer containing 6 M urea, 130 mM DTT, 30% glycerol, 112 mM Tris base, 4% sodium dodecyl sulfate (SDS), 0.002% bromophenol blue and acetic acid, and then with another buffer containing 6 M urea, 135 mM iodoacetamide, 30% glycerol, 112 mM Tris base, 4% SDS, 0.002% bromophenol blue and acetic acid. The focused IPG strips were then transferred onto 12% acrylamide slab gel and the second dimensional separation was performed in Hoefer miniVE system (GE Healthcare) with the current of 20 μA/gel for 1.5 h. The resolved

protein spots were then visualized by Coomassie Brilliant Blue or fluorescence dyes and 2-D gel images were captured by Typhoon laser scanner (GE Healthcare).

2.3. Quantitative intensity analysis

Image Master 2D Platinum (GE Healthcare) software was used for matching and analysis of protein spots on gels. A reference gel was created from an artificial gel combining all of the spots presenting in different gels into one image. The intensity volume in pixel unit (or summation of optical densities of each spot), which represented protein concentration or the amount of protein per spot, was used for quantification. Average mode of background subtraction was performed to normalize the intensity volume of each spot for the compatibility of intensity units across different gels. The reference gel was then used for determination of existence and difference of protein expression among different gels.

2.4. Statistical analysis

Unless indicated otherwise, there were at least 5 gels derived from 5 individual samples per each group for comparative proteomic analysis. Although several proteins were examined simultaneously, each protein spot was analyzed individually to define "differential protein expression". Our hypothesis was not to define that expression levels of all proteins were different among each individual sample but we wished to examine whether there was (were) any protein(s) that was (were) differentially expressed between the two different groups. Unpaired t-test was performed to determine differences in intensity volume of each corresponding spot between two groups of samples, whereas ANOVA with multiple comparisons was performed for comparative analysis among three or more groups. P values less than 0.05 were considered statistically significant.

2.5. Mass spectrometry

Proteins spots (from 2-D gels) or bands (from 1-D gels) were identified by quadrupole time-of-flight (Q-TOF) mass spectrometry (MS) and/or tandem MS (MS/MS) analyses. Briefly, the proteins were trypsinized and then premixed 1:1 with the matrix solution containing 5 mg/ml α-cyano-4-hydroxycinnamic acid (CHCA) in 50% ACN, 0.1% (v/v) TFA and 2% (w/v) ammonium citrate and deposited onto the 96-well MALDI target plate. The samples were analyzed by the Q-TOF Ultima mass spectrometer (Micromass; Manchester, UK), which was fully automated with predefined probe motion pattern and the peak intensity threshold for switching over from MS survey scanning to MS/MS, and from one MS/MS to another. Within each sample well, parent ions that met the predefined criteria (any peak within the m/z 800 – 3,000 range with intensity above 10 count ± include/exclude list) were selected for CID MS/MS using argon as the collision gas and a mass dependent ± 5 V rolling collision energy until the end of the probe pattern was reached. The MS and MS/MS data were extracted and outputted as the searchable .txt and .pkl files, respectively, for independent searches using the MASCOT search engine (http://www.matrixscience.com), assuming that peptides were monoisotopic. Fixed modification was carbamidomethylation at cysteine residues, whereas variable modification was oxidation at

methionine residues. Only one missed trypsin cleavage was allowed, and peptide mass tolerances of 100 and 50 ppm were allowed for peptide mass fingerprinting and MS/MS ions search, respectively.

2.6. Western blot analysis

A total of 10-30 µg proteins extracted from each sample were resolved by SDS-PAGE at 150 V for approximately 2 h using SE260 mini-Vertical Electrophoresis Unit (GE Healthcare). After the completion of SDS-PAGE, proteins were transferred onto a nitrocellulose membrane and non-specific bindings were blocked with 5% milk in PBS for 1 h. The membrane was then incubated with primary antibody at 4°C overnight. After washing, the membrane was further incubated respective secondary antibody conjugated with horseradish peroxidase at room temperature (RT) for 1 h. Reactive protein bands were then visualized by a chemiluminescence substrate and autoradiography.

3. Specific Methods for Individual Subprojects

3.1. Subproject #1: Proteomic analysis of changes in mitochondrial proteome in distal renal tubular cells induced by COM crystal adhesion

3.1.1. Cell culture and binding of CaOx crystals to renal tubular epithelial cells

MDCK cells were cultivated with complete Eagle's minimum essential medium (MEM) containing 10% fetal bovine serum (FBS), 1.2% penicillinG/ streptomycin and 2 mM glutamine in 75 cm² tissue culture flask. The cultured cells were maintained in a humidified incubator at 37°C with 5% CO₂ in presence or absence of COM crystals in culture medium (100 µg crystals/ml culture medium). The cells were incubated for a further 48 h and then harvested.

3.1.2. Mitochondrial isolation

Mitochondria were isolated from MDCK cells by subcellular fractionation. Briefly, the harvested cells were resuspended with ice-cold homogenized buffer (HB) (0.25 M sucrose, 1 mM EDTA, 10 mM HEPES; pH 7.5). The cell suspension was then disrupted. After disruption, the homogenate was centrifuged at 1,000 g for 10 min. The supernatant was collected and further centrifuged at 20,000 g for 25 min. The pellet was resuspended with fresh isolation buffer (HB without EDTA) and centrifuged at 20,000 g for 25 min. Purity of the isolated mitochondria was confirmed by Janus Green B staining, Western analysis and transmission electron microscopy.

The isolated mitochondria from COM-treated versus controlled cells were subjected to comparative proteomic analysis as detailed in **Section 2**.

3.2. Subproject #2: Proteomic identification of COM crystal-binding proteins on apical membranes of distal renal tubular cells

3.2.1. Cultivation of polarized renal tubular epithelial cells

MDCK cells were seeded at a density of 5-7.5 x 10⁴ cells/ml on permeable polycarbonate membrane (0.4 mm pore size) and cultivated for 4 days. The cells were grown in MEM supplemented with 10% FBS, 1.2% penicillinG/streptomycin and 2 mM L-glutamine. The cultured cells were maintained in humidified incubator at 37°C with 5% CO₂. The medium was changed every

other day. The polarization of renal tubular epithelial cells was confirmed by confocal microscopic examination to evaluate expression of Na⁺/K⁺-ATPase and ZO1, which represented basolateral membrane and tight junction, respectively. The expression of these three markers was examined to confirm the polarization.

3.2.2. Isolation of apical membranes and COM crystal binding

Confluent polarized MDCK cells on the permeable polycarbonate membrane insert were rinsed twice with ice-cold PBS and then harvested. The cells were washed again with ice-cold PBS and the cell pellet (collected using centrifugation at 2,500 rpm for 5 min) was resuspended in a buffer containing 250 mM sucrose, 12 mM Tris-HCl and 5 mM EDTA (pH 7.4). The cells were then lyzed by sonication and MgCl₂ was added to a final concentration of 12 mM. After incubation on ice for 10 min, the resuspension was centrifuged at 2,000 g for 15 min and the supernatant was further centrifuged at 21,000 g for 30 min. The resulting pellet was resuspended in a buffer containing 125 mM sucrose, 6 mM Tris-HCl and 2.5 mM EDTA (pH 7.4). MgCl₂ was added to a final concentration of 12 mM and these isolation methods based on differential centrifugal steps were repeated one more cycle. The purified apical membrane pellet was finally resuspended in a buffer containing 50 mM NaCl and 10 mM Tri-HCl (pH 7.4) and saved at -70°C until use.

3.2.3. Binding of CaOx crystals to apical membrane proteins and subsequent dissociation

The purified apical membranes were solubilized in 20 mM n-octyl- β -D-glucopyranoside. After removal of debris, COM crystals were added to the protein solution and the mixture was then incubated overnight at 4°C with a continuous rocker. The crystal-proteins complexes were isolated using centrifugation at 5,000 g for 10 min. The pellet was washed twice with ice-cold PBS and the adhered proteins were dissociated from crystals by adding 0.5 M EDTA (pH 8.0) with an overnight incubation at 4°C.

The resulting proteins were subjected to SDS-PAGE and mass spectrometric analysis as detailed in **Section 2.5**.

3.3. Subproject #3: Characterizations of secretome from distal renal tubular cells and its COMcrystal binding components

MDCK cells were cultivated with MEM supplemented with 10% FBS, 1.2% penicillinG/ streptomycin and 2 mM glutamine in 75 cm² tissue culture flask. The cultured cells were maintained in a humidified incubator at 37°C with 5% CO₂ until confluent. Culture supernatants were collected and subjected to sample preparation as detailed in *Section 2.1*. The recovered proteins were resolved in SDS-PAGE and identified by mass spectrometry. In a parallel experiment, culture supernatants were incubated with COM crystals (1 mg crystals/ml supernatant) for 1 h. After several washes with PBS, the bound proteins were eluted by a lysis buffer and subjected to SDS-PAGE and mass spectrometric analysis as detailed in *Section 2.5*.

3.4. Subproject #4: Insights into preventive mechanisms of green tea extract against oxalate-induced renal fibrosis: a proteomics approach

MDCK cells were cultivated with MEM supplemented with 10% FBS, 1.2% penicillinG/ streptomycin and 2 mM glutamine in 75 cm 2 tissue culture flask. The cultured cells were maintained in a humidified incubator at 37°C with 5% CO $_2$. Thereafter, the cells were seeded into 6-well plate to reach 40% confluency and were maintained in a growth medium for 24 h. Prior to treatment, cells were washed with serum-free medium and then pretreated with 25 μ M EGCG in maintenance medium for 1 h, followed by 500 μ M sodium oxalate to complete 24-h incubation.

Cell morphology was observed under a phase contrast microscope (Olympus CKX41; Tokyo, Japan) at the beginning and 24 h after treatment. For immunofluorescence study, the cells were stained with vimentin, cytokeratin, ZO-1 and F-actin. Briefly, cells were washed once with PBS and then fixed with 3.7% formaldehyde/PBS at RT for 10 min and permeabilized with 1% triton x-100/PBS at RT for 10 min. After washing step, the cells were incubated with appropriated primary antibody at 37°C for 1 h. The cells were extensively washed with PBS and incubated at RT for 1 h with respective secondary antibody conjugated with Cy3 or other labels. After washing, images were captured under a fluorescence microscope (Nikon; Tokyo, Japan).

Subsequently, cellular proteomes of the cells with or without EGCG pretreatment were subjected to comparative proteomic analysis as detailed in **Section 2**.

3.5. Subproject #5: Evaluation of altered proteome in macrophages in response to basolateral secretion of renal tubular epithelial cells treated with COM crystals

3.5.1. Cultivation of polarized renal tubular epithelial cells with and without COM crystals

Polarized MDCK cells were maintained as detailed in **Section 3.2.1**. These cells were treated with or without COM crystals (100 µg crystals/ml culture medium) for 48 h. Culture supernatant in the basolateral compartment was collected and used for treatment of macrophages.

3.5.2. Cultivation of macrophages

U937 cells (with a cell density of 1x10⁶ cells/ml) were seeded in each 75 cm² tissue culture flask and cultured in RPMI 1640 for 24 h. Then, the cells were maintained in 100 ng/ml phorbol 12-myristate 13-acetate (PMA)-containing medium for 48 h. Thereafter, the culture medium was replaced with RPMI 1640 fresh medium and the cells were further incubated for 48 h.

3.5.3. Treatment of macrophages

The resulting macrophages were treated with culture supernatant from basolateral compartment obtained from the COM-treated cells for 6-14 h, whereas those exposed to the basolateral supernatant obtained from the untreated cells served as the controls (See more details in **Section 3.5.1.**).

The treated and controlled macrophages were subjected to comparative cellular proteome analysis as detailed in **Section 2**.

3.6. Subproject #6: Proteomic analysis of Trimethoprim/Sulfamethoxazole-resistance Escherichia coli isolated from kidney stone

The proteomes of *Escherichia coli* isolated from kidney stone were studied. A total of 100 kidney stone patients who were born and had been living in Northeastern Thailand were recruited. Kidney stones were collected from the subjects within 12-h after surgical removal and stored at 4°C. All kidney stones were identified for *E. coli* and tested for Trimetoprim/Sulfamethoxazole (TMP/SMX) susceptibility. Stones were washed with sterile saline solution and crushed under aseptic condition. The resulting powder were cultivated in blood and MacConkey agar and incubated overnight at 37°C. Identification of *E. coli* isolates from kidney stone was done by colony morphology, Gram staining and standard biochemical tests. All *E. coli* isolates were subjected to disc diffusion for TMP/SMX susceptibility on Mueller-Hinton agar and incubated at 37°C.

Thereafter, the analyzed microbes were divided into two groups: TMP/SMX-susceptible and TMP/SMX-resistance groups. Both groups of bacterial samples were subjected to comparative proteomic analysis as detailed in **Section 2**.

3.7. Subproject #7: Biology of interactions between natural killer (NK) cells and dendritic cells in the pathogenesis of atherosclerosis in diabetes

3.7.1. Co-cultivation of KG-1 and NK92 cells

KG-1 cells were co-cultivated with NK92 cells in the presence of normal physiologic glucose or high glucose for 96 h in round-bottomed 96-well plates.

3.7.2. Determination of cell surface molecules

Flow cytometric analysis of surface molecules of KG-1 and NK92 cells were performed using monoclonal antibodies specific to the maturation and activation markers, adhesion molecules and chemokine receptors of DCs, activating and inhibitory receptors of NK cells.

3.7.3. Cytokine assay

To investigate the impact of DC on the cytokine production by NK cells and the influence of NK cells on cytokine secretion by DC, KG-1 cells and NK92 cells were co-cultivated in 24-well plates in the presence or absence of a separating porous membrane. Supernatants were collected and concentrations of IFN-γ, IL-12 and IL-10 were determined using a commercial ELISA kit.

3.7.4. NK cell toxicity assay

After 96 h of co-cultivation, NK92 cells were separated from KG-1 cells and cytotoxic activity of NK92 cells were analyzed against target cells K562. Percentages of dead K562 cells were determined by flow cytometry.

3.7.5. Comparative proteomic analysis

This part was performed as detailed in Section 2.

3.8. Subproject #8: Proteomics of lupus nephritis: A biomarker validation project

3.8.1. Criteria of active nephritis

Renal involvement was documented by having one of the following criteria:

- (1) A total urinary protein level of more than 0.5 g/day.
- (2) An increment of serum creatinine levels of more than 0.5 mg/dl during 1 month period of follow-up.
- (3) The presence of pyuria, hematuria, or urinary cast by microscopic examination.

3.8.2. Criteria of response to therapy

Therapeutic response was defined either by the improvement of pathological scores of activity and chronicity based on repeated kidney biopsies, or by the following clinical criteria, including:

- (1) Stabilization or improvement in renal function.
- (2) Decrease in hematuria to less than 10 RBC per high-power field.
- (3) Significant reduction in proteinuria (decrease to less than 3 g/day if baseline nephrotic range, or less than 1 g/day if baseline non-nephrotic) for at least 3 months.

3.8.3. Criteria of a loss of renal function

A loss of renal function was determined by doubling of serum creatinine calculated from the renal biopsy date or end-stage renal disease (ESRD). The criteria of ESRD include having a calculated MDRD-GFR below 15 ml/min or initiation of renal replacement therapy (dialysis or transplantation).

3.8.4. Urine collection and preparation

Mid-stream urine samples were collected from normal healthy individuals and LN patients (inactive, active, response, and non-response). The sample was centrifuged at 1,000 g, 4°C for 5 min to clear debris. The supernatant was stored at -80°C until further protein isolation procedures as detailed in **Section 2.1**. Comparative proteomic analysis was performed as detailed in **Section 2**. Potential biomarkers were validated by ELISA or other immunological methods in a large number of prospective urine samples.

3.8.5. Blood collection and preparation

Peripheral blood samples (10 ml) were collected in EDTA tubes and then centrifuged within 30 min at 1,500 g and RT for 10 min. The supernatant was collected and transferred into 15-ml tubes. For platelet removal, plasma samples were centrifuged at 2,500 g and RT for 15 min. The resulting supernatants were transferred into 1.5-ml microtubes on ice and kept at -80°C until use. For protein precipitation, 750 μ l of 100% ethanol was added into 150 μ l plasma samples and mixed. The mixtures were incubated on ice for 10 min and then centrifuged at 12,000 rpm for 10 min. The pellets were saved and then dissolved with a lysis buffer. Protein concentration of each sample was measured by spectrophotometry using the Bradford method.

3.9. Subproject #9: Changes in plasma proteome of β -thalassemia/HbE patients treated with anti-oxidant cocktail

3.9.1. Subject screening

Subjects were recruited from the project "Effect of antioxidant cocktail in β -thalassemia/HbE patients", which was extended to this study. The subjects were divided into 2 groups:

- (1) Patients who received daily dose of vitamin E 400 IU, N-acetylcysteine 200 mg, and deferiprone 50 mg/kg (n=10)
- (2) Patients who received daily dose of curcuminoids 500 mg, N-acetylcysteine 200 mg, and deferiprone 50 mg/kg (n=10)

3.9.2. Inclusion criteria

Hb typing is $\beta^{0/+}\beta^{E}$ with age between 18-50 years, Hb level at steady state 6-9 g/dL, non-splenectomized, no blood transfusion or iron chelation within 3 months before recruitment, and WHO performance status grade 0-2. All subjects had signed the informed consent.

3.9.3. Exclusion criteria

Pregnancy or lactation, administration of other drugs (except only for folic acid) within 30 days before recruitment, and presence of any severe diseases.

3.9.4. Blood collection and preparation

At the beginning of the study, fasting peripheral blood was collected in EDTA-coated tube and centrifuged at 1,500 g and 4°C for 10 min. The separated plasma was re-centrifuged at 3,000 g and 4°C for 10 min to obtain platelet-poor plasma for proteomic study. Platelet-poor plasma was aliquoted and kept at -80°C until used. All patients received anti-oxidant cocktail daily for 12 months. Platelet-poor plasma for proteomics study was prepared at baseline (0), 6, and 12 months after the treatment. The high-abundant proteins in plasma were eliminated using optimized technique including ultracentrifugation or affinity chromatography. The remaining low-abundant protein fractions were dialyzed, freeze-dried, rehydrated, and measured for protein concentrations using the Bradford method.

Comparative proteomic analysis was performed as detailed in Section 2.

3.10. Subproject #10: Development of 2-D Blue Native PAGE for protein interaction analysis in viral infected shrimp hemocytes

3.10.1. Sample preparation

Shrimp hemolymph was collected from 25-30 g SPF *P. monodon* rearing in artificial sea water. The total hemocytes in AC-1 anti-coagulant were loaded in Percoll gradient centrifugation to obtain the purified population for each hemocytic cell types. The isolated semi-granular cells were confirmed under microscopic examination and then subjected to protein extraction in lysis buffer, protein clean-up by precipitation and determination for protein concentration. Samples were collected from SPF shrimps in the controlled and disease groups, which were injected by buffer and purified Yellow Head Virus (YHV), respectively.

3.10.2. 2-D Blue Native PAGE

Optimization of buffers and lysis systems were required to obtain the suitable solubility and stabilization of the extracted hemocytic protein complexes. Various combinations of specific detergents such as digitonin and dodecylmaltoside were used and tested for optimal quantity and quality of protein samples in 1-D Blue Native PAGE. Once the condition was obtained, the extracted protein complexes were analyzed further by 2-D Blue Native PAGE. The first dimensional separation was done in a non-denaturing condition to keep protein complexes soluble and stabilized. The second separation was performed using a denaturing SDS-PAGE condition. Protein samples were examined in comparison between those extracted from controlled and from YHV infected cells. A series of time course for YHV infection was also investigated to monitor differential changes in their proteomic profiles as well as the changes in protein interaction patterns. Protein spots were stained either by silver staining method or by Colloidal Coomassie Blue to visualize the protein spots and mark for spot excision.

ผลผลิต/ผลลัพธ์ (Output/Outcome) ที่ได้จากโครงการ

1. ผลงานตีพิมพ์ (Publications)

Output จากนักวิจัยในโครงการที่ acknowledge สกว. (แสดงตัวหนาที่ชื่อของหัวหน้าโครงการและทีมวิจัย) โดยค่า Impact Factor เป็นค่าในปีที่ผลงานได้รับการตีพิมพ์

1.1. ผลงานตีพิมพ์ในวารสารวิชาการระดับนานาชาติ (* = Corresponding author)

1.1.1. Chutipongtanate S, Thongboonkerd V*.

Ceftriaxone crystallization and its potential role in kidney stone formation.

Biochem. Biophys. Res. Commun. 406(3): 396-402, 2011

(2011 IF = 2.484)

1.1.2. Chiangjong W, Sinchaikul S, Chen ST, Thongboonkerd V*.

Calcium oxalate dihydrate crystal induced changes in glycoproteome of distal renal tubular epithelial cells.

Mol. Biosyst. 7(6): 1917-1925, 2011

(2011 IF = 3.534)

1.1.3. Poungsawai J, Pattanakitsakul SN, **Thongboonkerd V***.

Subcellular localizations and time-course expression of dengue envelope and non-structural 1 proteins in human endothelial cells.

Microb. Pathog. 51(3): 225-229, 2011

(2011 IF = 1.938)

1.1.4. Zürbig P, Dihazi H, Metzger T, **Thongboonkerd V**, Vlahou A.

Urine proteomics in kidney and urogenital diseases: Moving towards clinical applications.

Proteomics Clin. Appl. 5(5-6): 256-268, 2011

(2011 IF = 1.970)

1.1.5. Mischak H, Thongboonkerd V, Schanstra JP, Vlahou A.

Renal and urinary proteomics.

Proteomics Clin. Appl. 5(5-6): 211-213, 2011

(2011 IF = 1.970)

1.1.6. Wongkamchai S, Chiangjong W, Sinchaikul S, Chen ST, Choochote W, Thongboonkerd V*

Identification of Brugia malayi immunogens by an immunoproteomics approach.

J. Proteomics 74(9): 1607-1613, 2011

(2011 IF = 4.878)

1.1.7. Fong-ngern K, Sinchaikul S, Chen ST, Thongboonkerd V*.

Large-scale identification of calcium oxalate monohydrate crystal-binding proteins on apical membrane of distal renal tubular epithelial cells.

J. Proteome Res. 10(10): 4463-4477, 2011

(2011 IF = 5.113)

1.1.8. Thanomsridetchai N, Singhto N, Tepsumethanon V, Shuangshoti S, Wacharapluesadee S, Sinchaikul S, Chen ST, Hemachudha T, Thongboonkerd V*.

Comprehensive proteome analysis of hippocampus, brainstem and spinal cord from paralytic and furious dogs naturally infected with rabies.

J. Proteome Res. 10(11): 4911-4924, 2011

(2011 IF = 5.113)

1.1.9. Thongboonkerd V*.

Proteomics in dengue virus infection: Host response in human endothelial cells.

J. Anal. Sci. Technol. 2(Suppl A): A46-A51, 2011

(2011 IF = Not applicable)

1.1.10. Tavichakorntrakool R, Prasongwattana V, Sungkeeree S, Saisud P, Sribenjalux P,

Pimratana C, Bovornpadungkitti S, Sriboonlue P, Thongboonkerd V*.

Extensive characterizations of bacteria isolated from catheterized urine and stone matrices in patients with nephrolithiasis.

Nephrol. Dial. Transplant. 27(11): 4125-4130, 2012

(2012 IF = 3.371)

1.1.11. Somparn P, Hirankarn N, Leelahavanichkul A, Khovidhunkit W, Thongboonkerd V,

Avihingsanon Y.

Urinary proteomics revealed prostaglandin H2D-isomerase, not Zn- α 2-glycoprotein, as a biomarker for active lupus nephritis.

J. Proteomics 75(11): 3240-3247, 2012

(2012 IF = 4.088)

1.1.12. Chaiyarit S, Thongboonkerd V*.

Changes in mitochondrial proteome of renal tubular cells induced by calcium oxalate monohydrate crystal adhesion and internalization are related to mitochondrial dysfunction.

J. Proteome Res. 11(6): 3269-3280, 2012

(2012 IF = 5.056)

1.1.13. Mischak H, Ioannidis JP, Argiles A, Attwood TK, Bongcam-Rudloff E, Broenstrup M,

Charonis A, Chrousos GP, Delles C, Dominiczak A, Dylag T, Ehrich J, Egido J, Findeisen P, Jankowski J, Johnson RW, Julian BA, Lankisch T, Leung H, Maahs D, Magni F, Manns MP, Manolis E, Mayer G, Navis G, Novak J, Ortiz A, Persson F, Peter K, Riese HH, Rossing P, Sattar N, Spasovski G, **Thongboonkerd V**, Vanholder R, Schanstra JP, Vlahou A.

Implementation of proteomic biomarkers: Making it work.

Eur. J. Clin. Invest. 42(9): 1027-1036, 2012

(2012 IF = 3.365)

1.1.14. Chutipongtanate S, Fong-ngern K, Peerapen P, Thongboonkerd V*.

High calcium enhances calcium oxalate crystal binding of renal tubular cells via increased surface ANXA1, but impairs their proliferation and healing.

J. Proteome Res. 11(7): 3650-3663, 2012

(2012 IF = 5.056)

1.1.15. Chutipongtanate S, Chaiyarit S, Thongboonkerd V*.

Citrate, not phosphate, can dissolve calcium oxalate monohydrate crystals and detach these crystals from renal tubular cells.

Eur. J. Pharmacol. 689(1-3): 219-225, 2012

(2012 IF = 2.592)

1.1.16. Polprasert C, Chiangjong W, Thongboonkerd V*.

Marked changes in red cell membrane proteins in hereditary spherocytosis: A proteomics approach.

Mol. Biosyst. 8(9): 2312-2322, 2012

(2012 IF = 3.350)

1.1.17. Roop-ngam P, Chaiyarit S, Pongsakul N, Thongboonkerd V*.

Isolation and characterizations of oxalate-binding proteins in the kidney.

Biochem. Biophys. Res. Commun. 423(3): 629-634, 2012

(2012 IF = 2.406)

1.1.18. Thongboonkerd V*.

The variability in tissue proteomics.

Proteomics Clin. Appl. 6(7-8): 340-342, 2012

(2012 IF = 2.926)

1.1.19. Chutipongtanate S, Watcharatanyatip K, Homvises T, Jaturongkakul K, Thongboonkerd V*.

Systematic comparisons of various spectrophotometric and colorimetric methods to measure concentrations of protein, peptide and amino acid: Detectable limits, linear dynamic ranges, interferences, practicality and unit costs.

Talanta 98: 123-129, 2012

(2012 IF = 3.498)

1.1.20. Chutipongtanate S, Thongboonkerd V*.

Phosphate inhibits calcium oxalate crystal growth and crystallization through reducing free calcium ions: A morphological analysis and calcium consumption assay.

Clin. Chem. Lab. Med. 50(9): 1697-1698, 2012

(2012 IF = 3.009)

1.1.21. Chaichompoo P, Kumya P, Khowawisetsut L, Chiangjong W, Chaiyarit S, Pongsakul N,

Sirithanaratanakul N, Fucharoen S, **Thongboonkerd V***, Pattanapanyasat K.

Characterizations and proteome analysis of platelet-free plasma-derived microparticles in β -thalassemia/hemoglobin E patients.

J. Proteomics 76: 239-250, 2012

(2012 IF = 4.088)

1.1.22. Chiangjong W, Thongboonkerd V*.

A novel assay to evaluate promoting effects of proteins on calcium oxalate crystal invasion through extracellular matrix based on plasminogen/plasmin activity.

Talanta 101: 240-245, 2012

(2012 IF = 3.498)

1.1.23. Thongboonkerd V*.

The promise and challenge of systems biology in translational medicine.

Clin. Sci. (Lond) 124(6): 389-390, 2013

(2013 IF = 4.859)

1.1.24. Hatairaktham S, Srisawat C, Siritanaratkul N, Chiangjong W, Fucharoen S,

Thongboonkerd V, Kalpravidh RW.

Differential plasma proteome profiles of mild versus severe β -thalassemia/Hb E.

Ann. Hematol. 92(3): 365-377, 2013

(2013 IF = 2.396)

1.1.25. Peerapen P, Thongboonkerd V*.

p38 MAPK mediates calcium oxalate crystal-induced tight junction disruption in distal renal tubular epithelial cells.

Sci. Rep. 3: 1041, 2013

(2013 IF = 5.078)

1.1.26. Chutipongtanate S, Sutthimethakorn S, Chiangjong W, Thongboonkerd V*.

Bacteria can promote calcium oxalate crystal growth and aggregation.

J. Biol. Inorg. Chem. 18(3): 299-308, 2013

(2013 IF = 3.164)

1.1.27. Kanlaya R, Fong-Ngern K, Thongboonkerd V*.

Cellular adaptive response of distal renal tubular cells to high-oxalate environment highlights surface alpha-enolase as the enhancer of calcium oxalate monohydrate crystal adhesion.

J. Proteomics 80C: 55-65, 2013

(2013 IF = 3.929)

1.1.28. Chanmee T, Phothacharoen P, Thongboonkerd V, Kasinrerk W, Kongtawelert P.

Characterization of monoclonal antibodies against a human chondrocyte surface antigen.

Monoclon. Antib. Immunodiagn. Immunother. (Formerly Hybridoma) 32(3):180-186, 2013

(2013 IF = 0.244)

1.1.29. Singhto N, Sintiprungrat K, Thongboonkerd V*.

Alterations in macrophage cellular proteome induced by calcium oxalate crystals: the association of HSP90 and F-actin is important for phagosome formation.

J. Proteome Res. 12(8): 3561-3572, 2013

(2013 IF = 5.001)

1.1.30. Kuakarn S, SomParn P, Tangkijvanich P, Mahachai V, Thongboonkerd V, Hirankarn N.

Serum proteins in chronic hepatitis B patients treated with peginterferon alfa-2b.

World J Gastroenterol. 19(31): 5067-5075, 2013

(2013 IF = 2.433)

1.2. ผลงานตีพิมพ์ในวารสารวิชาการระดับนานาชาติได้รับการคัดเลือกขึ้นปกของวารสาร Journal of Proteome Research (Volume 10, Issue 11, November 2011) (2011 IF = 5.113)

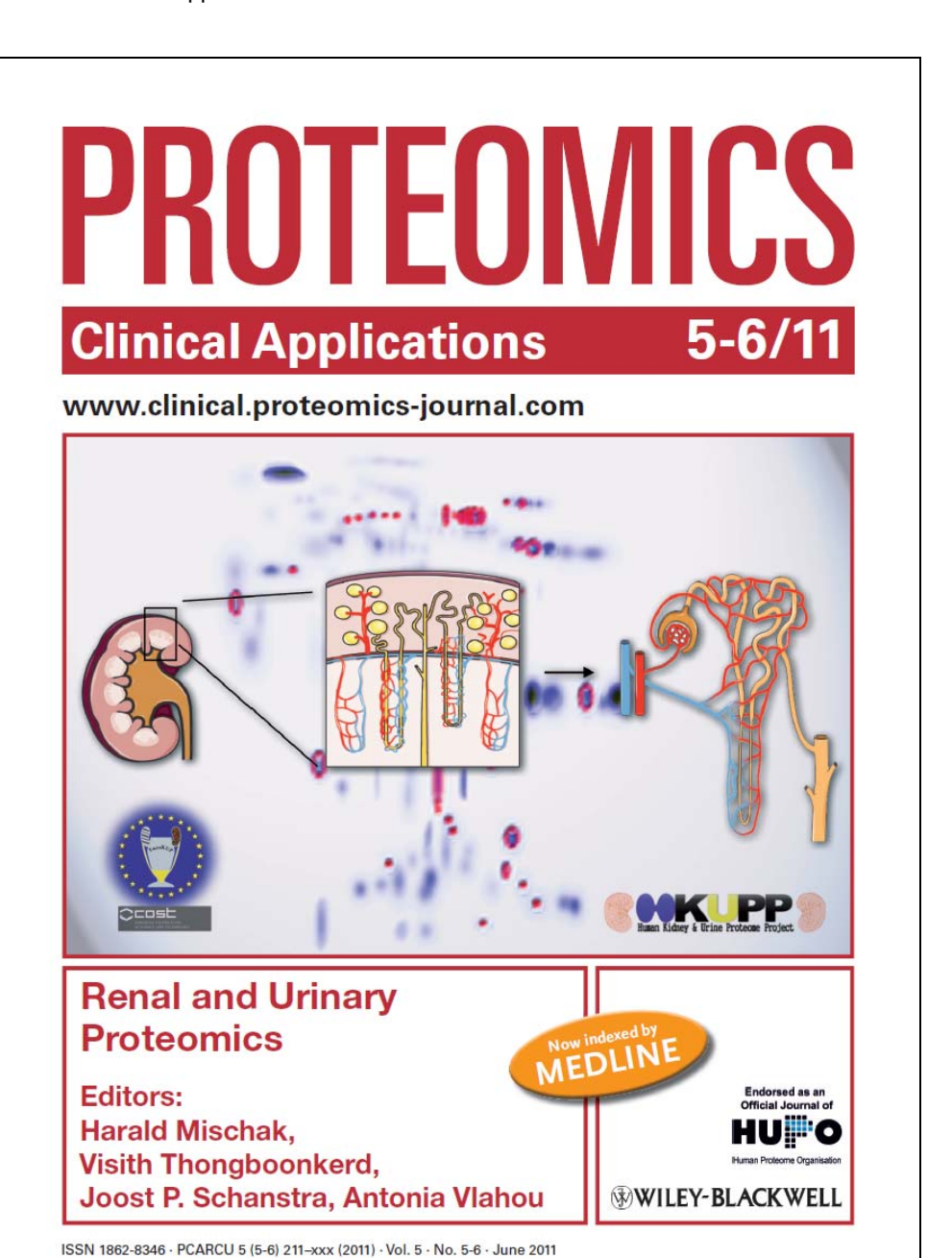


Cover Figure Caption:

"Calcium oxalate monohydrate (COM) crystal adhesion to apical surface of renal tubular epithelial cells can lead to kidney stone formation. Research published in the journal identified COM crystal-binding proteins using a large-scale approach. Depicted on the cover are Madin-Darby Canine Kidney cells which were used in immunofluorescence experiments in this study. Image courtesy of Fong-Ngern, K.; Peerapen, P.; Sinchaikul, S.; Chen, S. T.; **Thongboonkerd, V**. *J. Proteome Res. 2011, 10, 4463–4477.*"

1.3. Invited Guest Editor

ศ.นพ. วิศิษฏ์ ทองบุญเกิด ได้รับเชิญ จากสำนักพิมพ์ Wiley-VCH เป็น Guest Editor ร่วมกับนักวิจัยโปรตีโอ มิกส์ชั้นแนวหน้าของโลก สำหรับ Special Issue เรื่อง "Renal and Urinary Proteomics" ของวารสาร PROTEOMICS – Clinical Applications ฉบับที่ 5-6 ปี 2011



1.4. บทความในหนังสือนานาชาติ (สำนักพิมพ์ ต่างประเทศ)

1.4.1. Thongboonkerd V*.

Study of diabetic nephropathy in the proteomic era.

In: Diabetes and the Kidney (Contrib. Nephrol. vol 170)

Edited by Lai KN, Tang SC; Basel, Karger, pp. 172-183, 2011

2. เครือข่ายวิจัย (Networking)

2.1. Proteomics Network in Thailand

This project is a great opportunity to create a proteomics network in Thailand. This network has been joined by several scientists and clinicians, as well as their associates and students who are interested in proteome science. This network offers collaboration, consultation and discussion on trouble shootings in proteomics to enhance the rapid progress of proteomics in Thailand. In practical, this network has regular activities, at least an annual meeting, as part of the annual meeting of the Protein Society of Thailand.

หน่วยงานภายในประเทศที่มีความร่วมมือกันทำวิจัยทางด้านโปรตีโอมิกส์

- 2.1.1. คณะแพทยศาสตร์ศิริราชพยาบาล มหาวิทยาลัยมหิดล
- 2.1.2. คณะวิทยาศาสตร์ มหาวิทยาลัยมหิดล
- 2.1.3. คณะทันตแพทยศาสตร์ มหาวิทยาลัยมหิดล
- 2.1.4. คณะแพทยศาสตร์ จุฬาลงกรณ์มหาวิทยาลัย
- 2.1.5. คณะแพทยศาสตร์ มหาวิทยาลัยธรรมศาสตร์
- 2.1.6. คณะแพทยศาสตร์ มหาวิทยาลัยขอนแก่น
- 2.1.7. คณะแพทยศาสตร์ มหาวิทยาลัยศรีนครินทรวิโรฒ
- 2.1.8. คณะแพทยศาสตร์ มหาวิทยาลัยเชียงใหม่
- 2.1.9. คณะเทคนิคการแพทย์ มหาวิทยาลัยขอนแก่น
- 2.1.10. สถาบันชีววิทยาศาสตร์โมเลกุล มหาวิทยาลัยมหิดล
- 2.1.11. สถาบันจีโนม สำนักงานพัฒนาวิทยาศาสตร์และเทคโนโลยีแห่งชาติ (สวทช.)
- 2.1.12. ศูนย์ปฏิบัติการกลางด้านชีววิทยาศาสตร์คอมพิวเตอร์เพื่อการวิจัยแบบบูรณาการ มหาวิทยาลัยมหิดล
- 2.1.13. ศูนย์วิจัยด้านธาลัสซีเมีย มหาวิทยาลัยมหิดล

2.2. International Proteomics Networks

2.2.1. Human Kidney and Urine Proteome Project (HKUPP), Human Proteome Organisation (HUPO)

HKUPP is an international collaborative network officially approved by the HUPO as one of its initiatives. The mission of HKUPP is to encourage and facilitate applications of proteomics to better understand renal (patho)physiology and to define urinary biomarkers for kidney diseases and related disorders. Dr. Visith is a key member of HKUPP responsible for several projects, especially determination of standards and guidelines for kidney and urine proteome analyses.

2.2.2. European Network for Kidney and Urine Proteomics (EuroKUP)

EuroKUP has been established after HKUPP and focuses its activities within European countries. From approximately 50 participating PIs from almost all European countries, Dr. Visith is one among four members from outside Europe and has joined many EuroKUP projects. He is also responsible for determination of standards and guidelines for kidney and urine proteome analyses.

2.2.3. Institute of Biological Chemistry and Genomic Research Center, Academia Sinica, Taipei,
Taiwan (Prof. Shui-Tein Chen, PhD)

With a long-term collaboration, Prof. Chen is one of the key members in our network that are always helpful. Not only us, Prof. Chen has collaborated with many Thai scientists from various institutions.

- 2.2.4. Department of Medicine I, Charles University Medical School, Pilsen, Czech Republic
- 2.2.5. The University of Hong Kong, Hong Kong
- 2.2.6. Mosaiques Diagnostics and Therapeutics AG, Hannover, Germany
- 2.2.7. Nephrology and Rheumatology UMG, Georg-August University Goettingen, Germany
- 2.2.8. Biomedical Research Foundation Academy of Athens, Greece
- 2.2.9. Institute of Nephrology, Niigata University Graduate School of Medical and Dental Sciences, Niigata, Japan
- 2.2.10.Institut National de la Santé et de la Recherche Médicale (INSERM), U858, Toulouse, France and Université Toulouse III Paul-Sabatier, Institut de Médecine Moléculaire de Rangueil, Equipe n°5, IFR150, Toulouse, France
- 2.2.11. University of Alabama at Birmingham, Birmingham, Alabama, USA

3. การผลิตนักวิจัยรุ่นใหม่ (Training)

This study has offered training opportunities on proteomic analysis for a total of 2 post-docs, 7 research associates, 11 PhD students, and 8 MSc students. For all of the students, their thesis works were related to disease proteomics. They have obtained basic knowledge of methodologies in quantitative and qualitative proteomics and biochemical techniques to examine pathogenic mechanisms of diseases. Specifically, they are able to perform cell culture, cellular fractionation, sample preparation for proteomic analysis, 2-D PAGE, spot matching, quantitative intensity analysis, protein identification by mass spectrometry, and 1-D/2-D Western blotting. These knowledge and skills will make them be able to perform other proteomic studies independently. These really are opportunities to make this new biotechnology more widely used and applied in other areas with a high efficacy.

4. การนำผลงานไปใช้ประโยชน์ในเชิงพาณิชย์ เชิงสาธารณะ หรือเชิงนโยบาย

ยังไม่มี เนื่องจากกลุ่มวิจัยเน้นงานวิจัยเชิงลึกเพื่อให้ได้มาซึ่งองค์ความรู้ใหม่สำหรับต่อยอดนำผลงานไปใช้ ประโยชน์ในเชิงพาณิชย์ หรือเชิงสาธารณะ หรือเชิงนโยบายในอนาคต

5. วิทยากรรับเชิญในการประชุมที่สำคัญระดับชาติและระดับนานาชาติ

5.1. งานประชุมวิชาการระดับนานาชาติ

Sep 19-23, 2010 Thongboonkerd V

Title: "Proteomics for the Investigation of Host Responses in Dengue Virus

Infection"

In: HUPO 9th Annual World Congress, Sydney, AUSTRALIA

By: Human Proteome Organisation (HUPO)

Jun 21-23, 2011 Thongboonkerd V

Title: "Plasma proteome for early diagnosis of sepsis"

In: 9th Annual ISF Colloquium on: The Systems Biology of Sepsis, Genomics

and Beyond, Rockefeller University, New York, USA

By: International Sepsis Forum (ISF)

Nov 15-17, 2011 Thongboonkerd V

Title: "Proteomics in dengue virus infection"

In: International Symposium on Analytical Science and Technology, Daejeon,

KOREA

By: Korea Basic Science Institute (KBSI)

April 6-8, 2012 Thongboonkerd V

Title: "Proteomics in PD"

In: 5th Asian Chapter Meeting of International Society for Peritoneal Dialysis

(ISPD) 2011, Pattaya, THAILAND

By: The International Society for Peritoneal Dialysis (ISPD) and The

Nephrology Society of Thailand

May 5-7, 2012 Thongboonkerd V

Title: "Applications of proteomics to kidney stone disease"

In: AOHUPO 6th Congress, Beijing, CHINA

By: Asia-Oceania Human Proteome Organisation (AOHUPO)

5.2. งานประชุมวิชาการภายในประเทศ

29 กันยายน 2553 ศ.นพ. วิศิษฎ์ ทองบุญเกิด

หัวข้อ: "Proteomics in Medicine"

ใน: Biomedical and Technological Sciences Seminar (BTS's seminar)

จัดโดย: คณะแพทยศาสตร์ มหาวิทยาลัยสงขลานครินทร์

สถานที่: ห้องประชุมอดิเรก ณ ถลาง อาคารเรียนรวมและห้องสมุดคณะแพทยศาสตร์

มหาวิทยาลัยสงขลานครินทร์

เวลา: 13.00-15.00

21 ตุลาคม 2553 ศ.นพ. วิศิษฎ์ ทองบุญเกิด

หัวข้อ: "How to write an effective review article?"

ใน: การอบรมเพื่อพัฒนานักวิจัยสาขาวิทยาศาสตร์ชีวภาพและการแพทย์
 (ในโครงการจัดกิจกรรมเพื่อ เฉลิมพระเกียรติพระบาทสมเด็จพระจุลจอมเกล้า
 เจ้าอยู่หัวในโอกาสครบรอบ 100 ปี การสวรรคต "พระปิยมหาราชรำลึก 2553")

จัดโดย: คณะแพทยศาสตร์ จุฬาลงกรณ์มหาวิทยาลัย

สถานที่ ห้องประชุม 230/1 ชั้น 2 อาคารแพทยพัฒน์ คณะแพทยศาสตร์ จุฬาลงกรณ์

มหาวิทยาลัย

เวลา: 11.30-12.00

21 ตุลาคม 2553 ศ.นพ. วิศิษฎ์ ทองบุญเกิด

หัวข้อ: "How to write and get your work published (researcher view)?" ใน: การอบรมเพื่อพัฒนานักวิจัยสาขาวิทยาศาสตร์ชีวภาพและการแพทย์

(ในโครงการจัดกิจกรรมเพื่อ เฉลิมพระเกียรติพระบาทสมเด็จพระจุลจอมเกล้า เจ้าอยู่หัวในโอกาสครบรอบ 100 ปี การสวรรคต "พระปียมหาราชรำลึก 2553")

จัดโดย: คณะแพทยศาสตร์ จุฬาลงกรณ์มหาวิทยาลัย

สถานที่: ห้องประชุม 230/1 ชั้น 2 อาคารแพทยพัฒน์ คณะแพทยศาสตร์ จุฬาลงกรณ์

มหาวิทยาลัย

เวลา: 13.00-16.00

26 ตุลาคม 2553 ศ.นพ. วิศิษฎ์ ทองบุญเกิด

หัวข้อ: "Medical proteomics: The new hope for disease diagnostics, therapeutics

and prevention"

ใน: การประชุมวิชาการวิทยาศาสตร์และเทคโนโลยีแห่งประเทศไทย ครั้งที่ 36

จัดโดย: สมาคมวิทยาศาสตร์แห่งประเทศไทยในพระบรมราชูปถัมภ์ ร่วมกับคณะ

วิทยาศาสตร์และเทคโนโลยี มหาวิทยาลัยธรรมศาสตร์

สถานที่: ห้อง EH102 ศูนย์นิทรรศการและการประชุมไบเทค กรุงเทพฯ

เวลา: 14.00-17.00

1 ธันวาคม 2553 ศ.นพ. วิศิษฎ์ ทองบุญเกิด

หัวข้อ: "แพทย์ไทยสู่นักวิจัยโลก" จัดโดย: โรงเรียนมหิดลวิทยานุสรณ์

สถานที่: หอประชุมพระอุบาลีคุณูปมาจารย์ (ปั๊ญญา อินทปญโญ)โรงเรียนมหิดลวิทยา

นุสรณ์ ต. ศาลายา จ.นครปฐม

เวลา: 12.00-14.20

9 ธันวาคม 2553 ศ.นพ. วิศิษฏ์ ทองบุญเกิด

หัวข้อ: "สถานภาพงานวิจัยด้าน Protein Markers ที่เกี่ยวข้องกับโรคไต"

ใน: การประชุมหารือทิศทางงานวิจัยโรคไต

จัดโดย: สำนักงานพัฒนาวิทยาศาสตร์และเทคโนโลยีแห่งชาติ (สวทช.)

สถานที่: ห้องประชุม 720 ชั้น 7 อาคาร สวทช. – โยธี กระทรวงวิยาศาสตร์ ถนนพระราม

หก กรุงเทพฯ

เวลา: 9.35-11.00

17 ธันวาคม 2553 ศ.นพ. วิศิษฎ์ ทองบุญเกิด

หัวข้อ: "Proteomics and Kidney Disease"

ใน: การประชุมวิชาการนานาชาติ Mahidol – Kyoto Universities International

Symposium 2010

จัดโดย: มหาวิทยาลัยมหิดล ร่วมกับ Kyoto University

สถานที่: ห้องประชุมจุฬาภรณ์ ชั้น 2 ตึกสยามมินทร์ คณะแพทยศาสตร์ศิริราชพยาบาล

เวลา: 11.55-12.20

5 มกราคม 2554 ศ.นพ. วิศิษฎ์ ทองบุญเกิด

หัวข้อ: "งานวิจัยส่งเสริมอาชีพแพทย์สู่ความสำเร็จได้อย่างไร"

จัดโดย: คณะแพทยศาสตร์ มหาวิทยาลัยขอนแก่น

สถานที่: ห้องบรรยาย 1 อาคารเตรียมวิทยาศาสตร์คลินิก ชั้น 2 คณะแพทยศาสตร์

มหาวิทยาลัยขอนแก่น

เวลา: 14.00-16.00

21 มกราคม 2554 ศ.นพ. วิศิษฎ์ ทองบุญเกิด

หัวข้อ: "From Nephrologist To Scientist"

ใน: การสัมมนาโครงการผลิตอาจารย์แพทย์ และอาจารย์ทันตแพทย์ ครั้งที่ 10

จัดโดย: มหาวิทยาลัยมหิดล

สถานที่: อีสเทิรน์แกรนด์พาเลช พัทยา จังหวัดชลบุรี

เวลา: 11.15-12.15

8 มีนาคม 2554 ศ.นพ. วิศิษฎ์ ทองบุญเกิด

หัวข้อ: "Molecular Tools in Hematology"

ใน: การประชุมวิชาการประจำปี สมาคมโลหิตแห่งประเทศไทย ครั้งที่ 39

จัดโดย: สมาคมโลหิตแห่งประเทศไทย

สถานที่: ห้องเวิลด์บอลล์รูม ชั้น 23 โรงแรมเซ็นทาราแกรนด์ เซ็นทรัลวิลด์ กรุงเทพฯ

เวลา: 15.30-17.00

7 เมษายน 2554 ศ.นพ. วิศิษฎ์ ทองบุญเกิด

หัวข้อ: "Proteomics"

ใน: 3rd Biochemistry and Molecular Biology "From Basic to Translational

Research for Better Life"

จัดโดย: สมาคมวิทยาศาสตร์แห่งประเทศไทยในพระบรมราชูปถัมภ์ ร่วมกับคณะ

แพทยศาสตร์ มหาวิทยาลัยเชียงใหม่

สถานที่: ห้องประชุม โรงแรมดิเอ็มเพลสเชียงใหม่ จังหวัดเชียงใหม่

เวลา: 13.00-13.30

15 มิถุนายน 2554 ศ.นพ. วิศิษฎ์ ทองบุญเกิด

หัวข้อ: "Medical Proteomics: A Primer"

ใน: งานประชุมวิชาการร่วมระหว่างคณะแพทยศาสตร์สามสถาบัน พ.ศ. 2554: จุฬาฯ

รามาฯ – ศิริราช

จัดโดย: คณะแพทยศาสตร์ จุฬาลงกรณ์มหาวิทยาลัย คณะแพทยศาสตร์โรงพยาบาล

รามาธิบดี และ คณะแพทยศาสตร์ศิริราชพยาบาล มหาวิทยาลัยมหิดล

สถานที่: อาคารอิมแพ็คคอนเวนชั่น เซ็นเตอร์ ศูนย์ประชุมอิมแพ็คเมืองทองธานี จังหวัด

นนทบุรี

เวลา: 8.00-12.15

16 มิถุนายน 2554 ศ.นพ. วิศิษฎ์ ทองบุญเกิด

หัวข้อ: "Disease Proteomics"

ใน: งานประชุมวิชาการร่วมระหว่างคณะแพทยศาสตร์สามสถาบัน พ.ศ. 2554: จุฬาฯ

- รามาฯ - ศิริราช

จัดโดย: คณะแพทยศาสตร์ จุฬาลงกรณ์มหาวิทยาลัย คณะแพทยศาสตร์โรงพยาบาล

รามาธิบดี และ คณะแพทยศาสตร์ศิริราชพยาบาล มหาวิทยาลัยมหิดล

สถานที่: อาคารอิมแพ็คคอนเวนชั่น เซ็นเตอร์ ศูนย์ประชุมอิมแพ็คเมืองทองธานี จังหวัด

นนทบุรี

เวลา: 8.00-12.15

14 ตุลาคม 2554 ศ.นพ. วิศิษฏ์ ทองบุญเกิด

หัวข้อ: "Writing a manuscript: Review article vs. original article"

ใน: โครงการฝึกอบรมเพื่อพัฒนานักวิจัยสาขาวิทยาศาสตร์ชีวภาพและการแพทย์

(เนื่องในวโรกาส "วันปิยมหาราชรำลึก" พุทธศักราช 2554)

จัดโดย: คณะแพทยศาสตร์ จุฬาลงกรณ์มหาวิทยาลัย

สถานที่: ห้องประชุม 230/1 ชั้น 2 อาคารแพทยพัฒน์ คณะแพทยศาสตร์ จุฬาลงกรณ์

มหาวิทยาลัย

เวลา: 13.00-15.30

25 มกราคม 2555 ศ.นพ. วิศิษฎ์ ทองบุญเกิด

หัวข้อ: "การเขียนผลงานวิจัยให้โดนใจ ไร้การละเมิดทางวรรณกรรม"

ใน: Research Facilitating System

จัดโดย: คณะทันตแพทยศาสตร์ มหาวิทยาลัยมหิดล

สถานที่: ห้องประชุมอาคาร 2 ชั้น 5 คณะทันตแพทยศาสตร์ มหาวิทยาลัยมหิดล

เวลา: 13.00-15.00

28 มกราคม 2555 ศ.นพ. วิศิษฎ์ ทองบุญเกิด

หัวข้อ: "Proteomics: Applications in Nephrology"

ใน: New Frontiers in Nephrology จัดโดย: สมาคมโรคไตแห่งประเทศไทย

สถานที่: ห้องประชุมอาคาร 2 ชั้น โรงแรมบางกอกชฎา ถนนรัชดาภิเษก กรุงเทพฯ

เวลา: 09.00-10.00

29 มีนาคม 2555 ศ.นพ. วิศิษฏ์ ทองบุญเกิด

หัวข้อ: "เสวนากับนักวิทยาศาสตร์ระดับชาติ"

ใน: Thai Science Camp ครั้งที่ 4

จัดโดย: สมาคมวิทยาศาสตร์แห่งประเทศไทยในพระบรมราชูปถัมภ์

สถานที่: ห้องยูเรก้า องค์การพิพิธภัณฑ์วิทยาศาสตร์แห่งชาติ (อพวช.) กรุงเทพฯ

เวลา: 14.00-17.00

18 ตุลาคม 2555 ศ.นพ. วิศิษฎ์ ทองบุญเกิด

หัวข้อ: From Expression Proteomics to Functional Study

ใน: การประชุมวิชาการวิทยาศาสตร์และเทคโนโลยีแห่งประเทศไทย ครั้งที่ 38

จัดโดย: สมาคมวิทยาศาสตร์แห่งประเทศไทยในพระบรมราชูปถัมภ์ ร่วมกับคณะ

วิทยาศาสตร์ มหาวิทยาลัยเชียงใหม่

สถานที่: ศูนย์ประชุมนานาชาติเอ็มเพลสเชียงใหม่ จังหวัดเชียงใหม่

เวลา: 8.30-9.00

29 พฤศจิกายน 2555 ศ.นพ. วิศิษฎ์ ทองบุญเกิด

หัวข้อ: Adsorption Therapy for ESRD: Large Urmic Toxins by Proteomics

ใน: Renal Diseases & Biotechnology for Blood Purification (RB2012)

จัดโดย: หน่วยโรคไต ภาควิชาอายุรศาสตร์ คณะแพทยศาสตร์ มหาวิทยาลัยเชียงใหม่

ร่วมกับสมาคมโรคไตแห่งประเทศไทย

สถานที่: ศูนย์ประชุมนานาชาติเอ็มเพลสเชียงใหม่ จังหวัดเชียงใหม่

เวลา: 15.00-16.30

15 กุมภาพันธ์ 2556 ศ.นพ. วิศิษฎ์ ทองบุญเกิด

หัวข้อ: เทคนิคการเขียนบทความตีพิมพ์ในวารสารวิชาการ

ใน: เทคนิคการเขียนบทความตีพิมพ์ในวารสารวิชาการ

จัดโดย: มหาวิทยาลัยมหิดล

สถานที่: ห้องประชุม ศ.นพ.นที รักษ์พลเมือง

เวลา: 09.00-12.00

3 เมษายน 2556 ศ.นพ. วิศิษฎ์ ทองบุญเกิด

หัวข้อ: การนำเทคโนโลยีจีโนมไปประยุกต์ใช้ด้านโปรตีโอมิกส์ทางการแพทย์

ใน: การประชุมวิชาการประจำปี 2556 สวทช.

จัดโดย: สำนักงานพัฒนาวิทยาศาสตร์และเทคโนโลยีแห่งชาติ (สวทช.)

สถานที่: ห้องประชุม BT-127 อาคารไบโอเทค อุทยานวิทยาศาสตร์ประเทศไทย จ.

ปทุมธานี

เวลา: 15.00-15.30

6. รางวัลที่ได้รับระหว่างรับทุนส่งเสริมกลุ่มวิจัย

6.1. Awards

2010 TWAS Prize for Young Scientists in Thailand

The Academy of Sciences for The Developing World (TWAS), which links to

UNESCO and the National Research Council of Thailand (NRCT)

Awardee: Visith Thongboonkerd

2010 **Outstanding Scientist Award**

Foundation for the Promotion of Science and Technology under the Patronage of

His Majesty the King, Thailand

Visith Thongboonkerd Awardee:

2010 **Outstanding Researcher Award**

From: National Research Council of Thailand (NRCT)

Visith Thongboonkerd Awardee:

2010, 11 & 12 **Outstanding Staff Award**

Awardee:

From: Faculty of Medicine Siriraj Hospital Visith Thongboonkerd

6.2. Honors

(2011 IF = 1.970)

2011 - 2015 Invited to serve as an Associate Editor of Journal of Proteome Research

(2011 IF = 5.113)

Elected to serve as a HUPO (Human Proteome Organisation) Council Member 2013 - Present

A total of 3-consecutive 3-year terms (2007-2009, 2010-2012, 2013-2015)

Editorial Board: Proteomics (2011 IF = 4.505)

Expert Review of Proteomics (2011 IF = 3.685)

Proteome Science (2011 IF = 2.328)

Proteomics Insights

International Journal of Proteomics

Genome Medicine

The Open Spectroscopy Journal

Biomarkers in Medicine (2011 IF = 2.630)

Biomarker Insights

International Journal of Nephrology and Renovascular Disease

International Journal of Artificial Organs (2011 IF = 1.861)

American Journal of Nephrology (2011 IF = 2.539)

Editorial Advisory Board: Clinical Science (2011 IF = 4.317)

7. นักวิจัยในโครงการที่ได้รับรางวัลหรือได้รับทุนวิจัยอื่นในระหว่างที่รับทุนส่งเสริมกลุ่มวิจัย

7.1. รางวัล

2010 Merck Young Scientist Award (2nd Runner Up)

From: Merck Limited

Awardee: Rattiyaporn Kanlaya

2011 Outstanding Thesis Award

From: Faculty of Graduate Studies, Mahidol University

Awardee: Nilubon Singhto

2011 Outstanding Abstract Award

From: The Protein Society of Thailand

Awardee: Kitisak Sintiprungrat

2011 Outstanding Abstract Award

From: The Protein Society of Thailand

Awardee: Suneerat Hatairaktham

2011 Merck Young Scientist Award 2011 (Honorable Mention)

From: Merck KGaA

Awardee: Wararat Chiangjong

2011 รางวัลหน่วยปฏิบัติการวิจัย (RU) ที่มีผลงานดีเด่น สาขาวิทยาศาสตร์สุขภาพ

From: Chulalongkorn University

Awardee: Yingyos Avihingsanon

2011 รางวัลผลงานวิจัยดีมาก

From: Chulalongkorn University

Awardee: Nattiya Hirankarn

2011 รางวัลผลงานวิจัยดีเด่นระดับปรีคลินิก

From: Faculty of Medicine Siriraj Hospital

Awardee: Chatchawan Srisawat

2012 Outstanding Thesis Award

From: Faculty of Graduate Studies, Mahidol University

Awardee: Sakdithep Chaiyarit

2012 AOHUPO2012 Young Scientist Travel Award

From: Asia-Oceania Human Proteome Organisation (AOHUPO)

Awardee: Nilubon Singhto

2012 Best Poster Award for New TRF Scholars

From: The Thailand Research Fund (During the TRF Annual Meeting)

Awardee: Ratree Tavichakorntrakool

7.2. ทุนวิจัย

รศ.นพ. ยิ่งยศ อวิหิงสานนท์ หัวหน้าโครงการวิจัย

Biomarker Discovery in Lupus Nephritis: Omics approach

<u>แหล่งทุน</u> สำนักงานพัฒนาวิทยาศาสตร์และเทคโนโลยีแห่งชาติ

รศ.นพ. ยิ่งยศ อวิหิงสานนท์ หัวหน้าโครงการวิจัย

การวิจัยทางคลินิกแบบสหสถาบันศึกษาเพื่อทดสอบประสิทธิผลของตัวบ่งชื้ ทางชีวภาพที่ใช้ในการติดตามการรักษาและพยากรณ์โรคไตอักเสบลูปัส <u>แหล่งทุน</u>คณะกรรมการวิจัยวิจัยแห่งชาติ (วช.): เครือข่ายวิจัยกลุ่มสถาบัน

แพทยศาสตร์แห่งประเทสไทย (UResNet)

รศ.นพ. ยิ่งยศ อวิหิงสานนท์ หัวหน้าโครงการวิจัย

A Multicenter, Randomised, Double blind, Placebo-controlled, Proof of

concept study to evaluate efficacy and safety of treatment with CNTO136 administed intravenously in subjects with active lupus

nephritis

แหล่งทน Centocor Research and Development Inc.

รศ.นพ. ยิ่งยศ อวิหิงสานนท์ หัวหน้าโครงการวิจัย

A Multicenter, Randomised, Double blind, Placebo-controlled study to

evaluate efficacy and safety of treatement with subcutaneous

LY2127399 in subjects with SLE แหล่งทุน Lilly Research Laboratories

รศ.นพ. ยิ่งยศ อวิหิงสานนท์ หัวหน้าโครงการวิจัย

CRAD 001A2429

<u>แหล่งทุน</u>Novartis Pharma

รศ.ดร.พญ. ณัฏฐิยา หิรัญกาญจน์ หัวหน้าโครงการวิจัย

การค้นหาไคเมริกทรานสคริปจำเพาะที่มีความสัมพันธ์กับภาวะไฮโปเมทิ เลชั่น ที่ลำดับเบสของไลน์วันในทีเซลล์ชนิด CD4 และนิวโทรฟิลของผู้ป่วย

โรคเอสเอลอี

แหล่งทน สำนักงานพัฒนาวิทยาศาสตร์และเทคโนโลยีแห่งชาติ

รศ.ดร.พญ. ณัฏฐิยา หิรัญกาญจน์ หัวหน้าโครงการวิจัย

การประเมินประสิทธิภาพของชุดตรวจ อิเล็คซิส แอนติ-เอชซีวี รุ่นที่ 2

(Postlaunch)

แหล่งทุนบริษัท Roche Diagnostics ประเทศเยอรมันนี

ผศ.ดร.นพ. ชัชวาลย์ ศรีสวัสดิ์ หัวหน้าโครงการวิจัย

Nanosecond Pulsed Electric Field (nsPEF) System for Pancreatic

Tumor Regression

<u>แหล่งทุน</u> แพทยสมาคมแห่งประเทศไทย ในพระบรมราชูปถัมภ์

ผศ.ดร.นพ. ชัชวาลย์ ศรีสวัสดิ์ หัวหน้าโครงการวิจัย

Targeting aptamers specific to hepatocellular carcinoma

แหล่งทุน Nanotec-Mahidol University Center of Excellence for Cancer

Diagnosis and Treatment

รศ.ดร. ชาติชาย กฤตนัย หัวหน้าโครงการวิจัย

<u>แหล่งทุน</u> สกอ.

รศ.ดร. ชาติชาย กฤตนัย หัวหน้าโครงการวิจัย

แหล่งทุนมหาวิทยาลัยมหิดล

นพ.ดร. สมชาย ชุติพงศ์ธเนศ หัวหน้าโครงการวิจัย

แหล่งทุน ทุนพัฒนาศักยภาพในการทำงานวิจัยของอาจารย์รุ่นใหม่ สกว.

ดร. รัตติยาภรณ์ กัลยา หัวหน้าโครงการวิจัย

แหล่งทุน ทุนส่งเสริมนักวิจัยรุ่นใหม่ สกว.

ดร.พญ. จารุภา สูงสถิตานนท์ หัวหน้าโครงการวิจัย

<u>แหล่งทุน</u> ทุนพัฒนาศักยภาพในการทำงานวิจัยของอาจารย์รุ่นใหม่ สกว.

ดร.พญ. จารุภา สูงสถิตานนท์ หัวหน้าโครงการวิจัย

แหล่งทุนมหาวิทยาลัยมหิดล

ผศ.ดร. ราตรี ทวิชากรตระกูล หัวหน้าโครงการวิจัย

<u>แหล่งทุน</u> ทุนพัฒนาศักยภาพในการทำงานวิจัยของอาจารย์รุ่นใหม่ สกว.

ผศ.ดร. ราตรี ทวิชากรตระกูล หัวหน้าโครงการวิจัย

แหล่งทน มหาวิทยาลัยขอนแก่น

ดร. ศักดิเทพ ไชยฤทธิ์ หัวหน้าโครงการวิจัย

<u>แหล่งทุน</u>ทุนส่งเสริมนักวิจัยรุ่นใหม่ สกว.

ดร.จุฑาทิพย์ มานิสสรณ์ หัวหน้าโครงการวิจัย

<u>แหล่งทุน</u>ทุนส่งเสริมนักวิจัยรุ่นใหม่ สกว.

ดร.เกศรินทร์ ฟองเงิน หัวหน้าโครงการวิจัย

<u>แหล่งทุน</u> ทุนส่งเสริมนักวิจัยรุ่นใหม่ สกว.

รายชื่อกลุ่มวิจัย เมธีวิจัยอาวุโส สกว. (ศ.นพ. วิศิษฎ์ ทองบุญเกิด)

ชื่อ-หามสกุล		เริ่มเข้าร่วมโครงการ			สถานภาพปัจจุบัน	
	ตำแหน่ง	สังกัด	ตำแหน่งใน	ตำแหน่ง	สังกัด	หมายเหตุ
	วิชาการ		โครงการ	วิชาการ		
1. ศ.ดร.มรว. ชิษณุสรร สวัสดิวัตน์	ମ.	คณะวิทยาศาสตร์ มหาวิทยาลัยมหิดล	ที่ปรึกษา	ମ.	คณะวิทยาศาสตร์ มหาวิทยาลัยมหิดล	
		และสถาบันวิจัยจุฬาภรณ์	โครงการ		และสถาบันวิจัยจุฬาภรณ์	
2. ศ.นพ. วิศิษฎ์ ทองบุญเกิด	ମ.	สถานส่งเสริมการวิจัย คณะ	หัวหน้าโครงการ	ศ.	สถานส่งเสริมการวิจัย คณะ	
		แพทยศาสตร์ศิริราชพยาบาล			แพทยศาสตร์ศิริราชพยาบาล	
		มหาวิทยาลัยมหิดล			มหาวิทยาลัยมหิดล	
3. รศ.ดร. รัชนีกร กัลล์ประวิทธ์	รศ.	ภาควิชาชีวเคมี คณะแพทยศาสตร์ศิริราช	ผู้ร่วมโครงการ	รศ.	ภาควิชาชีวเคมี คณะแพทยศาสตร์ศิริราช	
		พยาบาล มหาวิทยาลัยมหิดล	(Co-investigator)		พยาบาล มหาวิทยาลัยมหิดล	
4. รศ.นพ. ยิ่งยศ อวิหิงสานนท์	รศ.	ภาควิชาอายุรศาสตร์ คณะแพทยศาสตร์	ผู้ร่วมโครงการ	ศ.	ภาควิชาอายุรศาสตร์ คณะแพทยศาสตร์	
		จุฬาลงกรณ์มหาวิทยาลัย	(Co-investigator)		จุฬาลงกรณ์มหาวิทยาลัย	
5. รศ.ดร.พญ. ณัฏฐิยา หิรัญกาญจน์	รศ.	ภาควิชาจุลชีววิทยา คณะแพทยศาสตร์	ผู้ร่วมโครงการ	ศ.	ภาควิชาจุลชีววิทยา คณะแพทยศาสตร์	
		จุฬาลงกรณ์มหาวิทยาลัย	(Co-investigator)		จุฬาลงกรณ์มหาวิทยาลัย	
6. รศ.นพ. วิทูรย์ ประสงค์วัฒนา	รศ.	ภาควิชาชีวเคมี คณะแพทยศาสตร์	ผู้ร่วมโครงการ	รศ.	ภาควิชาชีวเคมี คณะแพทยศาสตร์	
		มหาวิทยาลัยขอนแก่น	(Co-investigator)		มหาวิทยาลัยขอนแก่น	
7. รศ.ดร. ชาติชาย กฤตนัย	รศ.	สถาบันชีววิทยาศาสตร์โมเลกุล	ผู้ร่วมโครงการ	รศ.	สถาบันชีววิทยาศาสตร์โมเลกุล	
		มหาวิทยาลัยมหิดล	(Co-investigator)		มหาวิทยาลัยมหิดล	
8. ผศ.ดร.นพ. ชัชวาลย์ ศรีสวัสดิ์	ผศ.	ภาควิชาชีวเคมี คณะแพทยศาสตร์ศิริราช	ผู้ร่วมโครงการ	รศ.	ภาควิชาชีวเคมี คณะแพทยศาสตร์ศิริราช	
		พยาบาล มหาวิทยาลัยมหิดล	(Co-investigator)		พยาบาล มหาวิทยาลัยมหิดล	
9. นพ.ดร. สมชาย ชุติพงศ์ธเนศ	อาจารย์	สถานส่งเสริมการวิจัย คณะ	ผู้ร่วมโครงการ	อาจารย์	ภาควิชากุมารเวชศาตร์ คณะ	
		แพทยศาสตร์ศิริราชพยาบาล	(Co-investigator)		แพทยศาสตร์โรงพยาบาลรามาธิบดี	

	มหาวิทยาลัยมหิดล			(กำลังศึกษาต่อเฉพาะทาง)	
-	สถานส่งเสริมการวิจัย คณะ	ผู้ร่วมโครงการ	อาจารย์	สถานส่งเสริมการวิจัย คณะ	
	แพทยศาสตร์ศิริราชพยาบาล	(Co-investigator)		แพทยศาสตร์ศิริราชพยาบาล	
	มหาวิทยาลัยมหิดล			มหาวิทยาลัยมหิดล	
อาจารย์	ภาควิชาวิทยาภูมิคุ้มกัน คณะ	ผู้ร่วมโครงการ	อาจารย์	ภาควิชาวิทยาภูมิคุ้มกัน คณะ	
	แพทยศาสตร์ศิริราชพยาบาล	(Co-investigator)		แพทยศาสตร์ศิริราชพยาบาล	
	มหาวิทยาลัยมหิดล			มหาวิทยาลัยมหิดล	
อาจารย์	คณะเทคนิคการแพทย์	ผู้ร่วมโครงการ	ผศ.	คณะเทคนิคการแพทย์	
	มหาวิทยาลัยขอนแก่น	(Co-investigator)		มหาวิทยาลัยขอนแก่น	
-	สถานส่งเสริมการวิจัย คณะ	ผู้ร่วมโครงการ	-	สถานส่งเสริมการวิจัย คณะ	
	แพทยศาสตร์ศิริราชพยาบาล	(Co-investigator)		แพทยศาสตร์ศิริราชพยาบาล	
	มหาวิทยาลัยมหิดล			มหาวิทยาลัยมหิดล	
-	สถานส่งเสริมการวิจัย คณะ	นักวิจัย	-	คณะเวชศาสตร์เขตร้อน	
	แพทยศาสตร์ศิริราชพยาบาล			มหาวิทยาลัยมหิดล	
	มหาวิทยาลัยมหิดล				
-	สถานส่งเสริมการวิจัย คณะ	นักวิจัย	-	สถานส่งเสริมการวิจัย คณะ	
	แพทยศาสตร์ศิริราชพยาบาล			แพทยศาสตร์ศิริราชพยาบาล	
	มหาวิทยาลัยมหิดล			มหาวิทยาลัยมหิดล	
-	สถานส่งเสริมการวิจัย คณะ	ผู้ช่วยวิจัยระดับ	-	สถานส่งเสริมการวิจัย คณะ	-กำลังศึกษาต่อระดับ ป.
	แพทยศาสตร์ศิริราชพยาบาล	ป.โท		แพทยศาสตร์ศิริราชพยาบาล	เอก
	มหาวิทยาลัยมหิดล			มหาวิทยาลัยมหิดล	
-	สถานส่งเสริมการวิจัย คณะ	ผู้ช่วยวิจัยระดับ	อาจารย์	คณะเทคนิคการแพทย์ มหาวิทยาลัยเวส	
	แพทยศาสตร์ศิริราชพยาบาล	ป.โท		เทิร์น	
	มหาวิทยาลัยมหิดล				
-	สถานส่งเสริมการวิจัย คณะ	ผู้ช่วยวิจัยระดับ	-	คณะเวชศาสตร์เขตร้อน	
		- สถานส่งเสริมการวิจัย คณะ แพทยศาสตร์ศิริราชพยาบาล มหาวิทยาลัยมหิดล อาจารย์ ภาควิชาวิทยาภูมิคุ้มกัน คณะ แพทยศาสตร์ศิริราชพยาบาล มหาวิทยาลัยมหิดล อาจารย์ คณะเทคนิคการแพทย์ มหาวิทยาลัยขอนแก่น - สถานส่งเสริมการวิจัย คณะ แพทยศาสตร์ศิริราชพยาบาล มหาวิทยาลัยมหิดล	- สถานส่งเสริมการวิจัย คณะ ผู้ร่วมโครงการ (Co-investigator) มหาวิทยาลัยมหิดล (Co-investigator) มหาวิทยาลัยมหิดล อาจารย์ ภาควิชาวิทยาภูมิคุ้มกัน คณะ ผู้ร่วมโครงการ (Co-investigator) มหาวิทยาลัยมหิดล (Co-investigator) มหาวิทยาลัยมหิดล ผู้ร่วมโครงการ (Co-investigator) - สถานส่งเสริมการวิจัย คณะ ผู้ร่วมโครงการ (Co-investigator) มหาวิทยาลัยมหิดล (Co-investigator) มหาวิทยาลัยมหิดล - สถานส่งเสริมการวิจัย คณะ นักวิจัย แพทยศาสตร์ศิริราชพยาบาล มหาวิทยาลัยมหิดล - สถานส่งเสริมการวิจัย คณะ นักวิจัย แพทยศาสตร์ศิริราชพยาบาล มหาวิทยาลัยมหิดล - สถานส่งเสริมการวิจัย คณะ ผู้ช่วยวิจัยระดับ แพทยศาสตร์ศิริราชพยาบาล มหาวิทยาลัยมหิดล - สถานส่งเสริมการวิจัย คณะ ผู้ช่วยวิจัยระดับ แพทยศาสตร์ศิริราชพยาบาล มหาวิทยาลัยมหิดล - สถานส่งเสริมการวิจัย คณะ ผู้ช่วยวิจัยระดับ ป.โท มหาวิทยาลัยมหิดล	- สถานส่งเสริมการวิจัย คณะ แพทยศาสตร์ศีริราชพยาบาล มหาวิทยาลัยมหิดล อาจารย์ ภาควิชาวิทยาภูมิคุ้มกัน คณะ แพทยศาสตร์ศีริราชพยาบาล แพทยศาสตร์ศีริราชพยาบาล แพทยศาสตร์ศีริราชพยาบาล มหาวิทยาลัยมหิดล อาจารย์ คณะเทคนิคการแพทย์ มหาวิทยาลัยขอนแก่น (Co-investigator) - สถานส่งเสริมการวิจัย คณะ แพทยศาสตร์ศีริราชพยาบาล มหาวิทยาลัยมหิดล - สถานส่งเสริมการวิจัย คณะ ผู้ช่วยวิจัยระดับ แพทยศาสตร์ศีริราชพยาบาล มหาวิทยาลัยมหิดล - สถานส่งเสริมการวิจัย คณะ แพทยศาสตร์ศีริราชพยาบาล มหาวิทยาลัยมหิดล - สถานส่งเสริมการวิจัย คณะ ผู้ช่วยวิจัยระดับ มะการย์ แพทยศาสตร์ศีริราชพยาบาล มหาวิทยาลัยมหิดล	- สถานส่งเสริมการวิจัย คณะ แพทยศาสตร์ศิริราชพยาบาล มหาวิทยาลัยมหิดล อาจารย์ มาควิชาวิทยาภูมิคุ้มกัน คณะ แพทยศาสตร์ศิริราชพยาบาล มหาวิทยาลัยมหิดล อาจารย์ มาควิชาวิทยาภูมิคุ้มกัน คณะ แพทยศาสตร์ศิริราชพยาบาล มหาวิทยาลัยมหิดล อาจารย์ ภาควิชาวิทยาภูมิคุ้มกัน คณะ แพทยศาสตร์ศิริราชพยาบาล มหาวิทยาลัยมหิดล อาจารย์ คณะเทลนิคการแพทย์ มหาวิทยาลัยมหิดล อาจารย์ คณะแทยนิคการแพทย์ มหาวิทยาลัยมหิดล - สถานส่งเสริมการวิจัย คณะ แพทยศาสตร์ศิริราชพยาบาล มหาวิทยาลัยมหิดล

		แพทยศาสตร์ศิริราชพยาบาล	ป.โท		มหาวิทยาลัยมหิดล	
		มหาวิทยาลัยมหิดล				
19. Ms. Nutkridta Pongsakul	-	สถานส่งเสริมการวิจัย คณะ	ผู้ช่วยวิจัยระดับ	-	สถานส่งเสริมการวิจัย คณะ	
		แพทยศาสตร์ศิริราชพยาบาล	ป.โท		แพทยศาสตร์ศิริราชพยาบาล	
		มหาวิทยาลัยมหิดล			มหาวิทยาลัยมหิดล	
20. Ms. Kewalee Jaturongkakul	-	สถานส่งเสริมการวิจัย คณะ	ผู้ช่วยวิจัยระดับ	-	สถานส่งเสริมการวิจัย คณะ	
		แพทยศาสตร์ศิริราชพยาบาล	ป.โท		แพทยศาสตร์ศิริราชพยาบาล	
		มหาวิทยาลัยมหิดล			มหาวิทยาลัยมหิดล	
21. Ms. Teerada Homvises	-	สถานส่งเสริมการวิจัย คณะ	ผู้ช่วยวิจัยระดับ	-	สถานส่งเสริมการวิจัย คณะ	
		แพทยศาสตร์ศิริราชพยาบาล	ป.โท		แพทยศาสตร์ศิริราชพยาบาล	
		มหาวิทยาลัยมหิดล			มหาวิทยาลัยมหิดล	
22. Ms. Patcharin Keawboonraung	-	สถานส่งเสริมการวิจัย คณะ	ผู้ช่วยวิจัยระดับ	-	คณะแพทยศาสตร์โรงพยาบาลรามาธิบด์	1
		แพทยศาสตร์ศิริราชพยาบาล	ป.ตรี		มหาวิทยาลัยมหิดล	
		มหาวิทยาลัยมหิดล				
23. Ms. Kedsarin Fong-ngern	-	Immunology, Faculty of Medicine	นักศึกษาระดับ	-	สถานส่งเสริมการวิจัย คณะ	-จบการศึกษาแล้ว
		Siriraj Hospital, Mahidol University	ป.เอก		แพทยศาสตร์ศิริราชพยาบาล	-ปัจจุบันบรรจุเป็นนักวิจัย
					มหาวิทยาลัยมหิดล	ที่ศิริราช
24. Ms. Kitisak Sintiprungrat	-	Immunology, Faculty of Medicine	นักศึกษาระดับ	-	สถาบันวิจัยจุฬาภรณ์	-จบการศึกษาแล้ว
		Siriraj Hospital, Mahidol University	ป.เอก			
25. Ms. Paleerath Peerapen	-	Immunology, Faculty of Medicine	นักศึกษาระดับ	-	สถานส่งเสริมการวิจัย คณะ	-จบการศึกษาแล้ว
		Siriraj Hospital, Mahidol University	ป.เอก		แพทยศาสตร์ศิริราชพยาบาล	-ปัจจุบันทำงานเป็น
					มหาวิทยาลัยมหิดล	นักวิจัยที่ศิริราช
26. Mr. Siripat Aluksanasuwan	-	Immunology, Faculty of Medicine	นักศึกษาระดับ	-	Immunology, Faculty of Medicine	-กำลังศึกษา
		Siriraj Hospital, Mahidol University	ป.เอก		Siriraj Hospital, Mahidol University	
27. Ms. Taniya Kaewarpai	-	Immunology, Faculty of Medicine	นักศึกษาระดับ	-	Immunology, Faculty of Medicine	-กำลังศึกษา
•						

		Siriraj Hospital, Mahidol University	ป.เอก		Siriraj Hospital, Mahidol University	
28. Ms. Wararat Chiangjong	-	Immunology, Faculty of Medicine	นักศึกษาระดับ	-	สถานส่งเสริมการวิจัย คณะ	-จบการศึกษาแล้ว
		Siriraj Hospital, Mahidol University	ป.เอก		เพทยศาสตร์ศิริราชพยาบาล	-ปัจจุบันทำงานเป็น
					มหาวิทยาลัยมหิดล	นักวิจัยที่ศ ิริร าช
29. Ms. Suchitra Sutthimethakorn	-	Molecular Medicine, Faculty of	นักศึกษาระดับ	-	Molecular Medicine, Faculty of	-กำลังศึกษา
		Science, Mahidol University	ป.เอก		Science, Mahidol University	
30. Mr. Suparat Taengchaiyaphum	-	Molecular Genetics and Genetics	นักศึกษาระดับ	-	สถาบันชีววิทยาศาสตร์โมเลกุล	-จบการศึกษาแล้ว
		Engineering Program, Institute of	ป.เอก		มหาวิทยาลัยมหิดล	
		Molecular Biosciences, Mahidol				
		University				
31. Ms. Suneerat Hatairaktham	-	Biochemistry, Faculty of Medicine	นักศึกษาระดับ	-	ภาควิชาชีวเคมี คณะแพทยศาสตร์ศิริราช	-จบการศึกษาแล้ว
		Siriraj Hospital, Mahidol University	ป.เอก		พยาบาล มหาวิทยาลัยมหิดล	-ปัจจุบันทำงานเป็น
						นักวิจัยที่ศิริราช
32. Ms. Poorichaya Somparn	-	Multidisciplinary, Faculty of Medicine,	นักศึกษาระดับ	-	ภาควิชาจุลชีววิทยา คณะแพทยศาสตร์	-จบการศึกษาแล้ว
		Chulalongkorn University	ป.เอก		จุฬาลงกรณ์มหาวิทยาลัย	-ปัจจุบันบรรจุเป็นนักวิจัย
						ที่จุฬาฯ
33. Ms. Pattarin Tangtanatakul	-	Multidisciplinary, Faculty of Medicine,	นักศึกษาระดับ	-	Multidisciplinary, Faculty of Medicine,	-กำลังเตรียมตัวสอบป้อง
		Chulalongkorn University	ป.เอก		Chulalongkorn University	วิทยานิพนธ์
34. Mr. Channarong Changtong	-	Immunology, Faculty of Medicine	นักศึกษาระดับ	-	คณะแพทยศาสตร์โรงพยาบาลรามาธิบดี	-จบการศึกษาแล้ว
		Siriraj Hospital, Mahidol University	ป.โท		มหาวิทยาลัยมหิดล	
35. Ms. Chompunoot	-	Immunology, Faculty of Medicine	นักศึกษาระดับ	-	Immunology, Faculty of Medicine	-กำลังเตรียมตัวสอบป้อง
Kapincharanon		Siriraj Hospital, Mahidol University	ป.โท		Siriraj Hospital, Mahidol University	วิทยานิพนธ์
36. Mr. Issara Songmahachai	-	Biochemistry, Faculty of Medicine	นักศึกษาระดับ	-	ภาควิชาชีวเคมี คณะแพทยศาสตร์ศิริ	-จบการศึกษาแล้ว
		Siriraj Hospital, Mahidol University	ป.โท		ราชพยาบาล มหาวิทยาลัยมหิดล	
37. Ms. Sakuna Siriboonpipattana	-	Biochemistry, Faculty of Medicine	นักศึกษาระดับ	-	ภาควิชาอายุรศาสตร์ คณะ	-จบการศึกษาแล้ว

		Siriraj Hospital, Mahidol University	ป.โท		แพทยศาสตร์ศิริราชพยาบาล	
					มหาวิทยาลัยมหิดล	
38. Mr. Nattapong Veerataveeporn	-	Biochemistry, Faculty of Medicine	นักศึกษาระดับ	-	Biochemistry, Faculty of Medicine	-จบการศึกษาแล้ว
		Siriraj Hospital, Mahidol University	ป.โท		Siriraj Hospital, Mahidol University	
39. Ms. Suparaporn Onsathit	-	Immunology, Faculty of Medicine	นักศึกษาระดับ	-	Immunology, Faculty of Medicine	-จบการศึกษาแล้ว
		Siriraj Hospital, Mahidol University	ป.โท		Siriraj Hospital, Mahidol University	
40. Ms. Supatsa Dedsatit	-	Microbiology, Faculty of Medical	นักศึกษาระดับ	-	Microbiology, Faculty of Medical	-จบการศึกษาแล้ว
		Technology, Khon Kaen University	ป.โท		Technology, Khon Kaen University	
41. Ms. Sunida Kuakarn	-	Multidisciplinary, Faculty of Medicine,	นักศึกษาระดับ	-	ภาควิชาจุลชีววิทยา คณะแพทยศาสตร์	-จบการศึกษาแล้ว
		Chulalongkorn University	ป.โท		จุฬาลงกรณ์มหาวิทยาลัย	

ภาคผนวก

ผลงานตีพิมพ์ในวารสารวิชาการระดับนานาชาติและหนังสือ



Contents lists available at ScienceDirect

Biochemical and Biophysical Research Communications

journal homepage: www.elsevier.com/locate/ybbrc



Ceftriaxone crystallization and its potential role in kidney stone formation

Somchai Chutipongtanate, Visith Thongboonkerd*

Medical Proteomics Unit, Office for Research and Development, Faculty of Medicine Siriraj Hospital, and Center for Research in Complex Systems Science, Mahidol University, Bangkok, Thailand

ARTICLE INFO

Article history: Received 9 February 2011 Available online 15 February 2011

Keywords: Ceftriaxone Crystal adhesion Crystallization Kidney stone Nephrolithiasis

ABSTRACT

Drug-induced nephrolithiasis contributes to 1–2% of the incidence of renal calculi. We examined whether ceftriaxone at therapeutic doses could be crystallized in the urine and also explored its role in kidney stone formation. Crystallization was induced by mixing ceftriaxone sodium at therapeutic urinary excretion levels (0.5–4.0 mg/ml) to calcium chloride at physiologic urinary concentration (5 mM) in deionized (dl) water or artificial urine (AU). The results showed that ceftriaxone was crystallized with free calcium in dose- and time-dependent manner. These ceftriaxone/calcium crystals showed birefringence property under polarized microscope. Individual crystals had needle-shape (5–100 μ m in length), whereas the aggregated form had star-burst and irregular-plate shape (40–200 μ m in diameter) (note that the crystal sizes were much larger than renal tubular lumens). Calcium-depletion assay revealed that crystallization required free calcium as a substrate. In AU, crystallization remained although it was partially inhibited when compared to that in dl water. Finally, these crystals could tightly adhere onto renal tubular cell surface. Our data demonstrated that ceftriaxone at therapeutic levels could be crystallized with free calcium in the urine under physiologic condition. We hypothesize that tubular occlusion and crystal–cell adhesion may play important role in pathogenic mechanisms of ceftriaxone-induced nephrolithiasis.

© 2011 Elsevier Inc. All rights reserved.

1. Introduction

Nephrolithiasis is an outcome of sophisticated events involving numerous factors; e.g., supersaturation of inorganic salts, underlying genetic/metabolic disorders, and defects in stone modulators [1]. Medication has been considered as one of the pathogenic factors for nephrolithiasis [1,2]. Drug-associated nephrolithiasis contributes to approximately 1-2% of the incidence of renal calculi [2]. This drug adverse event most often affects patients who have received high-dose and/or long-term treatment of some drugs with lithogenic potential [2]. According to mechanisms of calculi formation, lithogenic drugs can be classified into two groups [2]. The first group composes of drugs that induce metabolic abnormalities (e.g., hypercalciuria [3,4] hypocitraturia [5,6], hyperuricosuria [7] and alteration of urine acidity [5,6]), which subsequently provoke formation of metabolic calculi; e.g., calcium-containing stones and uric acid nephrolithiasis [2]. Examples of drugs in the first group include calcium/vitamin D supplement [3], furosemide [4], carbonic anhydrase inhibitors [5], laxatives [6], and uricosuric drugs [7]. The second group composes of drugs that can be crystallized directly in the urine due to their high excretory levels and poor solubility [8-11]. A number of drugs (e.g., triamterine [8], sulfonamides [9], indinavir [10], and silicate-containing drugs [11]) belong to this group. It seems that the second group of lithogenic drugs predominates and causes higher incidence of drugassociated nephrolithiasis [2].

Recently, ceftriaxone (a third-generation cephalosporin with broad-spectrum antibiotic activity) has been recognized as a potentially lithogenic drug [12-14]. Intravenous administration of ceftriaxone is widely used for treatment of microbial infections, particularly organ infection and sepsis. Abnormal ceftriaxone crystallization has been recently recognized as one of its side effects [13–15]. Interestingly, these ceftriaxone-induced calculi can develop within a short period after its administration. Two prospective studies using renal ultrasonography have revealed that 1.4-7.8% of patients had developed renal calculi within 7 days after the standard course of ceftriaxone therapy [13,14]. Although predisposing factors of this drug complication remain unclear, patient's age and some congenital genitourinary anomalies may be involved in the increasing risk of the calculi development [13,14,16]. Most patients with ceftriaxone-associated calculi are asymptomatic [13,14]; however, a number of patients may have colicky pain, gross hematuria, anuria, and uremia [12,16-18].

Compositional analysis has revealed that the calculi obtained from patients receiving ceftriaxone therapy compose mainly of ceftriaxone compound [17], suggesting that the mechanism of calculi formation is based on direct drug crystallization. Nonetheless, unlike other lithogenic medications that are crystallized due to their poor solubility, direct ceftriaxone crystallization has been

^{*} Corresponding author. Address: Medical Proteomics Unit, Office for Research and Development, Siriraj Hospital, Mahidol University, 12th Fl. Adulyadej Vikrom Bldg., 2 Prannok Rd., Bangkoknoi, Bangkok 10700, Thailand. Fax: +66 2 4184793.

E-mail address: thongboonkerd@dr.com (V. Thongboonkerd).

thought to occur by interaction between ceftriaxone (anionic) and free calcium (cationic) [12–14,16,17]. However, this hypothesis has not yet been tested. Additionally, it remains unclear whether ceftriaxone can be crystallized in the urine with its therapeutic urinary excretion levels [19] and physiologic concentration of urinary calcium. Moreover, the mechanisms leading to ceftriaxone crystal retention in the kidney or urinary tract has not been previously elucidated.

The present study was therefore aimed to demonstrate direct interaction between ceftriaxone and calcium. Crystallization of ceftriaxone at therapeutic urinary excretion levels [19] together with calcium at physiologic urinary concentration was first examined in dI water and then evaluated under urinary environment simulated by AU condition. Size and morphology of ceftriaxone crystals were evaluated using phase-contrast and polarized microscopy. Calcium-depletion assay was employed to validate the interacting complex between ceftriaxone and calcium. Furthermore, crystal-cell adhesion was also examined to better understand pathogenic mechanisms of ceftriaxone-induced nephrolithiasis.

2. Materials and methods

2.1. Ceftriaxone crystallization

A previous pharmacokinetic study has demonstrated that approximately 67% of administered ceftriaxone was excreted as unchanged compound via renal clearance; thus, urinary excretion levels of ceftriaxone are directly proportional to the administered dose [19]. After intravenous administration of 0.5, 1.0, and 2.0 g ceftriaxone (which are generally used in clinical practice) for 2 h, urinary ceftriaxone levels were 0.53 ± 0.30 , 0.99 ± 0.73 , and 2.69 ± 1.40 mg/ml, respectively [19]. Therefore, ceftriaxone concentrations of 0.5–4.0 mg/ml were used in our present study to represent therapeutic urinary excretion levels of ceftriaxone in patients.

Ceftriaxone stock solution was prepared by dissolving ceftriaxone sodium powder (Rocephin®, Roche Pharmaceuticals Inc., NJ) in dI water (18.2 M Ω ·cm) to the final concentration of 100 mg/ml and kept at -20 °C until used. This stock solution has clear colorless appearance without any precipitates or undissolved particles remained. Ceftriaxone crystallization was performed in each well of a 24-well polystyrene plate (with lid) (Corning Inc.; Corning, NY) as follows. Various amounts of ceftriaxone stock solution were added into dI water containing 5 mM calcium chloride (CaCl₂) (equivalent to 5 mM free calcium, a physiologic urinary calcium concentration) to make the final drug concentration of 0.5, 1.0, 2.0. and 4.0 mg/ml. Each crystallized reaction was further incubated for 2, 6, 12, and 24 h at 25 °C. To investigate ceftriaxone crystallization under urinary environment, AU formula (containing 5 mM CaCl₂, 200 mM urea, 4 mM creatinine, 5 mM Na₃C₆H₅O₇·2H₂O, 54 mM NaCl, 30 mM KCl, 15 mM NH₄Cl, 2 mM MgSO₄·7H₂O, 9 mM Na₂SO₄, pH 6.2) was used in stead of dI water during the crystallization reaction. This AU formula is very similar (almost identical) to the normal human urine considering physico-chemical properties as concentrations of individual compositions are within their physiologic ranges in the normal human urine [20]. In addition, this AU formula excluded oxalate, phosphate, and uric acid to prevent unwanted crystallization of calcium oxalate, calcium phosphate, and uric acid, respectively. All these experiments were done in triplicate (independently). Ceftriaxone crystals and reaction supernatants were further examined as follows.

2.2. Morphological evaluation of ceftriaxone crystals

Ceftriaxone crystal morphology was evaluated by phase-contrast and polarized microscopic examinations. At 2, 6, 12, and

24 h after crystallization, each reaction well was evaluated for ceftriaxone crystal size and morphology using Olympus CKX41 inverted phase-contrast microscope (Olympus Co. Ltd.; Tokyo, Japan). In addition, to gain further information on birefringence property, ceftriaxone crystals were also examined under crossed polarized light, generating by two polarized filters of Nikon ECLIPSE 80i microscope (Nikon Corp.; Tokyo, Japan).

2.3. Calcium-depletion assay

According to the hypothesis that the interaction between ceftriaxone and calcium led to ceftriaxone crystallization, free calcium ions in the solution would be depleted from the solution because they were consumed into the crystal complex as a substrate. Therefore, direct interaction between ceftriaxone and calcium could be demonstrated by a novel calcium-depletion assay established recently [21]. Briefly, the assay was performed by transferring 3 µl supernatant from each sample well into 200 µl of Arsenazo III reagent (0.2 mM Arsenazo III in a buffer containing 75 mM imidazole, pH 6.5) (BioSystems S.A.: Barcelona, Spain) in 96-well polystyrene plate (Corning Inc.: Corning, NY). The samples were gently mixed and then incubated for 5 min at 25 °C. The reaction intensity was measured using Anthos HTII Microplate Reader (Anthos Labtec Instruments; Salzburg, Austria) using a λ620 nm filter to measure the color intensity, which reflected AIII-calcium reaction and level of free calcium ions. All measurements were normalized by subtraction with the intensity background obtained from the blank AIII reagent (because the 620 nm light could be partially absorbed by AIII reagent). The standard curve was generated by using CaCl₂ at the following concentrations: 0, 0.312, 0.625, 1.250, 2.500, and 5.000 mM. The concentration of free calcium ions (Free Ca²⁺) in each sample well was calculated using the following equation:

Free
$$Ca^{2+}(mM) = \frac{(A_{620} - Constant of the standard curve)}{Slope of the standard curve}$$

Where A_{620} was the absorbance of the sample at $\lambda 620$ nm. All these experiments were done in triplicate (three independent experiments).

2.4. Renal tubular cell culture and crystal-cell adhesion

Approximately 1×10^5 Madin–Darby Canine Kidney (MDCK) cells, which represent cells derived from distal nephron [22], were inoculated in each well of a 24-well, polystyrene, disposable cell culture cluster (with lid) (Corning Inc.) containing complete Eagle's minimum essential medium (MEM) (GIBCO, Invitrogen Corporation; Green Island, NY) supplemented with 10% fetal bovine serum (FBS), 1.2% penicillinG/streptomycin, and 2 mM glutamine. The cultured cells were maintained in a humidified incubator at 37 °C with 5% CO₂ for 24 h. Thereafter, the culture medium in each well was replaced with 1 ml of AU (containing compositions as aforementioned) to simulate intraluminal urinary environment in vivo. Various amounts of ceftriaxone stock solution were added into each culture well to the final concentrations of 0.5, 1.0, 2.0, and 4.0 mg/ml, and the cells were then further incubated in a humidified incubator at 37 °C with 5% CO₂ for 2 h. Thereafter, the cells were vigorously washed three times with isotonic phosphate buffered saline (PBS) to remove non-adhered crystals before visualization using an inverted phase-contrast microscope (Olympus Co. Ltd.). All these experiments were done in triplicate (three independent experiments).

2.5. Statistical analysis

All the quantitative data are reported as mean ± SEM. Multiple comparisons were performed using ANOVA with Tukey's post

hoc test (SPSS, version 11.5). *P* values < 0.05 were considered statistically significant.

3. Results

3.1. Ceftriaxone crystal morphology

Size and morphology of ceftriaxone crystals were revealed under phase-contrast and crossed polarized light microscopes. Ceftriaxone crystals were present as individual crystals and also as the aggregates. Individual crystals had needle-shape with a size of approximately 5–100 μm in length (Fig. 1; panel A). Under crossed polarized light, the individual crystals showed birefringence property. The aggregated crystals had two morphological patterns; including star-burst (Fig. 1; panels B and C) and irregular-plate shape (Fig. 1; panels D–F). Size of the aggregated crystals varied in the range of 40–200 μm in diameter or length, which was much larger than the individual crystals. Under crossed polarized light, the aggregated crystals also exhibited birefringence property.

3.2. Factors determining degree of ceftriaxone crystallization

To determine whether ceftriaxone at therapeutic urinary excretion levels could be crystallized together with physiologic urine level of free calcium, various concentrations of 0.5, 1.0, 2.0, and 4.0 mg/ml ceftriaxone were crystallized with 5 mM CaCl $_2$ in dl water. Fig. 2A demonstrates that these concentrations of ceftriaxone could be crystallized with free calcium to form the aggregates in the time- and dose-dependent manner. Both number and size of crystals were directly proportional to drug concentration and incubation time, consistent to the simple rule of chemical reaction.

Also, various concentrations of ceftriaxone were added into AU containing 5 mM CaCl₂ to evaluate ceftriaxone crystallization under human urine environment *in vitro*. Our present study selected AU instead of fresh human urine as to reduce inter- and intra-individual variability of urinary components. Additionally, in contrast to the fresh human urine, this AU had no oxalate, phosphate and uric acid; therefore, unwanted crystallization of calcium oxalate, calcium phosphate and uric acid could be excluded from this study.

Fig. 2B demonstrates that ceftriaxone could be crystallized in the AU environment, but with the less extent as compared to crystallization in dI water (Fig. 2A). In AU, ceftriaxone crystals were observed only with high doses (2.0 and 4.0 mg/ml), but number and size of the crystals were fewer and smaller, respectively, as compared to crystallization in dI water. These results implicated that AU had some inhibitory effects against ceftriaxone crystallization.

3.3. Ceftriaxone crystallization required free calcium as a substrate

Consumption of free calcium during crystallization was validated using a calcium-depletion assay. Fig. 3A demonstrates calcium depletion after ceftriaxone crystallization in dI water. Degree of calcium depletion was dose- and time-dependent. While the lower doses (0.5 and 1.0 mg/ml) showed minimal degree of calcium depletion, the higher doses (2.0 and 4.0 mg/ml) were accompanied with marked decrease in free calcium levels. At 24 h after crystallization in dI water using 0.5, 1.0, 2.0, and 4.0 mg/ml ceftriaxone, remaining levels of free calcium were $4.54\pm0.26, 3.63\pm0.13, 2.00\pm0.10,$ and 0.10 ± 0.05 mM, respectively (significantly reduced from the basal level of 5 mM). This data indicated that ceftriaxone crystallization required free calcium as a substrate.

Fig. 3B demonstrates calcium depletion after ceftriaxone crystallization in AU. Degree of calcium depletion was dose- and time-dependent. However, as expected, degree of calcium depletion in AU was lower than that in dI water at all doses and time-points. At the dose of 0.5 mg/ml, there was no calcium depletion observed, whereas there was only minimal degree of calcium-depletion observed at the dose of 1.0 mg/ml. However, calcium depletion was more obvious using higher doses (2.0 and 4.0 mg/ml) ceftriaxone. These data were consistent with the microscopic findings shown in Fig. 2B. At 24 h after crystallization in AU using 0.5, 1.0, 2.0, and 4.0 mg/ml ceftriaxone, remaining levels of free calcium were 4.90 ± 0.15 , 4.13 ± 0.24 , 3.01 ± 0.14 , and 1.60 ± 0.11 mM, respectively. These data also suggested that AU might have some inhibitory effects against ceftriaxone crystallization.

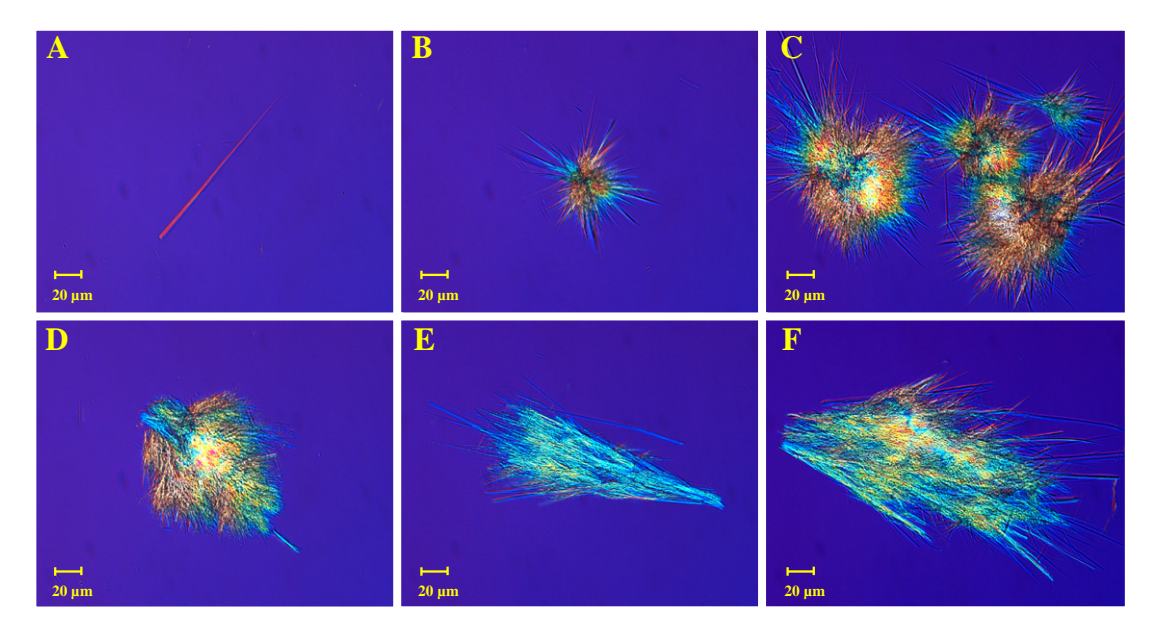


Fig. 1. Ceftriaxone crystal morphology. Crystals were generated by mixing 2.0 mg/ml ceftriaxone with 5 mM CaCl₂ in dI water. After 2 h incubation, the crystals were subjected to evaluation by phase-contrast and polarized microscopy. Individual crystals were present with needle shape (panel A), whereas the aggregated forms had starburst pattern (panels B and C) and irregular-plate shape (panels D-F). Original magnification = $400 \times$ for all panels.

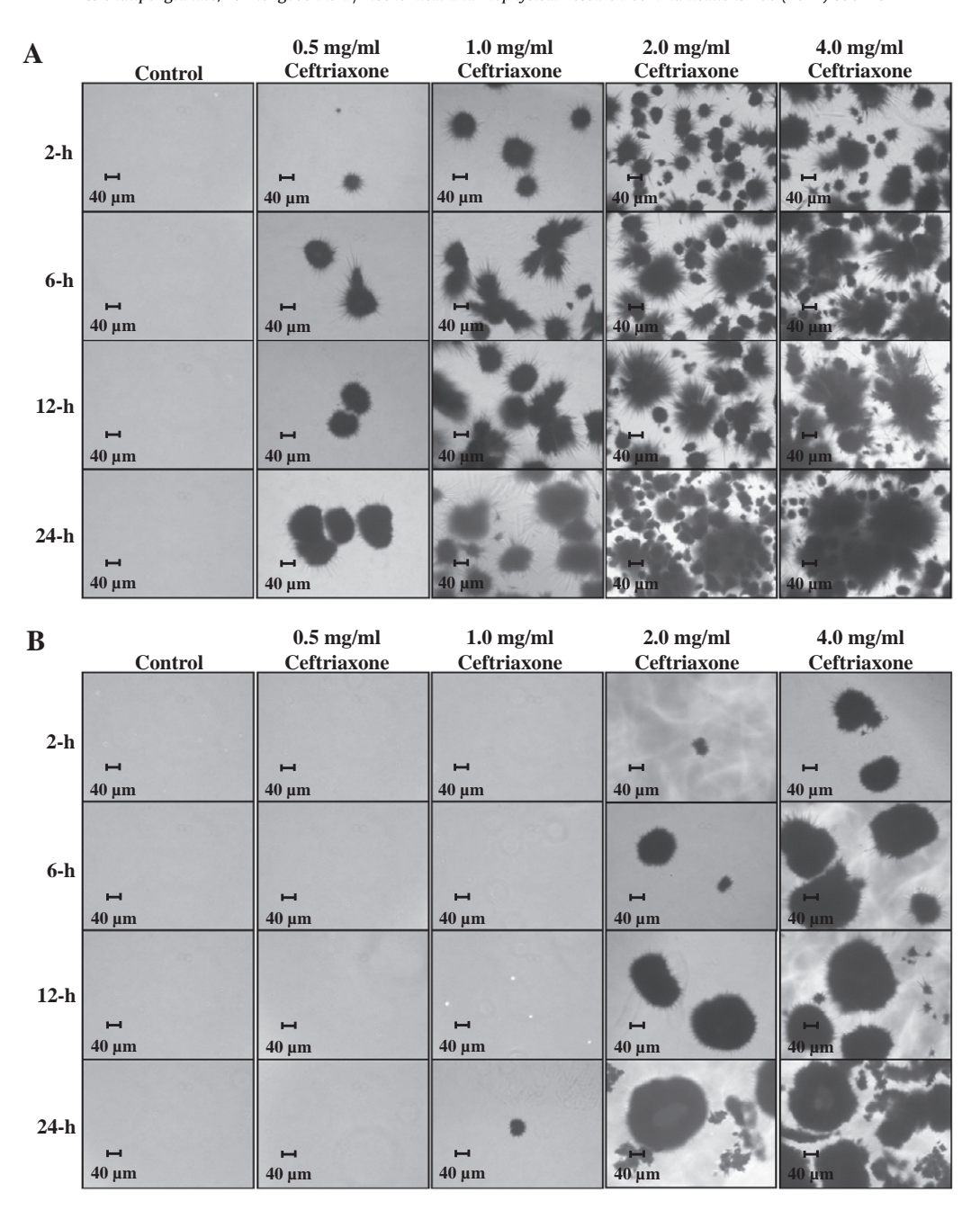


Fig. 2. Ceftriaxone crystallization with varying doses and incubation periods. Ceftriaxone at 0.5, 1.0, 2.0, and 4.0 mg/ml were mixed with 5 mM CaCl₂ in dl water (A) or AU (B). The mixtures were then incubated for 2, 6, 12, and 24 h at 25 °C, and crystal images were taken by phase-contrast microscopy. Original magnification = $200 \times$ for all panels.

3.4. Ceftriaxone crystals tightly adhered onto MDCK cell surface

Crystal adhesion is considered as one of the most crucial pathogenic mechanisms of renal calculi because this cell-crystal interaction leads to crystal retention in the kidney [23]. Previously, there was no evidence demonstrating that crystal adhesion plays any roles in drug-associated nephrolithiasis. We thus examined the interaction between ceftriaxone crystals and renal tubular (MDCK) cells under simulated urine environment. Fig. 4 shows that ceftriaxone/calcium crystals tightly adhered onto MDCK cell surface as the crystals remained after vigorous washing, particularly when higher doses (2.0 and 4.0 mg/ml) of ceftriaxone were used. As this experiment was performed under the AU environment, crystal adhesion was not obvious when lower doses (0.5–1.0 mg/

ml) were used, consistent with the inhibitory effects of AU on ceftriaxone crystallization as also shown in Figs. 2B and 3B. Our data suggested that adhesion of ceftriaxone crystals onto renal tubular cell surface may promote crystal aggregation and crystal retention in the kidney.

4. Discussion

It has been proposed that ceftriaxone-induced nephrolithiasis is a result of direct interaction between ceftriaxone and free calcium in the urine [12–14,16,17]. However, it was unclear in the past whether ceftriaxone could be crystallized with calcium, particularly under physiologic urinary condition. The results in our

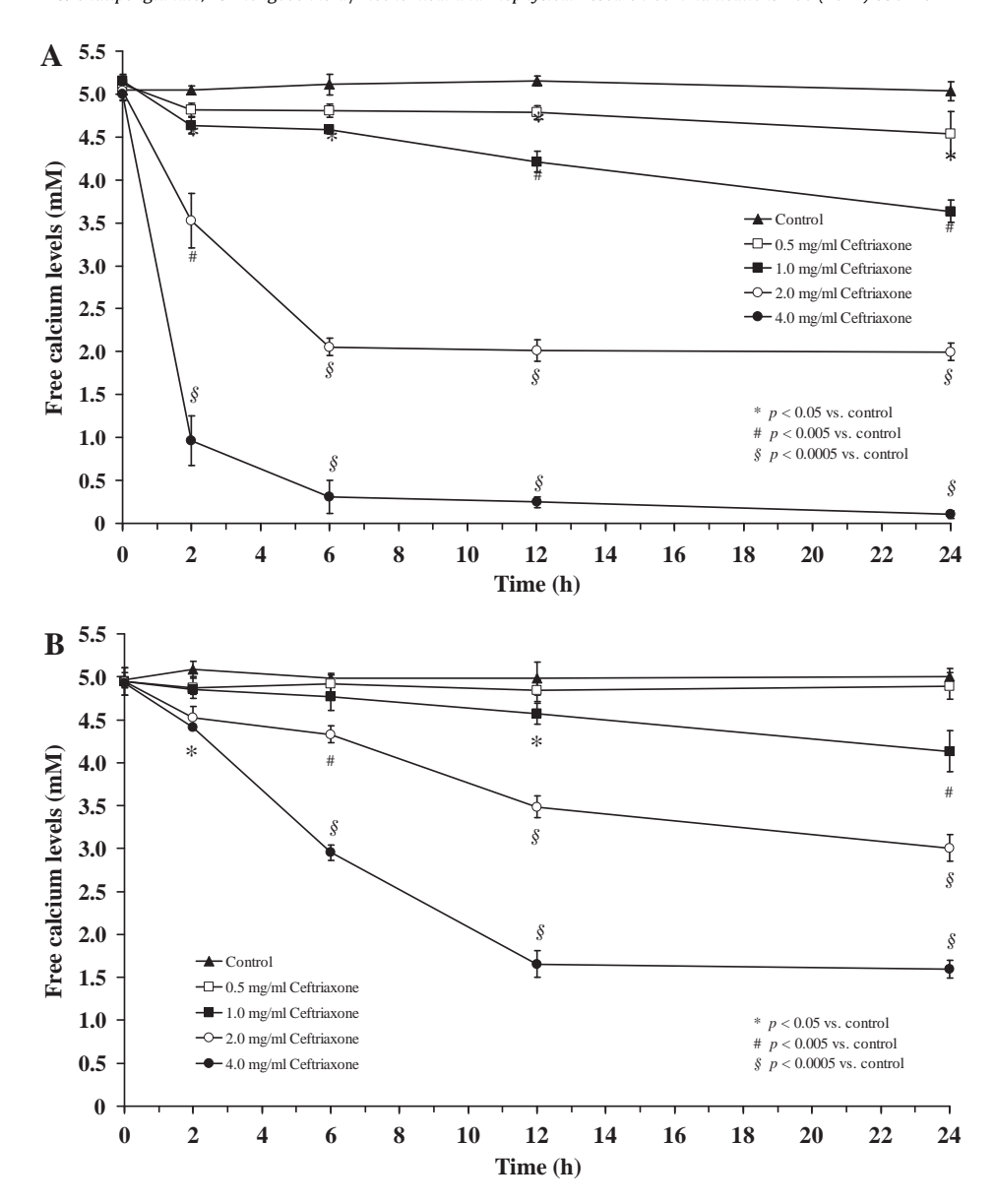


Fig. 3. Calcium-depletion assay. The consumption of free calcium during ceftriaxone crystallization was validated by calcium-depletion assay. Calcium depletion (which reflected consumption of free calcium) was monitored in each crystallization reaction performed in dI water (A) or AU (B) (detailed in Section 2). Each data point was derived from three independent experiments and the data are reported as mean ± SEM.

present study clearly demonstrated that ceftriaxone at therapeutic urinary excretion levels [19] could directly interact with free calcium at physiologic urinary concentration to generate ceftriaxone/calcium crystals. Several factors including drug concentration and incubation time are very important for determining the degree of ceftriaxone/calcium crystallization (Fig. 2A and B). According to our data, ceftriaxone crystallization was dose- and time-dependent reaction. Therefore, high-dose ceftriaxone administration (which leads to increasing urinary ceftriaxone levels) and urinary stasis by any causes (which leads to retention of ceftriaxone crystals in urinary tract, allowing crystal growth and aggregation) may aggravate ceftriaxone calculi formation.

Another interesting factor that may be involved in the pathogenic mechanisms of ceftriaxone-induced nephrolithiasis is urinary environment. Our present study has demonstrated that AU exhibited some degree of inhibitory effects on ceftriaxone crystallization (Figs. 2B and 3B). It has been hypothesized that some substances in AU (e.g., citrate and magnesium) may be responsible for these inhibitory effects. Citrate may bind to free calcium to reduce

the remaining free calcium, which is the substrate for ceftriaxone crystallization. In addition to citrate and magnesium, other anionic and cationic urinary composition [24,25] may also act as the modulators to prevent ceftriaxone crystallization. Nevertheless, it still occurs when the high doses of ceftriaxone is administered. Further studies are required to elucidate this hypothesis.

Similar to several other lithogenic drugs [2], the data in this study also suggested that ceftriaxone/calcium calculi may be developed after tubular occlusion. The size of ceftriaxone crystal aggregates was approximately 40–200 μm in diameter (Figs. 1 and 2), whereas the luminal diameters of proximal tubules, distal tubules and collecting ducts are approximately 50–60, 20–30, and 50–60 μm , respectively, which are much smaller than ceftriaxone/calcium crystals. Therefore, the ceftriaxone crystal aggregates can easily obstruct renal tubules, leading to tubular occlusion and ceftriaxone calculi formation.

Furthermore, we have also demonstrated that crystal-cell adhesion may play significant roles in the pathogenic mechanisms of ceftriaxone-induced nephrolithiasis. Our findings showed that

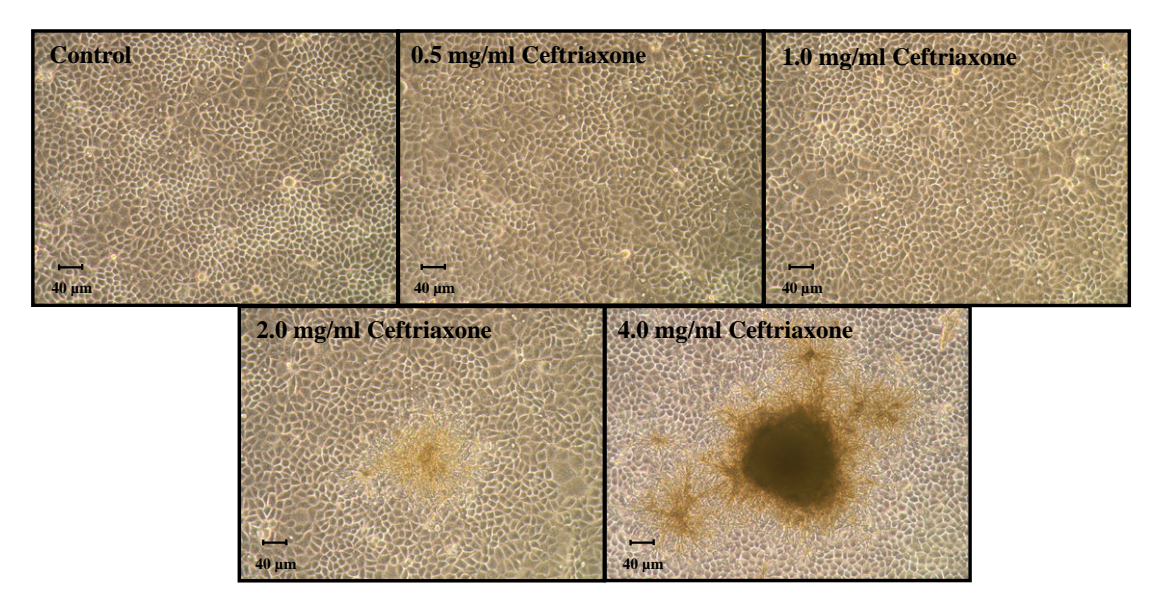


Fig. 4. Adhesion of ceftriaxone crystals onto renal tubular cell surface. Ceftriaxone crystallization was performed in MDCK cell culture well containing AU (detailed in Section 2). After 2 h incubation, the cells were vigorously washed three times with isotonic PBS solution. The remainings were then imaged using a phase-contrast microscope. Original magnification = 200× for all panels. All experiments were done in triplicate.

ceftriaxone crystals could tightly adhere onto renal tubular cell surface (Fig. 4), suggesting the high adhesive force between ceftriaxone crystals and renal tubular cell surfaces. Although the mechanism for such crystal-cell adhesion is still unknown, one possibility is that ceftriaxone/calcium crystals may adhere onto cell surface via ionic interaction and/or hydrogen bond, similar to other calcium-containing crystals (e.g., calcium oxalate, calcium phosphate) [26]. Another possibility is that MDCK cell surface may present some (unknown) receptors for ceftriaxone crystals. These hypotheses should be further elucidated.

Although our data clearly demonstrated that ceftriaxone could be crystallized in the urine at physiologic condition, only a few numbers of patients receiving ceftriaxone therapy have been reported to develop ceftriaxone-containing calculi in routine clinical practice. One explanation is that most of patients with ceftriaxoneinduced nephrolithiasis have asymptomatic calculi and thus this complication has been neglected by patients or overlooked by clinicians until severe clinical symptoms are present. This explanation is also supported by a prospective clinical study [13]. In this study, all patients were investigated with renal ultrasonography before and after ceftriaxone therapy to demonstrate the presence or absence of renal calculi. After 50 mg/kg/day intramuscular administration and 100 mg/kg/day intravascular injection of ceftriaxone for 7 days, 7.4% and 8.3%, respectively, of patients developed novel episode of renal calculi [13]. Interestingly, all calculi-affected patients were asymptomatic and had spontaneous recovery with stone passage after conservative treatments. Without renal ultrasonography, these asymptomatic calculi would not be recognized and ceftriaxone-induced nephrolithiasis remains underinvestigated. According to this evidence, the accurate incidence of ceftriaxone-associated nephrolithiasis may be higher than that was initially anticipated from clinical experience. Because ceftriaxone is one of the most commonly used drugs in clinical practice, the occurrence of this drug-induced stone should be concerned to avoid or prevent inevitable renal complications (e.g., renal failure) in some cases.

In summary, our present study has shown that ceftriaxone could be crystallized in the urine under physiologic condition. The size of ceftriaxone crystal aggregates was much larger than the diameter of renal tubular lumens, implicating that tubular

occlusion may be the major mechanism for subsequent development of ceftriaxone calculi. In addition, crystal adhesion onto renal tubular cell surface may also play important role for the initiation of ceftriaxone-induced nephrolithiasis.

5. Conflict of interest

Both authors declare no conflicts of interest and have no financial relationships with companies that make products relevant to the paper.

Acknowledgments

This study was supported by Office of the Higher Education Commission and Mahidol University under the National Research Universities Initiative, and The Thailand Research Fund to VT and SC (VT is a Senior TRF Research Scholar, whereas SC is a New TRF-CHE Research Scholar). Both SC and VT are also supported by "Chalermphrakiat" Grant, Faculty of Medicine Siriraj Hospital.

References

- [1] F.L. Coe, A. Evan, E. Worcester, Kidney stone disease, J. Clin. Invest. 115 (2005) 2598–2608.
- [2] M. Daudon, P. Jungers, Drug-induced renal calculi: epidemiology, prevention and management, Drugs 64 (2004) 245–275.
- [3] C.Y. Pak, K. Sakhaee, T.I. Hwang, G.M. Preminger, J.A. Harvey, Nephrolithiasis from calcium supplementation, J. Urol. 137 (1987) 1212–1213.
- [4] H.N. Noe, J.F. Bryant, S. Roy III, F.B. Stapleton, Urolithiasis in pre-term neonates associated with furosemide therapy, J. Urol. 132 (1984) 93–94.
- [5] C. Ahlstrand, H.G. Tiselius, Urine composition and stone formation during treatment with acetazolamide, Scand. J. Urol. Nephrol. 21 (1987) 225–228.
- [6] W.H. Dick, J.E. Lingeman, G.M. Preminger, L.H. Smith, D.M. Wilson, W.L. Shirrell, Laxative abuse as a cause for ammonium urate renal calculi, J. Urol. 143 (1990) 244–247.
- [7] D.A. McLain, F.J. Garriga, O.S. Kantor, Adverse reactions associated with ticrynafen use, JAMA 243 (1980) 763–764.
- [8] R.W. Grunberg, S.J. Silberg, Triamterene-induced nephrolithiasis, JAMA 245 (1981) 2494–2495.
- [9] L.A. Farina, R.J. Palou, T.G. Chechile, Reversible acute renal failure due to sulfonamide-induced lithiasis in an AIDS patient, Arch. Esp. Urol. 48 (1995) 418-419
- [10] M. Daudon, L. Estepa, J.P. Viard, D. Joly, P. Jungers, Urinary stones in HIV-1-positive patients treated with indinavir, Lancet 349 (1997) 1294–1295.
- [11] J.H. Farrer, J. Rajfer, Silicate urolithiasis, J. Urol. 132 (1984) 739-740.

- [12] G. Feher, A. Benczik, E. Szabo, I. Rethy, M. Berenyi, Renal gravel formation inducing renal insufficiency as a side-effect of ceftriaxon, Orv. Hetil. 140 (1999) 769-771.
- [13] Z. Avci, A. Koktener, N. Uras, F. Catal, A. Karadag, O. Tekin, H. Degirmencioglu, E. Baskin, Nephrolithiasis associated with ceftriaxone therapy: a prospective study in 51 children, Arch. Dis. Child. 89 (2004) 1069–1072.
- [14] M. Mohkam, A. Karimi, A. Gharib, H. Daneshmand, A. Khatami, N. Ghojevand, M. Sharifian, Ceftriaxone associated nephrolithiasis: a prospective study in 284 children, Pediatr. Nephrol. 22 (2007) 690–694.
- [15] E. Steadman, D.W. Raisch, C.L. Bennett, J.S. Esterly, T. Becker, M. Postelnick, J.M. McKoy, S. Trifilio, P.R. Yarnold, M.H. Scheetz, Evaluation of a potential clinical interaction between ceftriaxone and calcium, Antimicrob. Agents Chemother. 54 (2010) 1534–1540.
- [16] V. Stojanovic, V.G. Djuric, Nephrolithiasis caused by ceftriaxone in a 3-year-old child with ureteropelvic junction obstruction, Case Rep. Med. 2009 (2009) 365962.
- [17] R.A. de Moor, A.C. Egberts, C.H. Schroder, Ceftriaxone-associated nephrolithiasis and biliary pseudolithiasis, Eur. J. Pediatr. 158 (1999) 975–977.
- [18] V. Tasic, A. Sofijanova, V. Avramoski, Nephrolithiasis in a child with acute pyelonephritis. Ceftriaxone-induced nephrolithiasis and biliary pseudolithiasis, Pediatr. Nephrol. 20 (2005) 1510–1513.

- [19] I.H. Patel, S. Chen, M. Parsonnet, M.R. Hackman, M.A. Brooks, J. Konikoff, S.A. Kaplan, Pharmacokinetics of ceftriaxone in humans, Antimicrob. Agents Chemother. 20 (1981) 634–641.
- [20] S. Chutipongtanate, V. Thongboonkerd, Systematic comparisons of artificial urine formulas for in vitro cellular study, Anal. Biochem. 402 (2010) 110–112.
- [21] S. Chutipongtanate, V. Thongboonkerd, Establishment of a novel colorimetric assay for high-throughput analysis of calcium oxalate crystal growth modulation, Analyst 135 (2010) 1309–1314.
- [22] M.H. Saier Jr., Growth and differentiated properties of a kidney epithelial cell line (MDCK), Am. J. Physiol. 240 (1981) C106–C109.
- [23] J.C. Lieske, S. Deganello, Nucleation, adhesion, and internalization of calciumcontaining urinary crystals by renal cells, J. Am. Soc. Nephrol. 10 (Suppl 14) (1999) S422–S429.
- [24] R.L. Ryall, Glycosaminoglycans, proteins, and stone formation: adult themes and child's play, Pediatr. Nephrol. 10 (1996) 656–666.
- [25] V. Thongboonkerd, S. Chutipongtanate, T. Semangoen, P. Malasit, Urinary trefoil factor 1 is a novel potent inhibitor of calcium oxalate crystal growth and aggregation, J. Urol. 179 (2008) 1615–1619.
- [26] Y.I. Rabinovich, M. Esayanur, S. Daosukho, K.J. Byer, H.E. El Shall, S.R. Khan, Adhesion force between calcium oxalate monohydrate crystal and kidney epithelial cells and possible relevance for kidney stone formation, J. Colloid Interf. Sci. 300 (2006) 131–140.

Session I – Bioanalysis I

Open Access

Proteomics in Dengue Virus Infection: Host Response in Human Endothelial Cells

Visith Thongboonkerd^{1,2*}

¹Medical Proteomics Unit, Office for Research and Development, Faculty of Medicine Siriraj Hospital,
Mahidol University, Bangkok, Thailand

²Center for Research in Complex Systems Science, Mahidol University, Bangkok, Thailand

*Corresponding author:

Visith Thongboonkerd, Email: thongboonkerd@dr.com (or) vthongbo@yahoo.com

From 2011 International Symposium on Analytical Science and Technology (ISAST)

Daejeon, Republic of Korea, 15-17 November, 2011

Abstract

This mini-review highlights important findings obtained from a series of our recent proteomic studies of human endothelial cells in response to dengue virus infection, which remains common in tropical/subtropical countries. These findings shed light onto mechanisms of vascular leakage, which is a fatal complication of this disease.

Key words: Dengue; Endothelial cell; Proteome; Proteomics; Vascular leakage

Introduction

Dengue virus (DENV) infection remains a common disease in tropical and subtropical regions with periodic outbreaks. The World Health Organization (WHO) has recently estimated that there are more than 2 billion people worldwide who are at risk of DENV infection and there may be 50-100 million individuals infected with DENV annually (among these, approximately 500,000 patients require hospitalization) [1].

The DENV-infected individuals may or may not have symptoms, which vary from mild to severe. The severe

or fatal forms of DENV infection include dengue hemorrhagic fever (DHF) and dengue shock syndrome (DSS) with the hallmarks of vascular leakage, bleeding and shock. However, pathogenic mechanisms of vascular leakage in DHF and DSS remain unclear. Our group therefore performed a series of proteomic studies to address expression and functional changes of human endothelial cells in response to DENV infection [2,3]. The important findings obtained from these studies are highlighted as follows.

Results and Discussion

The optimal condition of DENV infection for proteome analysis of host response in human endothelial cells was carefully defined. This condition should provide the high percentage of infectivity but on the other hand should have the minimal degree of cell death,

because the study focused mainly to early responses of the infected cells, not the changes caused by cell death. After obtaining such optimal condition, expression proteome analysis was performed followed by highly focused functional studies to address functional significance of the expression data (Fig. 1).

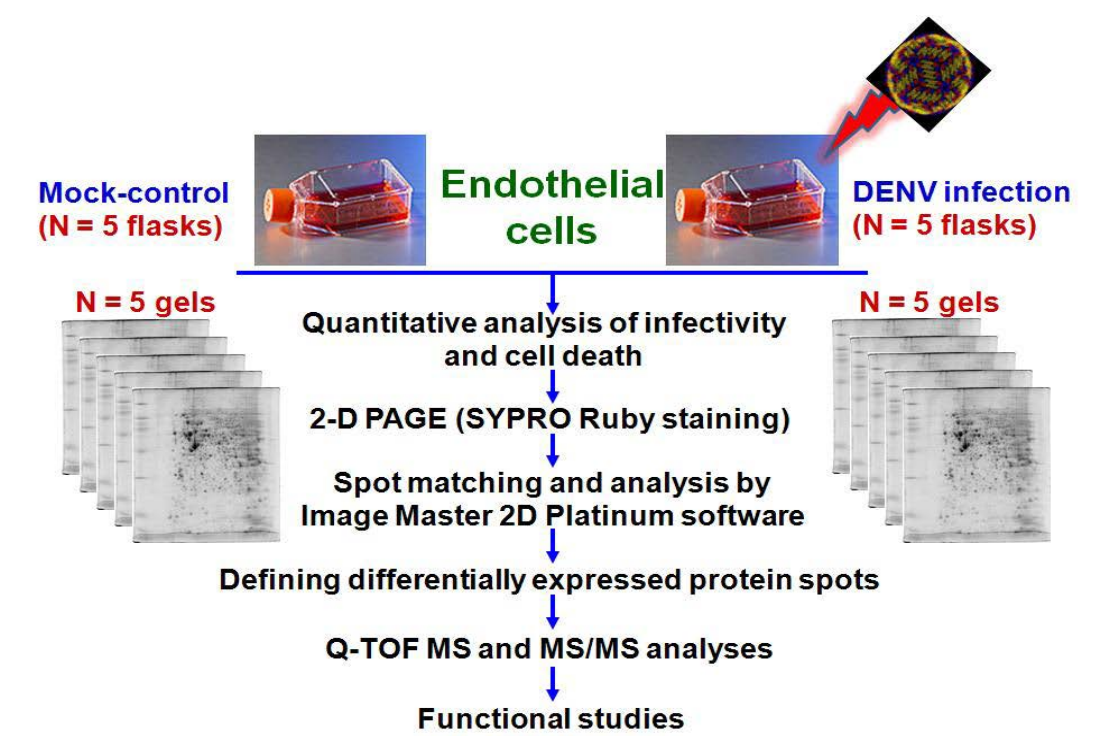


Fig. 1. Schematic summary of analytical approach

Human endothelial cells (EA.hy926) were challenged with DENV at various multiplicities of infection (MOI; or proportional amount of the viral particles per number of cells) (at 1, 5 and 10) for 2 h with 12, 24 and 48 h post-infection incubation periods. Non-infected (mock) cells served as the controls. The infectivity was quantitated by flow cytometric analysis of DENV envelope protein.

The results showed that the cells had the highest percentage of infection at 24 h post-infection with the MOI of 10, whereas prolonged incubation to 48 h did not significantly increase the infectivity. Morphological examination revealed that the DENV-infected cells at 12 and 24 h post-infection had similar morphology to the mock-control cells without any obvious changes regardless of the MOI used. However, at 48 h post-infection, particular with the MOI of 5 and 10, the infected cells showed characteristics of cell death, including cellular detachment and rounding.

Quantitative analysis of cell death by flow cytometry using annexin V/propidium iodide co-staining showed that total cell death (early/late apoptosis and necrosis) at 24 h post-infection with the MOI of 10 was not increased significantly. Based on these infectivity and cell death data, the MOI of 10 with 24 h post-infection period was used for all subsequent proteome analyses [2].

Cellular proteins were extracted, resolved by two-dimensional polyacrylamide gel electrophoresis (2-D PAGE), and visualized by SYPRO Ruby fluorescence stain. Comparative proteomics was performed by spot matching and intensity analysis, which revealed 15 protein spots, whose levels were significantly altered by DENV infection. All of them were successfully identified by quadrupole time-of-flight (Q-TOF) mass spectrometry (MS) and tandem mass spectrometry (MS/MS) (Fig. 2) [2].

11 Increased 4 Decreased

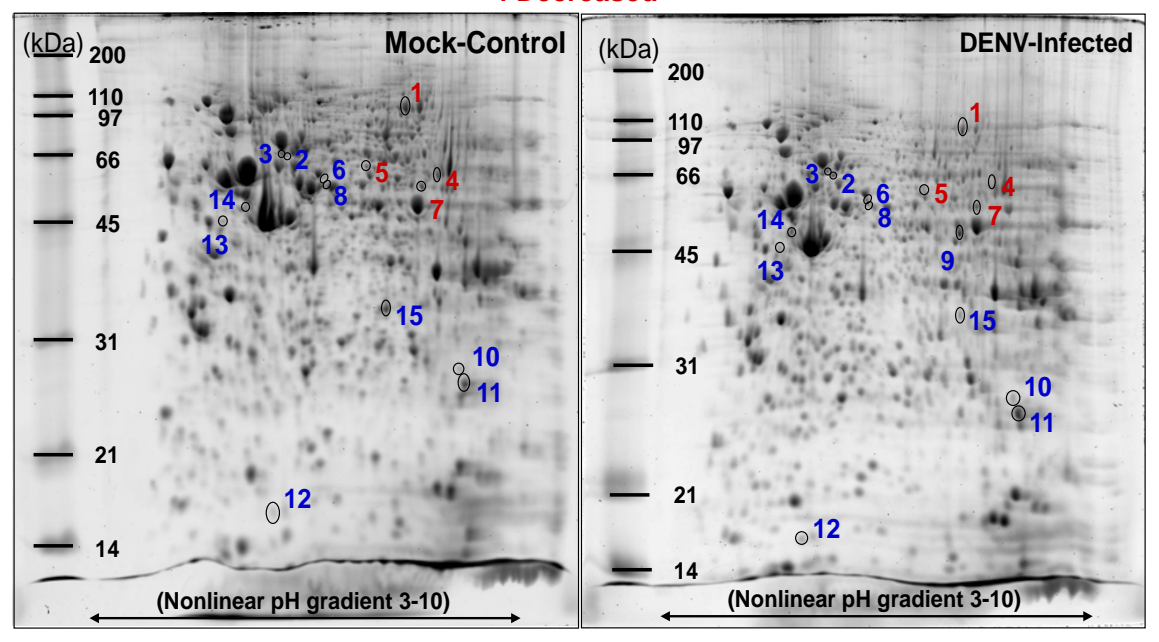


Fig. 2. The proteome map of significantly altered proteins in human endothelial cells in response to DENV infection (n = 5 gels per group derived from 5 individual culture flasks). Modified from Ref [2]. with permission from the American Chemical Society (ACS).

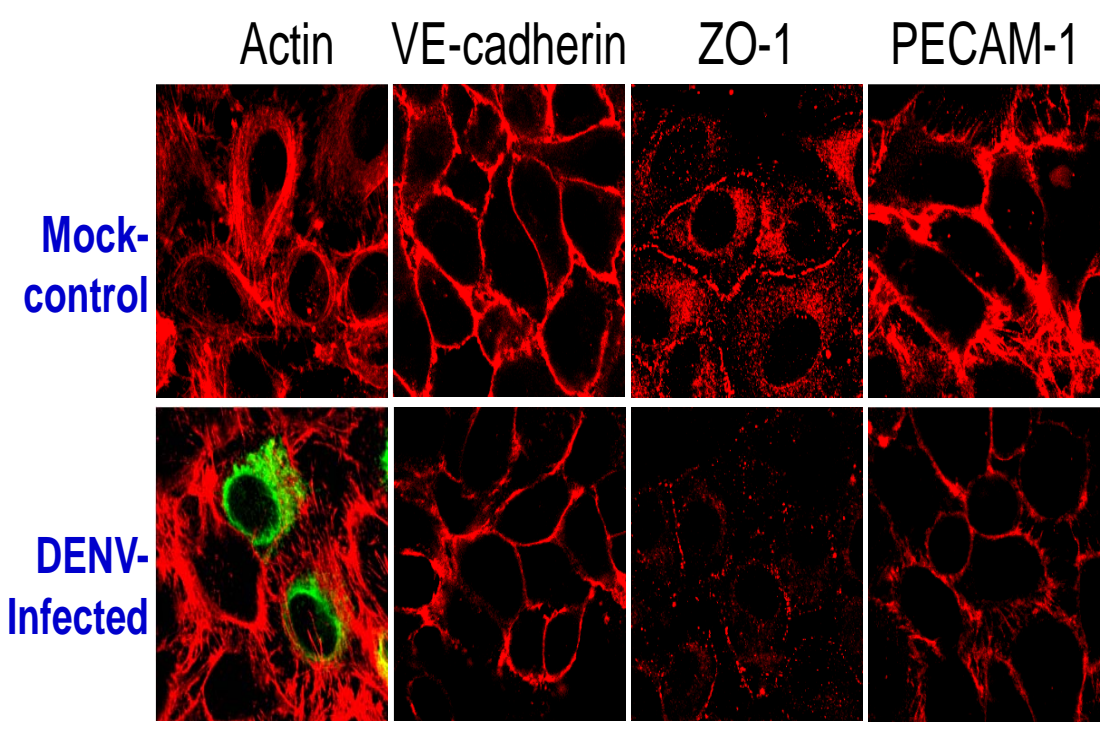


Fig. 3. Expression and organization of actin, VE-cadherin, ZO-1 and PECAM-1 upon DENV infection (showed in red, whereas DENV envelope protein is illustrated in green). Modified from Ref.[2] with permission from the American Chemical Society (ACS).

Among the 15 significantly altered proteins, level of actin was decreased. Actin plays a critical role in cellular structure and integrity of the cells, and is related to tight junction and adhesion molecules, which are crucial for controlling vascular permeability [4]. Actin cytoskeletal assembly and expression of junctional protein complex [5], which includes vascular endothelial cadherin (VE-cadherin), zonula occludens-1 (ZO-1) and plateletendothelial cell adhesion molecule-1 (PECAM-1), were then evaluated. Laser-scanning confocal microscopic examination revealed decreased expression and reorganization of actin filament in the DENV-infected cells. Moreover, the results showed markedly reduced expression of VE-cadherin, ZO-1 and PECAM-1 (Fig. 3). This is the first proteome dataset to demonstrate the

defects in cytoskeletal assembly and junctional protein complex induced by DENV infection [2].

To further address the significance of these findings, alterations in actin and junctional proteins during transendothelial migration of leukocytes, which frequently occurs in DENV infection, were investigated. The transendothelial migration event, particularly at the step of PECAM-1 engagement, was simulated by PECAM-1 cross-linking. The data showed that PECAM-1 cross-linking had the synergistic effects with DENV infection on the decreases of actin, VE-cadherin and ZO-1, strengthening the important role of transendothelial migration of leukocytes in vascular leakage observed in DHF and DSS (Fig. 4) [2].

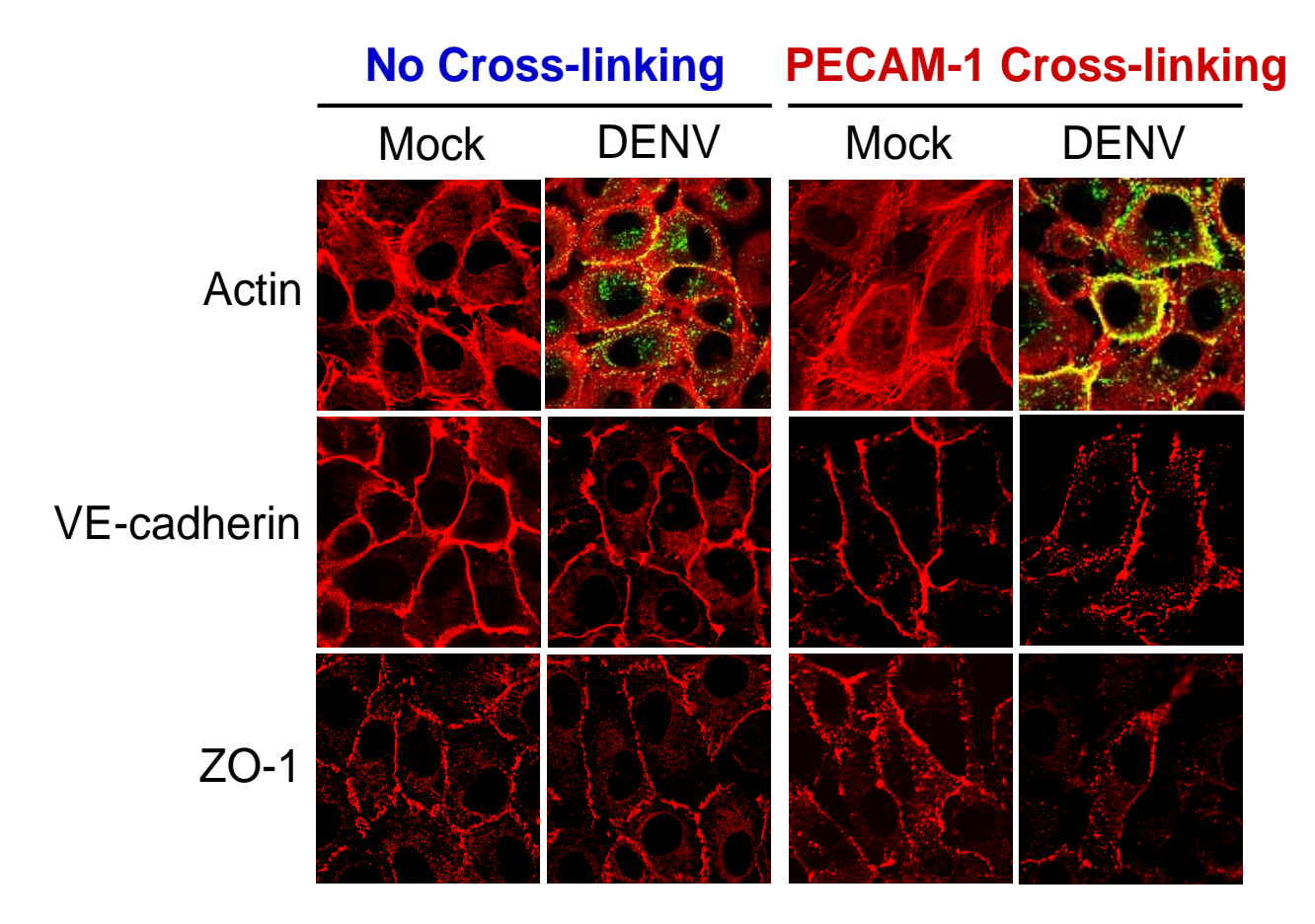


Fig. 4. Expression and organization of actin, VE-cadherin and ZO-1 (showed in red, whereas DENV envelope protein is illustrated in green) after PECAM-1 engagement. Modified from Ref.[2] with permission from the American Chemical Society (ACS).

On the other hand, five forms of heterogeneous nuclear ribonucleoproteins (hnRNPs) were increased. The functional significance of these proteins in response to DENV infection was addressed by functional proteomics study to identify hnRNPs-interacting proteins in the DENV-infected endothelial cells.

Immunoprecipitation followed by 2-D PAGE and Q-TOF MS and MS/MS analyses revealed 18 and 13 interacting partners of hnRNP C1/C2 and hnRNP K, respectively [3]. Among these interacting proteins, interestingly, vimentin was a common partner for both hnRNPs. The interaction between vimentin and these hnRNPs was confirmed by reciprocal immunoprecipitation followed by Western blot analysis. In addition, this interaction was also confirmed by double

immunofluorescence co-staining and confocal microscopic examination. Moreover, disruption of vimentin filament by sub-lethal dose of acrylamide caused dissociation of this protein complex [3].

Not only host-host but also host-virus protein-protein interactions were observed. Double immuno-fluorescence co-staining showed that vimentin was strongly associated with DENV nonstructural protein-1 (NS1). The disruption of vimentin filament by sub-lethal dose of acrylamide dissociated this host-virus protein complex and also reduced DENV NS1 protein expression. More importantly, the disruption of vimentin filament by sub-lethal dose of acrylamide markedly reduced both replication and release of DENV (Fig. 5) [3]

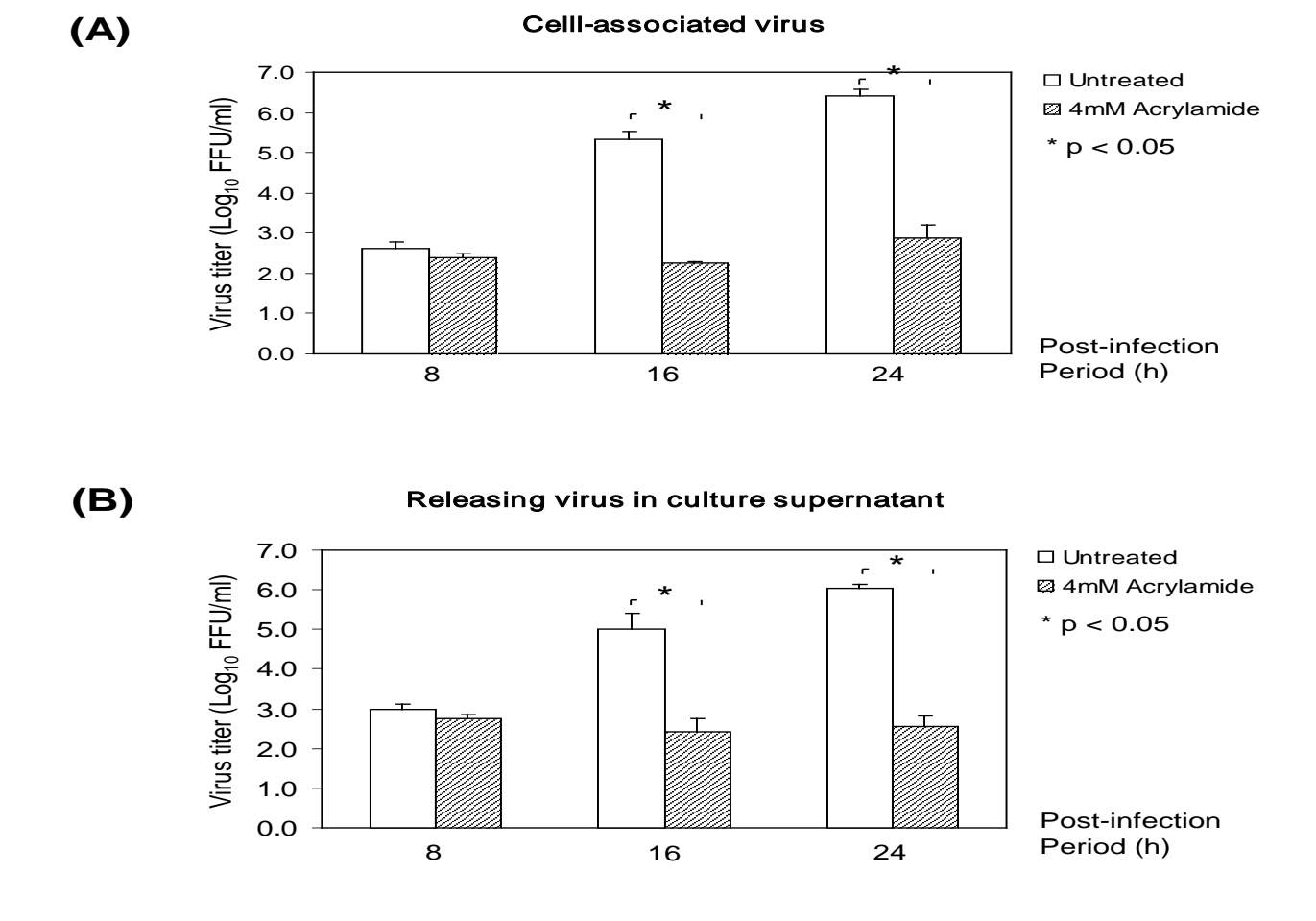


Fig. 5. Effects of vimentin disruption on DENV replication (A) and release (B). Modified from Ref.[3] with permission from the Royal Society of Chemistry (RSC).

In summary, the data obtained from this series of the study indicate that:

- DENV infection causes defects in tight junction (ZO-1), adherens junction (VE-cadherin) and adhesion molecule (PECAM-1) of human endothelial cells.
- Vimentin in human endothelial cells interacts with hnRNPs and DENV NS1 protein. These interactions are important for DENV replication and release.
- These findings provide novel insights into responses of human endothelial cells to DENV infection and better understanding of the pathogenic mechanisms of vascular leakage in DHF and DSS.

Acknowledgement

This work was supported by The Thailand Research Fund (RTA5380005), Office of the Higher Education Commission and Mahidol University under the National Research Universities Initiative. The author is also supported by "Chalermphrakiat" Grant.

References

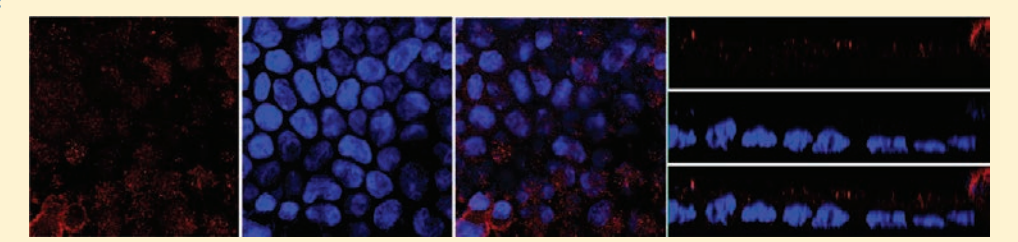
- 1. Halstead, S. B. Dengue. Lancet 2007, 370, 1644-1652.
- Kanlaya, R.; Pattanakitsakul, S. N.; Sinchaikul, S.; Chen, S. T.; Thongboonkerd, V. Alterations in actin cytoskeletal assembly and junctional protein complexes in human endothelial cells induced by dengue virus infection and mimicry of leukocyte transendothelial migration. *J Proteome. Res.* 2009, 8, 2551-2562.
- Kanlaya, R.; Pattanakitsakul, S. N.; Sinchaikul, S.; Chen, S. T.; Thongboonkerd, V. Vimentin interacts with heterogeneous nuclear ribonucleoproteins and dengue nonstructural protein 1 and is important for viral replication and release. *Mol. Biosyst.* 2010, 6, 795-806.
- Basu, A.; Chaturvedi, U. C. Vascular endothelium: the battlefield of dengue viruses. FEMS Immunol. Med. Microbiol. 2008, 53, 287-299.
- 5. Vandenbroucke, E.; Mehta, D.; Minshall, R.; Malik, A. B. Regulation of endothelial junctional permeability. *Ann. N. Y. Acad Sci* **2008**, *1123*, 134-145.



Large-scale Identification of Calcium Oxalate Monohydrate Crystal-binding Proteins on Apical Membrane of Distal Renal Tubular Epithelial Cells

Kedsarin Fong-ngern, †,† Paleerath Peerapen, †,† Supachok Sinchaikul, § Shui-Tein Chen, § and Visith Thongboonkerd $^{*,\dagger,\parallel}$

ABSTRACT:



Adhesion of calcium oxalate monohydrate (COM) crystals onto apical surface of renal tubular epithelial cells is a crucial mechanism for crystal retention, leading to kidney stone formation. Various proteins on apical membrane may bind to COM crystals; however, these crystal-binding proteins remained unidentified. The present study therefore aimed to identify COM crystal-binding proteins on apical membrane of distal renal tubular epithelial cells. Madin-Darby Canine Kidney (MDCK) cells were cultivated to be polarized epithelial cells and apical membrane was isolated from these cells using a peeling method established recently. Enrichment and purity of isolated apical membrane were confirmed by Western blot analysis for specific markers of apical (gp135) and basolateral (Na⁺/K⁺-ATPase) membranes. Proteins derived from the isolated apical membrane were then resuspended in artificial urine and incubated with COM crystals. The bound proteins were eluted, resolved by SDS-PAGE, and analyzed by Q-TOF MS and MS/MS, which identified 96 proteins. Among these, expression and localization of annexin II on apical surface of MDCK cells were confirmed by Western blot analysis, immunofluorescence staining, and laser-scanning confocal microscopic examination. Finally, the function of annexin II as the COM crystal-binding protein was successfully validated by COM crystal-binding assay. This large data set offers many opportunities for further investigations of kidney stone disease and may lead to the development of new therapeutic targets.

KEYWORDS: apical membrane, calcium oxalate, crystal adhesion, crystal-binding protein, kidney stone, nephrolithiasis, proteomics, renal tubular cells

■ INTRODUCTION

Kidney stone disease (nephrolithiasis) remains a common disease with a high recurrent rate (approximately 50% within 5–10 years and 75% within 20 years after surgical removal). The recurrent rate is even higher after the first recurrence. The initial processes of kidney stone formation include crystallization and crystal retention. The former occurs by supersaturation of ionic compounds in renal tubular fluid, whereas the latter develops thereafter by adhesion of causative crystals (mainly calcium oxalate monohydrate or COM, which is most commonly found in kidney stone matrices) onto apical or luminal surface of epithelial cells lining along renal tubules. Crystal adhesion can cause many downstream cascades of renal cellular responses. 3–6

Moreover, crystal adhesion can also enhance the adhesion of additional crystals, leading to crystal aggregation and retention inside renal tubules, and finally stone formation.^{7,8}

In many previous studies using rat models, hyperoxaluria and calcium oxalate crystalluria were induced in rats by intraperitoneal injection of sodium oxalate or oral administration of 0.75% ethylene glycol through drinking water. Their kidney tissues were then investigated under polarized light or scanning electron microscope (SEM). The results showed that many calcium oxalate crystals were initially attached on renal tubular cell surface

Received: March 17, 2011 **Published:** August 22, 2011



[†]Medical Proteomics Unit, Office for Research and Development, Faculty of Medicine Siriraj Hospital, Mahidol University, Bangkok, Thailand

[‡]Department of Immunology and Immunology Graduate Program, Faculty of Medicine Siriraj Hospital, Mahidol University, Bangkok, Thailand

[§]Institute of Biological Chemistry and Genomic Research Center, Academia Sinica, Taipei, Taiwan

Center for Research in Complex Systems Science, Mahidol University, Bangkok, Thailand

in association with microvilli. Thereafter, some of those crystals were found in the intercellular space, whereas some were internalized into the cells. ^{9,10} In a human study, kidney tissues were obtained from patients with calcium oxalate nephrolithiasis. From these, approximately 50% of the specimens had crystals adhered on renal tubular epithelial cells and some of them were seen inside the cells. These findings strengthen the crucial role of crystal adhesion in kidney stone disease.

The mechanisms underlying COM crystal adhesion on the cell surface are quite complicated. Surface charge is an important factor mediating crystal adhesion as the data obtained from previous studies revealed that COM crystals adhered to the cell surface at anionic sites and could be blocked by specific cations. 11 Adhesive property, electrostatic binding and specific interactions are also believed to be other important factors mediating crystal adhesion. During the past decade, several studies had attempted to identify surface molecules on renal tubular cells that might serve as the receptors for COM crystal adhesion with the ultimate goal to inhibit or block these bindings for disease prevention. Indeed, the apical membrane of renal tubular cells comprises various types of membrane proteins. 12 Many of these apical membrane proteins are expected to play a role in facilitating crystal-cell adhesion. However, only a small number of calcium oxalate crystal-binding proteins have been identified, including sialic acid-containing proteins,8 annexin II,13 nucleolin-related protein, 14,15 osteopontin, 16 and surface receptor CD44. 16,17 However, there should be many more calcium oxalate crystalbinding proteins, which remained unidentified.

The present study therefore aimed to identify all of potential COM crystal-binding proteins on apical membrane of distal renal tubular epithelial cells using a proteomics approach. Polarized MDCK cells were maintained and their apical membranes were isolated using a peeling method established recently. Purity of apical membrane isolation was checked and proteins were then solubilized from the purified apical membranes. After an overnight incubation with COM crystals, the unbound proteins were discarded, whereas the bound proteins were resolved with SDS-PAGE and identified by Q-TOF MS and MS/MS analyses. The proteomic data were then confirmed by Western blot analysis, immunofluorescence staining, and laser-scanning confocal microscopic examination.

■ MATERIALS AND METHODS

Cultivation and Polarization

MDCK cells were grown in Eagle's minimum essential medium (MEM) (GIBCO, Invitrogen Corporation; Grand Island, NY) supplemented with 10% fetal bovine serum (FBS), 1.2% penicillinG/streptomycin and 2 mM L-glutamine and maintained in a humidified incubator with 5% CO₂ at 37 °C. For polarization, MDCK cells at a density of approximately 5.0–7.5 \times 10⁴cells/mL were seeded and grown on prewetted collagen-coated permeable polycarbonate membrane in Transwells (0.4 μ m pore size; Corstar; Cambridge, MA) for four days. The culture medium was refreshed every other day. Polarization was confirmed by immunofluorescence staining and laser-scanning confocal microscopy (described with more details below).

Isolation of Apical Membrane and Solubilization of Apical Membrane Proteins

Apical membrane of the polarized MDCK cells was isolated by a peeling method established recently. ¹⁸ Briefly, after the cells were maintained in Transwells for four days, the culture medium

was removed and the polarized cells were rinsed twice with icecold membrane preserving buffer (1 mM MgCl₂ and 0.1 mM CaCl₂ in PBS). Thereafter, Whatman filter paper (0.18-mmthick, Whatman International Ltd.; Maidstone, U.K.) prewetted with deionized water was placed onto the polarized cell monolayer. After a 5-min incubation period, the filter paper was peeled out and the apical membranes retained at the filter paper surface were harvested by rehydration in deionized water and gentle scrapping. The apical membrane-enriched fraction was then lyophilized. Dried apical membrane was solubilized in 1× Laemmli's buffer and then dialyzed against deionized water at 4 °C overnight with three changes of deionized water. After lyophilization, apical membrane protein powder was stored at -80 °C until used. Enrichment and purity of isolated apical membrane were confirmed by Western blot analysis for specific markers of apical (gp135) and basolateral (Na⁺/K⁺-ATPase) membranes (described with more details below).

Preparation of COM Crystals

COM crystals were prepared as previously described. Briefly, 10 mM calcium chloride dihydrate ($CaCl_2 \cdot 2H_2O$) was mixed with 10 mM sodium oxalate ($Na_2C_2O_4$) in Tris buffer containing 90 mM NaCl (pH 7.4) to make their final concentrations to 5 mM and 0.5 mM, respectively. The mixture was incubated at 25 °C overnight and COM crystals were harvested by a centrifugation at 3000 rpm for 5 min. Supernatant was discarded and the crystals were resuspended in methanol. After another centrifugation at 3000 rpm for 5 min, methanol was discarded and the crystals were dried at 37 °C overnight.

COM Crystal Adhesion and Separation of COM Crystal-Binding Proteins

Apical membrane protein powder was resuspended into 1 mL protein-free artificial urine (containing 5 mM CaCl₂, 200 mM urea, 4 mM creatinine, 5 mM Na₃C₆H₅O₇·2H₂O, 54 mM NaCl, 30 mM KCl, 15 mM NH₄Cl, 2 mM MgSO₄·7H₂O, and 9 mM Na_2SO_4 ; pH = 6.2 and osmolality = 446 mOsm/kg).²⁰ Thereafter, 5 mg COM crystals were added and apical membrane proteins were allowed to interact with COM crystals in the artificial urine on a continuous rotator at 4 °C overnight. The crystal-protein complexes were then collected by a centrifugation at 3000 rpm for 5 min at 4 °C and the unbound proteins were discarded. Thereafter, the crystal-protein complexes were washed three times with PBS and other three times with 4 mM EDTA in PBS. After the final wash with PBS, COM crystal-binding proteins were eluted by 1× Laemmli's buffer and separated in 12% SDS-PAGE gel. The resolved COM crystal-binding proteins were visualized by Coomassie Brilliant Blue G-250 stain. All the procedures in this step are summarized in Figure 1.

In-Gel Tryptic Digestion

A total of 40 gel slices were excised from the whole lane of COM crystal-binding proteins in a preparative gel derived from 6×10^7 cells. The excised gel slices were washed twice with 200 μ L of 50% acetonitrile (ACN)/25 mM NH₄HCO₃ buffer (pH 8.0) at room temperature for 15 min, and then washed once with 200 μ L of 100% ACN. After washing, the solvent was removed and the gel pieces were dried by a SpeedVac concentrator (Savant; Holbrook, NY). The dried gel plugs were then rehydrated with 10 μ L of 1% (w/v) trypsin (Promega; Madison, WI) in 25 mM NH₄HCO₃. After rehydration, the gel pieces were crushed with siliconized blue stick and incubated at 37 °C for at least 16 h. Peptides were subsequently extracted twice with 50 μ L

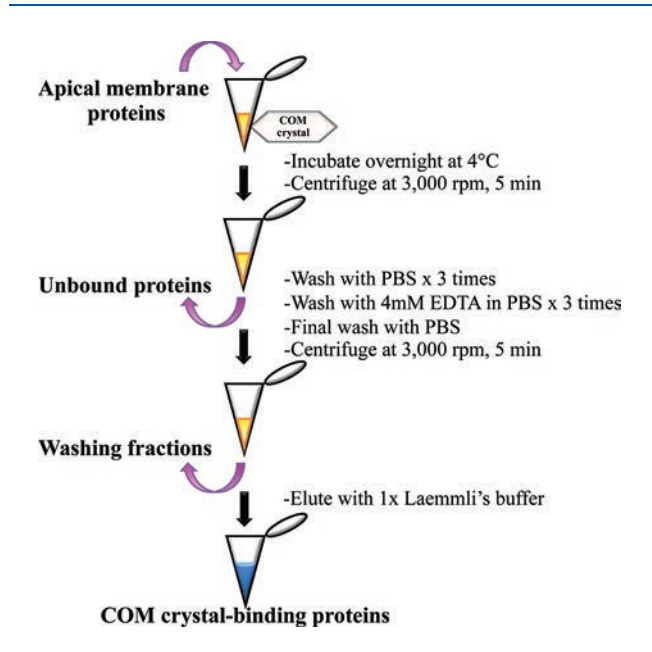


Figure 1. Schematic summary of methodologies to prepare COM crystal-binding proteins. Apical membrane proteins were incubated with COM crystals overnight at 4 $^{\circ}$ C. After centrifugation, unbound proteins were excluded and the remaining COM crystal-binding proteins were vigorously washed with PBS and 4 mM EDTA. Finally, COM crystal-binding proteins were eluted with $1\times$ Laemmli's buffer.

of 50% ACN/5% trifluoroacetic acid (TFA); the extracted solutions were then combined and dried with the SpeedVac concentrator. The peptide pellets were resuspended with 10 μ L of 0.1% TFA and purified using ZipTip_{C18} (Millipore; Bedford, MA). The peptide solution was drawn up and down in the ZipTip_{C18} 10 times and then washed with 10 μ L of 0.1% formic acid by drawing up and expelling the washing solution three times. The peptides were finally eluted with 5 μ L of 75% ACN/0.1% formic acid.

Quadrupole Time-of-Flight Mass Spectrometry and Tandem Mass Spectrometry (Q-TOF MS and MS/MS)

The trypsinized samples were premixed 1:1 with the matrix solution containing 5 mg/mL α-cyano-4-hydroxycinnamic acid in 50% ACN, 0.1% (v/v) TFA and 2% (w/v) ammonium citrate, and deposited onto the 96-well MALDI (matrix-assisted laser desorption/ionization) target plate. The samples were analyzed by Q-TOF Ultima mass spectrometer (Micromass; Manchester, U.K.), which was fully automated with predefined probe motion pattern and the peak intensity threshold for switching over from MS survey scanning to MS/MS, and from one MS/MS to another. Within each sample well, parent ions that met the predefined criteria (any peak within the m/z 800–3000 range with intensity above 10 count ± include/exclude list) were selected for CID MS/MS using argon as the collision gas and a mass dependent ± 5 V rolling collision energy until the end of the probe pattern was reached. The instrument was externally calibrated to less than 5 ppm accuracy over the mass range of m/z 800–3000 using a sodium iodide and PEG 200, 600, 1000, and 2000 mixtures and further adjusted with Glu-Fibrinopeptide B as the near-point lock mass calibrant during data processing. At a laser firing rate of 10 Hz, individual spectra from 5 s integration period acquired for each of the MS survey and MS/MS performed were combined, smoothed, deisotoped (fast option) and centroided using the Micromass ProteinLynxT Global Server (PGS) 2.0 data processing software. The procedure was processed according to the instruction of Micromass data processing software. The combined peptide mass fingerprinting (PMF) and MS/MS ion meta data were searched in concert against the specified protein database within the PGS 2.0 workflow. Additionally, the MS and MS/MS ions data were extracted and outputted as MASCOT-searchable .txt and .pkl files for independent searches using the publicly available MASCOT search engine (http://www.matrixscience.com) to query to the NCBI mammalian protein database, assuming that peptides were monoisotopic. Fixed modification was carbamidomethylation at cysteine residues, whereas variable modification was oxidation at methionine residues. Only one missed trypsin cleavage was allowed, and peptide mass tolerances of 100 and 50 ppm were allowed for PMF and MS/MS ions search, respectively.

Western Blot Analysis

To evaluate the yield and purity of enrichment or isolation of apical membrane, Western blot analysis for specific markers of apical (gp135) and basolateral (Na+/K+-ATPase) membranes was performed. Proteins derived from whole cell lysate and purified apical membrane (with an equal amount of 20 μ g) were resolved in 12% SDS-PAGE and then transferred onto a nitrocellulose membrane (Whatman; Dassel, Germany) using a semidry transfer apparatus (Bio-Rad; Milano, Italy) at 75 mA for 1-h. Nonspecific bindings were blocked with 5% skim milk in PBS at room temperature for 1-h. The membrane was then incubated with rabbit polyclonal anti-gp135 (Santa Cruz Biotechnology; Santa Cruz, CA) (1:200 in 5% skim milk/PBS) or mouse monoclonal anti-Na⁺/K⁺-ATPase-α1 subunit (Santa Cruz Biotechnology) (1:1000 in 5% skim milk/PBS) at 4 °C overnight. Thereafter, the membrane was washed three times with PBS and further incubated with respective secondary antibody conjugated with horseradish peroxidase (1:2000 in 5% skim milk/PBS) at room temperature for 1 h. The immunoreactive bands were then visualized by SuperSignal West Pico chemiluminescence substrate (Pierce Biotechnology, Inc.; Rockford, IL) and autoradiography.

To confirm the presence of annexin II in apical membrane and COM crystal-binding fractions, an equal amount (20 μ g) of proteins derived from whole cell lysate, purified apical membrane, and COM-binding fraction was loaded in each lane and resolved by 12% SDS-PAGE. Western blot analysis was performed as aforementioned using goat polyclonal antiannexin II (Santa Cruz Biotechnology) (1:1000 in 5% skim milk/PBS) as the primary antibody.

Immunofluorescence Staining and Laser-Scanning Confocal Microscopy

To confirm polarization of MDCK cells, the polarized MDCK monolayer was washed with membrane preserving buffer (1 mM MgCl₂ and 0.1 mM CaCl₂ in PBS), and then fixed with 3.7% formaldehyde in PBS at 25 °C for 10 min and permeabilized with 0.1% Triton X-100 at 25 °C for 10 min. After extensive washing with membrane preserving buffer, MDCK cells were incubated with mouse monoclonal antibody against zonula occludens-1 (ZO-1) (tight junction marker) (Invitrogen/Molecular Probes; Camarillo, CA), mouse monoclonal anti-Na $^+/K^+$ -ATPase- α 1 subunit (basolateral membrane marker) (Santa Cruz Biotechnology), or rabbit polyclonal anti-gp135 (apical membrane marker) (Santa Cruz Biotechnology) (all with a dilution of 1:50 in 1% BSA/PBS) at 37 °C for 1 h. The cells were then rinsed with PBS three times and then incubated with respective secondary antibody conjugated

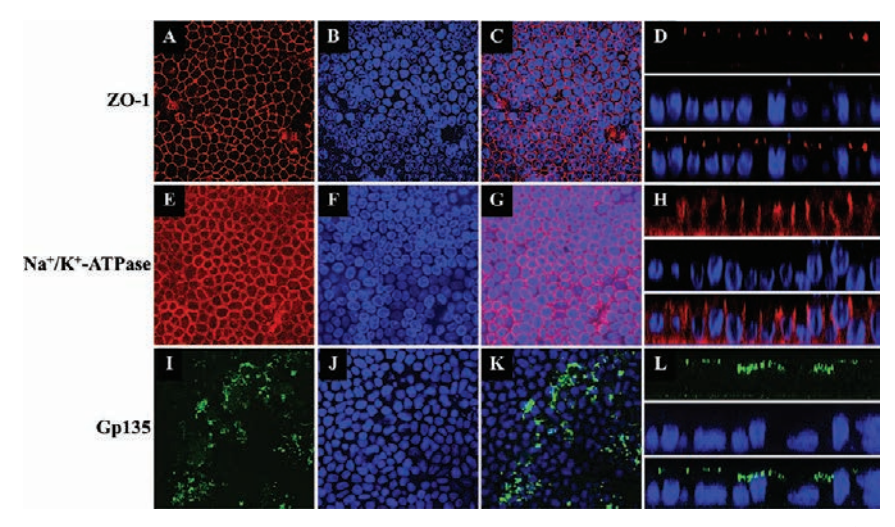


Figure 2. Confirmation of polarization of MDCK cells. Immunofluorescence study was performed to stain markers for (A-D) tight junction (ZO-1), (E-H) basolateral membrane $(Na^+/K^+$ -ATPase α -subunit), and (I-L) apical membrane (gp135). These markers were then visualized and images were taken by laser-scanning confocal microscopy in both horizontal (the first three columns) and sagittal (the last column; panels D, H and L) views. Expression of ZO-1 and Na^+/K^+ -ATPase is shown in red, whereas that of gp135 is in green. Blue illustrates nuclei stained with Hoechst dye. Original magnification powers were $400\times$ in the first three columns and $630\times$ in the last column (D, H and L).

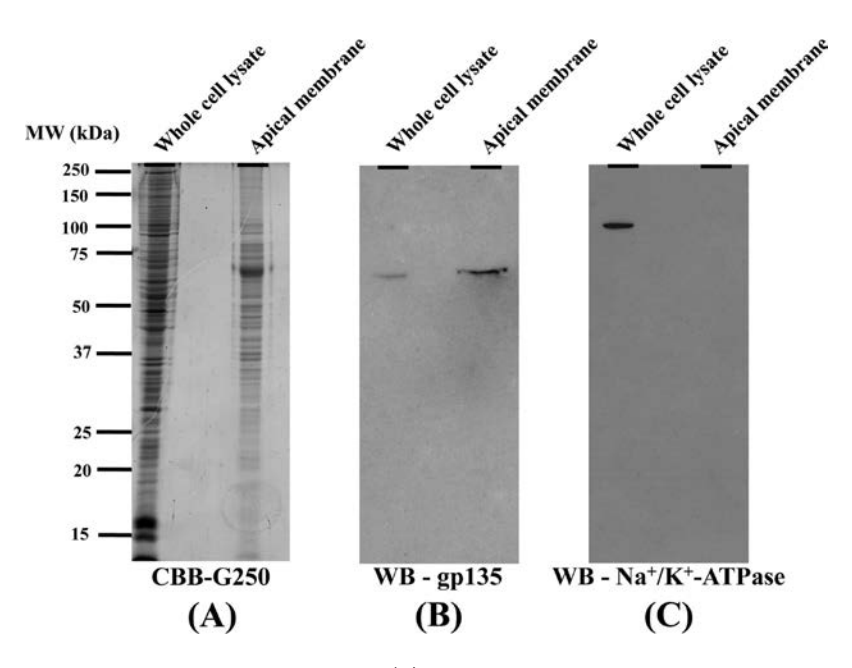


Figure 3. Yield of enrichment and purity of apical membrane isolation. (A) In total, $20 \mu g$ of proteins derived from MDCK whole cell lysate and isolated apical membrane were resolved by 12% SDS-PAGE and visualized by Coomassie Brilliant Blue G-250 stain. The resolved proteins were then transferred onto a nitrocellulose membrane and subjected to Western blot analysis using (B) rabbit polyclonal anti-gp135 (apical membrane marker) or (C) mouse monoclonal anti-Na $^+$ /K $^+$ -ATPase- α 1 subunit (basolateral membrane marker).

with rhodamine or AlexaFluor-488 (Invitrogen/Molecular Probes) (1:5000 in 1% BSA/PBS) containing 0.1 μ g/mL Hoechst dye (DNA staining for nuclear localization) (Invitrogen/Molecular Probes) at 37 °C for 1 h. Thereafter, the cells were examined by a laser-scanning confocal microscope equipped with an LSM5 Image Browser (LSM 510 Meta, Carl Zeiss; Jena, Germany).

To confirm the apical surface expression of annexin II, polarized MDCK cells were rinsed with membrane preserving buffer and then fixed with 3.7% formaldehyde in PBS at 25 °C for 15 min. After extensive washing with membrane preserving buffer, MDCK cells were incubated with goat polyclonal antiannexin II (Santa Cruz Biotechnology) (1:50 in 1% BSA/PBS) at 37 °C for 1 h.

The cells were then rinsed with PBS three times and then incubated with rhodamine-conjugated antigoat IgG antibody (Invitrogen/Molecular Probes) (1:5000 in 1% BSA/PBS) containing $0.1\,\mu\text{g/mL}$ Hoechst dye (Invitrogen/Molecular Probes) at 37 °C for 1 h. Thereafter, the cells were examined by a laser-scanning confocal microscope equipped with an LSMS Image Browser (LSM 510 Meta, Carl Zeiss; Jena, Germany).

COM Crystal-Binding Assay

This set of experiments was performed in cell culture incubator at 37 °C with 5% CO₂. After MDCK cells were confluent, culture medium was removed and the cells were rinsed twice with

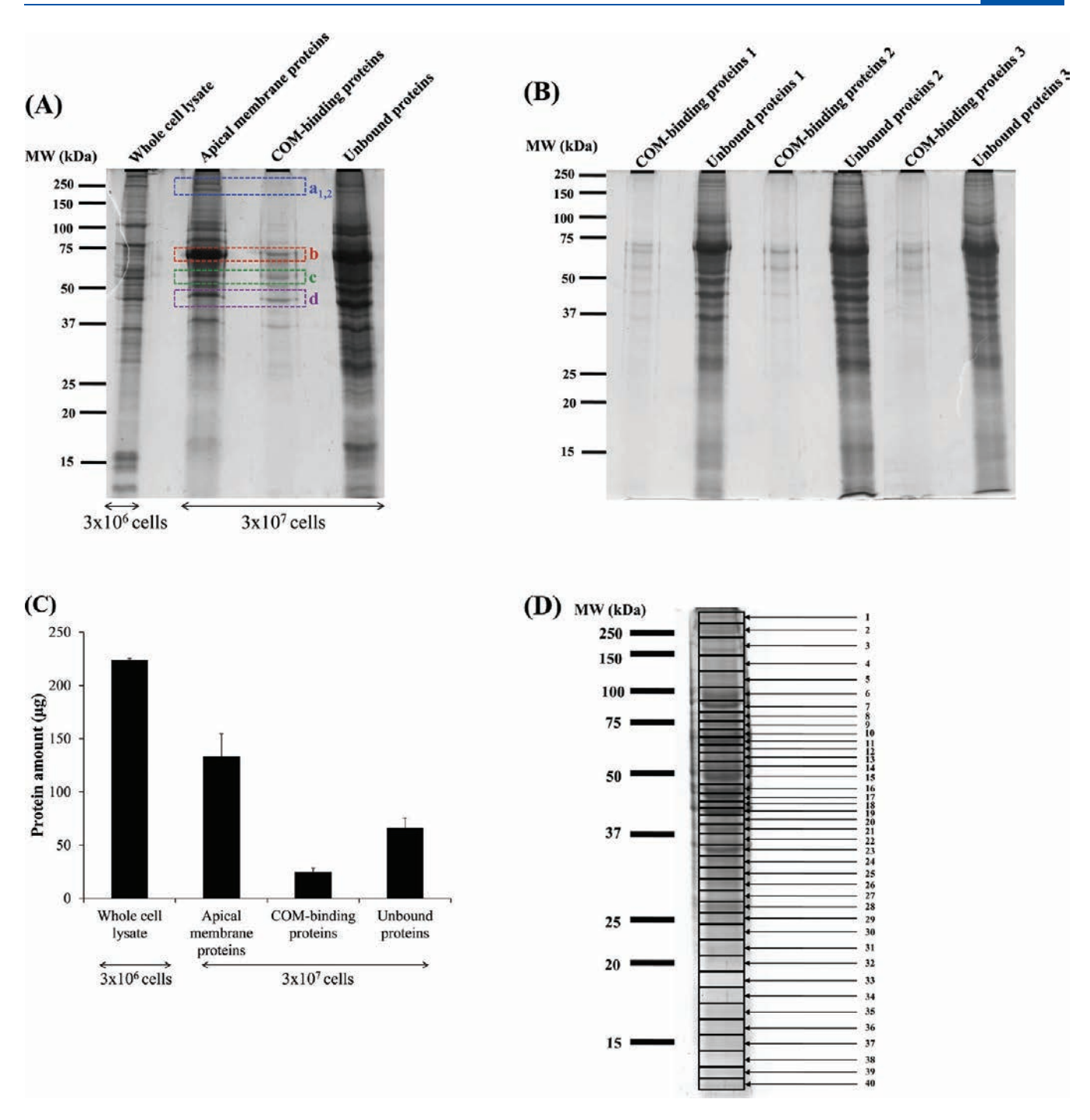


Figure 4. Isolation of COM crystal-binding proteins from apical membrane of polarized renal tubular epithelial cells. (A) COM crystal-binding proteins derived from 3×10^7 cells obtained from methodologies detailed in Figure 1 were resolved in 12% SDS-PAGE gel compared to purified apical membrane proteins and the unbound proteins derived from 3×10^7 cells, as well as whole cell lysate derived from 3×10^6 cells. The highlighted bands a, b, c, and d illustrate the selectivity of COM crystal binding of the COM crystal-binding proteins, as compared to the starting apical membrane fraction. (B) Reproducibility of isolation of COM crystal-binding proteins was confirmed in additional three independent experiments. (C) Amount of proteins derived from each fraction was quantitated. (D) COM crystal-binding proteins derived from 6×10^7 cells were resolved in a preparative gel. A total of 40 gel slices were excised and identified by Q-TOF MS and MS/MS (see also Table 1).

membrane preserving buffer. Nonspecific bindings were then blocked with 1% BSA in membrane preserving buffer for 15 min. Thereafter, the blocking solution was discarded and the cells were washed with membrane preserving buffer four times. MEM supplemented with 10% FBS was then added to the cells without (control) or with 0.2 μ g/mL goat polyclonal antiannexin II

(Santa Cruz Biotechnology) or goat IgG (nonspecific antibody) (Santa Cruz Biotechnology) for 30 min. Thereafter, the cells were rinsed with membrane preserving buffer four times and further incubated with COM crystals (100 μ g/mL in MEM supplemented with 10% FBS) for 1 h. The unbound crystals were then removed by rigorous wash five times with PBS.

Journal of Proteome Research

Table 1. Summary of COM Crystal-Binding Proteins Derived from Isolated Apical Membranes Identified by Q-TOF MS and/or MS/MS Analyses^a

		٥		1		•			
band no.	protein name	NCBI ID	identified by	identification scores (MS, MS/MS)	%cov (MS, MS/MS)	no. of matched peptides (MS, MS/MS)	pI M	MW (kDa)	BLAST link report ^b
1	Microtubule-actin	gi 194207660 MS	MS	96, NA	8, NA	34, NA	5.20	673.37	
	cross-linking factor 1 isoform 1								
1	Man1a2-prov protein	gi 149633134	MS	73, NA	25, NA	10, NA	6.55	53.52	
7	Protein C9orf55	gi 73971036	MS	78, NA	11, NA	15, NA	6.11 2	212.96	DENN/MADD domain containing 4C
	isoform 1								isoform 1
7	Spectrin, beta, nonerythrocytic	gi 109102947	MS	72, NA	12, NA	20, NA	5.34	251.96	
	1 isoform 2								
8	Hypothetical protein	gi 114576746	MS	72, NA	22, NA	14, NA	9.53	109.76	
	isoform 2								
3	Membrane protein, palmitoylated	gi 73963296	MS	56, NA	18, NA	10, NA	5.80	77.47	
	5 isoform 1								
4	Hypothetical protein	gi 149632550	MS	82, NA	24, NA	10, NA	5.76	80.98	Temporarily Assigned Gene name family member (tag-278) isoform 7
4	Adenylosuccinate lyase 1	gi 126338737	MS	75, NA	30, NA	10, NA	8.49	56.824	0
4	Glutamate receptor 3 isoform	gi 74008280	MS	50, NA	17, NA	12, NA	8.77	101.74	
	flip precursor isoform 2								
s	Dedicator of cytokinesis protein	gi 109463063 MS	MS	71, NA	16, NA	17, NA	6.40	183.48	
	1 (180 kDa protein downstream								
	of CRK) (DOCK180) isoform 1								
S	Plasma membrane calcium	gi 73984626	MS	67, NA	15, NA	13, NA	5.75	132.79	
	ATPase 2 isoform b isoform 6								
S	Hypothetical protein XP_539070	gi 73973961	MS	66, NA	22, NA	12, NA	5.33	95.16	BEN domain-containing protein 3
S	Ephrin type-B receptor 1	gi 194663612	MS	71, NA	14, NA	12, NA	6.34	109.10	
	precursor (Tyrosine-								
	protein kinase receptor								
	EPH-2) (NET) (HEK6) (ELK)								
9	Alpha-actinin 4	gi 126329095 MS	MS	105, NA	20, NA	16, NA	5.12	104.98	
9	Centrobin (LYST-interacting	gi 149438417	MS	74, NA	26, NA	10, NA	5.99	47.25	
	protein 8), partial								
9	Acyl-CoA thioesterase 9	gi 31980998	MS	77, NA	29, NA	11, NA	8.74	50.81	
7	Heat shock protein 1,	gi 73964029	MS, MS/MS	135, 219	35, 9	17,4	5.15	71.04	
	alpha isoform 3								
7	Hypothetical protein	gi 6807647	MS	183, NA	35, NA	21, NA	5.26	85.19	Heat shock protein
1	rCG43497. isoform	MS 6626901110	MS	NA 741	34. NA	17.NA	4 79	69 22.	rist 90-beta Heat shock motein HSP 90-
	CRA_a	12,000,11		Y7NT () L T	47×1 (1-0	4791(/1	Ì	77:	alpha (HSP 86) isoform 2

Heat shock 70 kDa protein 8 Four and a half LIM domains containing 4C isoform 1 containing 4C isoform 1 BLAST link report DENN/MADD domain DENN/MADD domain protein 1 isoform 6 MW (kDa) 212.96 66.33 48.62 143.14 68.89 212.96 47.83 222.12 20.98 32.76 50.81 32.63 47.54 153.03 183.46 52.84 237.27 64.01 248.71 NA 6.16 6.11 8.74 5.06 5.42 9.33 5.47 6.53 4.64 8.08 5.53 8.54 9.04 5.70 5.08 6.71 9.32 6.11 I^{d} ΝA peptides (MS, MS/MS) no. of matched NA, NA 15, NA 17, NA 14, NA 17, NA 17, NA 12, NA 20, NA 16, NA 10, NA 13, NA 12, NA 20, NA 20, NA NA, 2 8, NA 8, NA 8, NA 16,1 15,2 (MS, MS/MS) NA, NA 11, NA 10, NA 39, NA 36, NA 25, NA 17, NA 11, NA 15, NA 26, NA 37, NA 12, NA 17, NA 33, NA 13, NA 35, NA 50, NA NA,4 34,5 34,2 scores (MS, MS/MS) identification 100, NA NA, NA 145, NA 102, 58 117,58 45, NA 95, NA 58, NA NA, 87 86, NA 76, NA 79, NA 73, NA 72, NA 82, NA 74, NA 89, NA 57, NA MS, MS/MS MS, MS/MS identified by MS/MS MS MS MS MS NA MS gi|114644159 gi|157820041 gi|114584353 gi|259017317 gi|149041392 gi|148688105 gi|109069453 gi|73948972 gi|73968068 gi|73945732 gi|31980998 gi|73954621 gi|74000359 gi|73971036 gi|73951984 gi|73972128 gi|62088966 gi|73985236 gi|73971036 NCBI ID ΝA Adenomatous polyposis coli protein Ezrin (p81) (Cytovillin) (Villin-2) Hypothetical protein LOC302773 Heat shock protein 8 isoform 3 protein precursor (GRP 78) Immunoglobulin heavy chain rCG57965, isoform CRA b protein grp78) isoform 4 protein name (APC protein) isoform 1 lumenal Ca(2+) binding Retinoblastoma-associated Protein C9orf55 isoform 1 Protein C9orf55 isoform 1 (Endoplasmic reticulum 78 kDa glucose-regulated Golgi autoantigen, golgin binding protein) (BiP) Acyl-CoA thioesterase 9 protein 140 isoform 4 subfamily a, 4 variant MHC class I antigen Flotillin-1 isoform 2 Vimentin isoform 9 Talin 2 isoform 5 RAB5B protein Tubulin, beta 2 Crocc protein Table 1. Continued mCG142584 Unidentified isoform 3 band no. 10 Ξ Ξ 12 12 12 13 14 14 14 15 15 ^1 00 **% 6**

Tumor necrosis factor type 1 receptor associated protein BLAST link report MW (kDa) 43.23 74.10 35.71 25.83 11.08 41.34 78.58 216.84 457.18 532.76 55.66 117.41 19.90 32.86 10.25 40.94 36.20 50.81 32.45 20.26 36.07 5.56 5.80 5.78 6.03 5.23 5.33 99.9 6.27 8.74 7.74 5.93 8.20 8.88 9.40 5.90 8.62 9.43 9.45 5.71 I^{d} peptides (MS, MS/MS) no. of matched 20, NA 16, NA 10, NA 19, NA 25, NA 31, NA 10, NA 10, NA 10, NA 15, NA 11,NA 11, NA 7, NA 6, NA 8, NA 5, NA 8, NA 6, NA 12, 4 13, 1 9,4 (MS, MS/MS) 13, NA 10, NA 37, NA 63, NA 60, NA 41, NA 28, NA 21, NA 56, NA 37, NA 38, NA 13, NA 37, NA 29, NA 25, NA 43, NA 39, 15 42, 13 9, NA 9, NA scores (MS, MS/MS) 56, NA 73, NA 69, 166 87, NA 84, NA 77, NA 71, NA 84, NA 82, NA 75, NA 88, NA 77, NA 71, NA 73, NA 73, NA 80, NA 72, NA 96, 108 70, NA 59, NA gi|118419975 MS, MS/MS MS, MS/MS MS, MS/MS identified by MS MS MSMS MS gi|148676944 MS MS MS MS MS MS gi|109103632 MS MS MS MS MS MS gi|162951862 gi|119609671 gi|112700066 gi|149641845 gi|119597993 gi|109093687 gi|73973081 g|31980998 gi|23271726 gi|50978862 gi|73956740 gi|73952378 gi|73953205 gi|4210492 NCBI ID gi|3126874 gi|6467990 19998891 gi|809561 (NNE) (Enolase 1) (Phosphopyruvate hydratase) (C-myc promoter-binding Dynein heavy chain at 16F CG7092-PA Alpha enolase (2-phospho-D-glycerate F-box and WD-40 domain protein 10 Unknown (protein for MGC:38398) hydro-lyase) (Non-neural enolase) Mitochondrial uncoupling protein 4 MIF4G domain containing, isoform S100 calcium binding protein, zeta PDZ domain actin binding protein Dynein, axonemal, heavy chain 5, (Plasminogen-binding protein) (UCP 4) (Solute carrier family (Vascular anticoagulant-beta) Dynamin-like protein Dymple protein) (MBP-1) (MPB-1) Immunoglobulin heavy chain Glyceraldehyde-3-phosphate Annexin A8 (Annexin VIII) protein name Acyl-CoA thioesterase 9 (VAC-beta) isoform 3 MHC class II antigen Hypothetical protein Hypothetical protein isoform CRA a 25, member 27) dehydrogenase variable region ART5 protein Gamma-actin Table 1. Continued isoform 14 Annexin A2 Beta-actin isoform band no. 16 16 16 17 18 18 19 19 19 20 20 21 22 23 24 25 26 26 21

Table 1.	Table 1. Continued								
band no.	protein name	NCBIID	identified by	identification scores (MS, MS/MS)	%cov (MS, MS/MS)	no. of matched peptides (MS, MS/MS)	Id	MW (kDa)	BLAST link report^b
26	Hypothetical protein	gi 149254381	MS	78, NA	36, NA	8, NA	9.90	31.55	
26	Hypothetical protein isoform 2	gi 114576746	MS	72, NA	27, NA	13, NA	9.53	109.76	
26	Protein C9orf55 isoform 1	gi 73971036	MS	67, NA	8, NA	12, NA	6.11	212.96	DENN/MADD domain containing 4C isoform 1
27	Unidentified	NA	NA	NA, NA	NA, NA	NA, NA	NA	NA	
28	Phosphoglycerate mutase 1 (Phosphoglycerate mutase isozyme B) (PGAM-B) (BPG-	gi 73998120	MS, MS/MS	86, 137	42, 9	10,2	5.93	26.00	
	dependent PGAM 1) isoform 2	<u>.</u>		į		,	,	;	
78	Protein C9orf55 isoform 1	gi 73971036	MS	90, NA	10, NA	14, NA	6.11	212.96	DENN/MADD domain containing 4C isoform 1
28	Unnamed protein product	gi 194379894	MS	71, NA	26, NA	8,NA	4.42	21.66	Synapse-associated protein 1
29	Triosephosphate isomerase (TIM) (Triose-phosphate isomerase) isoform 5	gi 73997316	MS, MS/MS	122, 59	61, 9	11,1	8.29	23.18	
29	Hypothetical protein	gi 149638196 MS	MS	73, NA	24, NA	10, NA	4.81	54.40	Androgen receptor associated protein 54
29	256 kD golgin	gi 1236759	MS	75, NA	12, NA	23, NA	5.34	256.67	
29	MTAI	gi 126290061	MS	73, NA	20, NA	14, NA	9.36	85.80	
29	MHC class II antigen	gi 186703093	MS	105, NA	80, NA	7, NA	5.80	10.02	
29	Hypothetical protein isoform 2	gi 114576746	MS	87, NA	22, NA	15, NA	9.53	109.76	
30	Heterogeneous nuclear ribonucle	gi 112421201	MS	83, NA	35, NA	12, NA	9.50	34.31	
	oprotein A1								
30	mCG117968	gi 148682805	MS	72, NA	29, NA	11, NA	9.44	34.02	
30	Protein C9orf55 isoform 1	gi 73971036	MS	66, NA	12, NA	16, NA	6.11	212.96	DENN/MADD domain
31	Peroxiredoxin 2 (Thioredoxin	gi 73986497	MS	60, NA	38, NA	6, NA	5.23	22.11	containing 4C isoform 1
	peroxidase 1) (Thioredoxin-								
	dependent peroxide reductase 1) (Thiol-specific antioxidant protein)								
	(TSA) (PRP) (Natural killer								
	cell enhancing factor B)								
	(NKEF-B) isoform 1								
31	mCG1051031	gi 148691331 MS	MS	71, NA	26, NA	8, NA	99.9	31.33	MHC class I antigen
32	Hypothetical protein	gi 149258923	MS	75, NA	68, NA	6,NA	11.92	8.81	
32	Isopentenyl-diphosphate delta	gi 109505998	MS	77, NA	32, NA	6, NA	8.53	17.68	
	isomerase 2								
33	Unidentified	NA	NA	NA, NA	NA, NA	NA, NA	NA	NA	

Table 1. Continued

Table 1.	Table 1. Continued		•	•		,			
			identified	identification	%cov	no. of matched			BLAST link
band no.	protein name	NCBI ID	by	scores (MS, MS/MS)	(MS, MS/MS)	peptides (MS, MS/MS)	I^{d}	MW (kDa)	report^b
34	Adenylosuccinate lyase 1	gi 126338737 MS	MS	77, NA	25, NA	9, NA	8.49	56.82	
35	Sulfotransferase family, cytosolic,	gi 71896574 MS	MS	79, NA	39, NA	11, NA	8.17	34.96	
	1C, member 2								
35	Glucosamine-6-phosphate deaminase	gi 73974964 MS	MS	65, NA	30, NA	9, NA	6.41	31.35	
	2 isoform 1								
35	MHC class II antigen	gi 186703093 MS	MS	74, NA	80,NA	5, NA	5.80	10.02	
36	Peptidylprolyl isomerase A	gi 28189771	MS, MS/MS	83, 57	66, 20	10, 2	8.46	17.09	
	(cyclophilin A)								
36	TRIMCyp	gi 76576111	MS	70, NA	54, NA	8, NA	8.26	18.19	
36	Vav-3 protein	gi 73959967	MS	66, NA	20, NA	13, NA	6.22	96.55	
36	Acyl-CoA thioesterase 9	gi 31980998	MS	74, NA	26, NA	10, NA	8.74	50.81	
36	Peptidyl-Pro cis trans isomerase	gi 119902257 MS	MS	73, NA	50, NA	7, NA	7.68	18.06	
	isoform 1								
37	rCG21715	gi 149063079 MS	MS	90, NA	32, NA	9, NA	11.98	26.54	
37	Leucine rich repeat containing 42	gi 73956299 MS	MS	65, NA	19, NA	6, NA	8.49	52.34	
	isoform 1								
38	Nestin	gi 2209202	MS	74, NA	70, NA	S,NA	8.50	6.56	
39	Acyl-CoA thioesterase 9	gi 31980998	MS	74, NA	25, NA	10,NA	8.74	50.81	
39	Hypothetical protein isoform 2	gi 114576746 MS	MS	74, NA	19, NA	13,NA	9.53	109.76	
40	Rims2 protein	gi 111600267 MS	MS	73, NA	16, NA	20, NA	9.39	175.87	
40	Leucine rich repeat containing	gi 73956299 MS	MS	67, NA	28, NA	10, NA	8.49	52.34	
	42 isoform 1								
40	GDP dissociation inhibitor 1	gi 50978936 MS	MS	78, NA	24, NA	9,NA	5.00	51.06	
40	Dynamin 1-like, isoform 4	gi 126338701 MS	MS	73, NA	23, NA	12, NA	8.89	82.32	
,									

 a NCBI = National Center for Biotechnology Information; %cov = %sequence coverage [(number of the matched residues/total number of residues in the entire sequence) \times 100%; NA = Not applicable. Only proteins with \geq 80% identities are included.

4472

Table 2. Functional Classification of the Identified COM Crystal-Binding Proteins

function	protein name
Calcium-dependent phospholipid-binding	Annexin A2 a,b Annexin A8 (Annexin VIII) (Vascular anticoagulant-beta) (VAC-beta) isoform $3^{a,b}$
Calcium ion-binding	Man1a2-prov protein ^{a,b} S100 calcium binding protein, zeta ^{b}
Cell cycle	MTA1
Cellular structure	Centrobin (LYST-interacting protein 8), partial Microtubule-actin cross-linking factor 1 isoform 1 ^b Spectrin, beta, nonerythrocytic 1 isoform 2 Adenomatous polyposis coli protein
	(APC protein) isoform 1 Ezrin (p81) (Cytovillin) (Villin-2) isoform 3^a Vimentin isoform 9
	Crocc protein ^a Talin 2 isoform 5 ^a Tubulin, beta 2
	Beta-actin Gamma-actin
	PDZ domain actin binding protein Shroom a Leucine rich repeat containing 42 isoform 1^a Nestin
	Dynein heavy chain at 16F CG7092-PA Dynein, axonemal, heavy chain 5, isoform CRA a
Immune response	MHC class I antigen ^a MHC class II antigen ^a Immunoglobulin heavy chain variable region
Ion transporter	Tumor necrosis factor type 1 receptor associated protein Plasma membrane calcium ATPase 2 isoform b isoform 6 ^{a,b}
Metabolism	Mitochondrial uncoupling protein 4 (UCP 4) (Solute carrier family 25, member 27) ^{a,b} Alpha enolase (2-phospho-D-glycerate hydro-lyase) (Non-neural enolase)
INICLADOIISIII	(NNE) (Enolase 1) (Phosphopyruvate hydratase) (C-myc promoter-binding protein) (MBP-1) (MPB-1) (Plasminogen-binding protein) isoform 14 ^{a,b}
	Glyceraldehyde-3-phosphate dehydrogenase ^a Phosphoglycerate mutase 1 (Phosphoglycerate mutase isozyme B) (PGAM-B) (BPG-dependent PGAM 1) isoform 2
	Triosephosphate isomerase (TIM) (Triose-phosphate isomerase) isoform 5 ^a Sulfotransferase family, cytosolic, 1C, member 2 Glucosamine-6-phosphate deaminase 2 isoform 1
mRNA processing	Heterogeneous nuclear ribonucleoprotein A1 Peptidyl-Pro cis trans isomerase isoform 1
Protein and vesicular transport	DENN/MADD domain containing 4C isoform 1^a Alpha-actinin 4^b RABSB protein ^a
	Golgi autoantigen, golgin subfamily a, 4 variant ^a Rims2 protein ^a GDP dissociation inhibitor 1
	Flotillin-1 isoform 2 ^a Dynamin-like protein Dymple isoform ^a 256 kD golgin ^a
Protein folding and protein biosynthesis Receptor	Dynamin 1-like, isoform 4 ^a TRIMCyp Glutamate receptor 3 isoform flip precursor isoform 2 ^a

Table 2. Continued

Miscellaneous

function protein name

Ephrin type-B receptor 1 precursor (Tyrosine-protein kinase receptor EPH-2) (NET) (HEK6) (ELK)^a

Signal transduction Vav-3 protein

Stress response Heat shock protein HSP 90-beta^{a,b}

Heat shock protein HSP 90-alpha (HSP 86) isoform $2^{a,b}$ Heat shock protein 1, alpha isoform $3^{a,b}$

78 kDa glucose-regulated protein precursor (GRP 78) (Immunoglobulin heavy chain binding protein) (BiP) (Endoplasmic reticulum lumenal

Ca(2+) binding protein grp78) isoform $4^{a,b}$ Heat shock 70 kDa protein 8 isoform 2 isoform $2^{a,b}$

Heat shock protein 8 isoform $3^{a,b}$

Peroxiredoxin 2 (Thioredoxin peroxidase 1) (Thioredoxin-dependent peroxide reductase 1) (Thiol-specific antioxidant protein) (TSA) (PRP) (Natural killer cell enhancing factor B) (NKEF-B) isoform 1

Membrane protein, palmitoylated 5 isoform 1^a

Dedicator of cytokinesis protein 1 (180 kDa protein downstream of

CRK) (DOCK180) isoform 1^a

Temporarily Assigned Gene name family member (tag-278) isoform $7\,$

BEN domain-containing protein 3

Adenylosuccinate lyase 1

Acyl-CoA thioesterase 9

ART5 protein^a

Hypothetical protein isoform 2

Peptidylprolyl isomerase A (cyclophilin A)

Retinoblastoma-associated protein 140 isoform 4

Four and a half LIM domains protein 1 isoform 6

Hypothetical protein LOC302773

Unknown (protein for MGC:38398)

MIF4G domain containing, isoform CRA_c

F-box and WD-40 domain protein 10

Isopentenyl-diphosphate delta isomerase 2

mCG117968

rCG21715

Androgen receptor associated protein 54

Synapse-associated protein 1

Hypothetical protein^c

The remained COM crystals on MDCK apical surface were counted in random 15 high power fields (HPF) under phase contrast microscope (Olympus CKX41; Olympus Co. Ltd., Tokyo, Japan).

Statistical Analysis

The quantitative data are presented as mean \pm SEM. Comparisons among groups were performed by one-way analysis of variance (ANOVA) with Tukey's posthoc test (SPSS; version 13.0). *P* values <0.05 were considered as statistical significant.

■ RESULTS AND DISCUSSION

This study aimed to identify all of potential COM crystalbinding proteins on apical membrane of distal renal tubular epithelial cells using a proteomics approach. Renal tubular epithelial cells have characteristics of polarization, in which plasma membranes are divided to apical and basolateral portions by a function of tight junction. These two different membrane compartments have unique sets of proteins and lipids according to their differential cellular functions. Apical or luminal membrane is exposed to renal tubular fluid where COM crystals are formed. Madin-Darby Canine Kidney (MDCK) cells, which were derived from distal nephron and used widely as the representing cells of distal renal tubules, 21,22 were used in our present study because the distal nephron is considered as an originating site for COM kidney stone formation. We focused our attention to identification of COM-binding proteins only on apical membrane because of their biological relevance in vivo—only apical membrane, not basolateral membrane and intracellular compartments, contacts to luminal COM crystals.

The polarization of MDCK epithelial cells was confirmed by immunofluorescence staining of markers for tight junction (ZO-1), basolateral membrane (Na $^+$ /K $^+$ -ATPase α -subunit), and apical membrane (gp135). The data showed the presence of these markers in respective locales and thus confirmed the full polarization of MDCK cells (Figure 2). Apical membrane was then isolated using a recently established peeling method, of

^a Cell membrane localization. ^b Calcium-binding activity. ^c Has 3 different GI numbers (gi|109093687, gi|149254381 and gi|149258923).

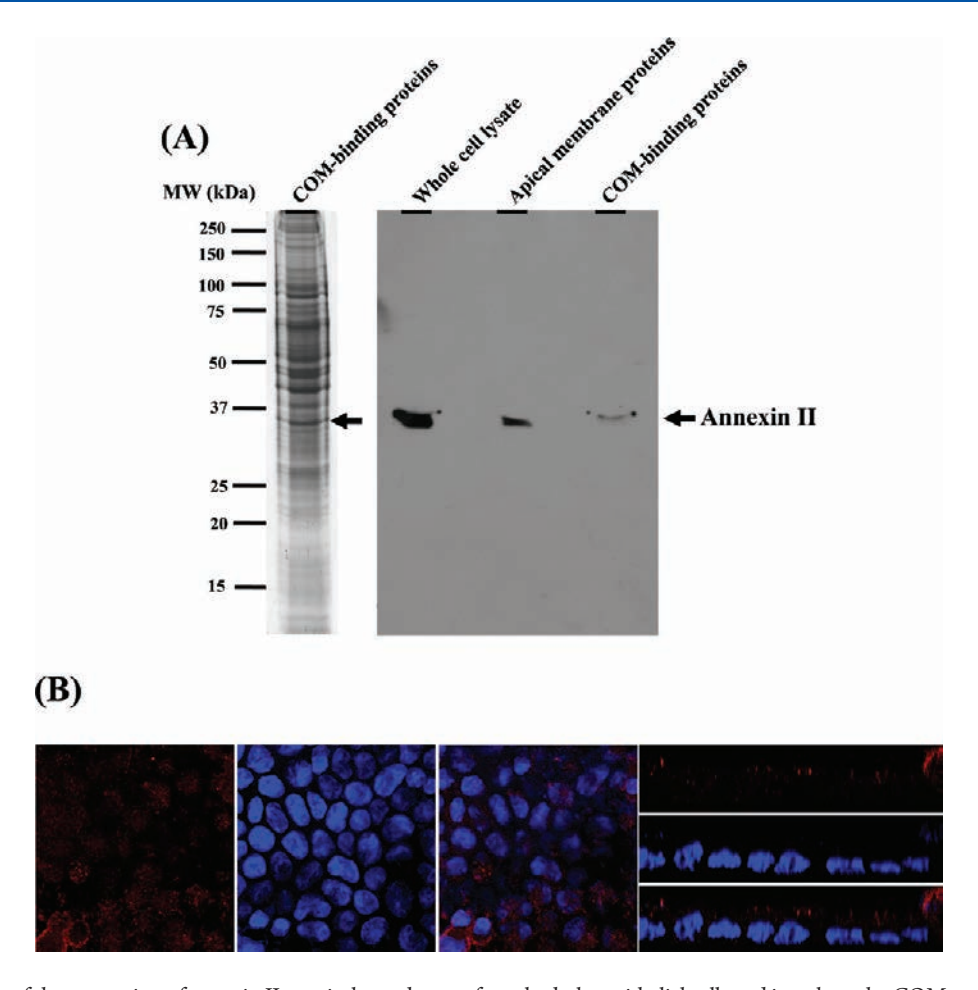


Figure 5. Validation of the expression of annexin II at apical membrane of renal tubular epithelial cells and its role as the COM crystal-binding protein. (A) Proteins derived from whole cell lysate, purified apical membrane, and COM crystal-binding fraction (with an equal amount of $20\,\mu g$) were resolved by 12% SDS-PAGE and subjected to Western blot analysis using goat polyclonal antiannexin II as the primary antibody. (B) Immunofluorescence staining of annexin II followed by laser-scanning confocal microscopic examination. The expression of annexin II is illustrated in red, whereas nuclear counter-stain is shown in blue. The confocal micrographs were obtained from both horizontal (first three panels) and sagittal (last three panels) sections. Original magnification = $630\times$ in all panels.

which principle is based on hydrous affinity and/or ionic interaction. 18- Our previous study has demonstrated that this novel method is simple and highly effective for isolation of apical membrane. 18 In the present study, the yield and purity of apical membrane isolation were also evaluated. The results showed that this novel method, based on peeling, was highly effective for enrichment of apical membrane. Figure 3A shows SDS-PAGE profile of the isolated apical membrane proteins, which obviously differed from that of the whole cell lysate. In addition, a typical apical membrane protein (gp135)²⁵ was effectively enriched by the peeling method as demonstrated by the more prominent gp135 band in Western blot analysis as compared to such band in the sample derived from whole cell lysate (Figure 3B). Moreover, this peeling method also provided the high purity of apical membrane proteins as there was no contamination of basolateral membrane marker $(Na^+/K^+$ -ATPase α -subunit)²⁶ in the isolated apical membrane fraction (Figure 3C). Therefore, this method would offer a high confident data for the analysis of apical membrane proteins.

Highly purified apical membrane fraction was solubilized with $1 \times \text{Laemmli's}$ buffer to obtain the mixture of apical membrane proteins. To avoid effects of detergent and reducing agents on crystal-protein interaction/binding, the protein solution was

extensively dialyzed against deionized water. After lyophilization, the purified apical membrane proteins were resuspended into the protein-free artificial urine and then incubated with COM crystals overnight. The reason that we used protein-free artificial urine instead of human urine because there are several proteins present in the normal human urine that can interfere with data interpretation (the urinary proteins can also bind to COM crystals). The pH and osmolality of artificial urine used in our present study were 6.2 and 446 mOsm/kg, respectively. Differential levels of pH and osmolality may affect the COM crystal binding capacities of proteins. To demonstrate the selective binding of proteins eluted from COM crystals, the SDS-PAGE profile of COM-binding proteins was examined compared to those of starting apical membrane proteins and unbound fraction (Figure 4A). The data showed that COM crystalbinding proteins had a distinct SDS-PAGE profile that was much different from that of the unbound fraction, which was similar to the profile of the starting apical membrane proteins, indicating the highly selective bindings of proteins in the bound fraction. The reproducibility of isolation of COM crystalbinding proteins was confirmed in additional three independent experiments (Figure 4B), and the amount of proteins derived from each fraction was quantitated (Figure 4C).

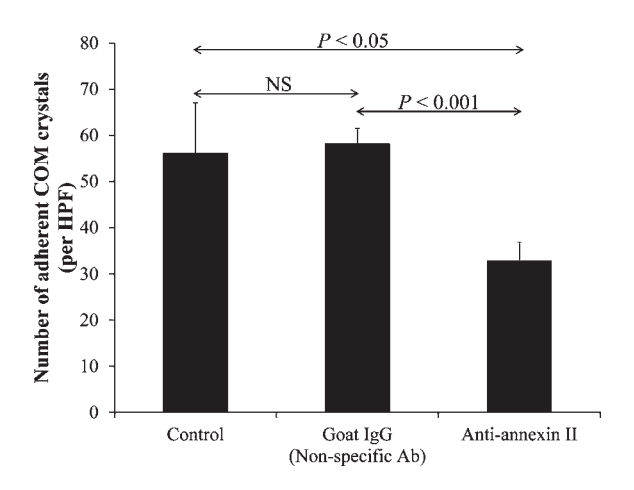


Figure 6. Functional validation of annexin II as the COM crystal-binding protein. COM crystal-binding assay was performed without (control) or with goat polyclonal antiannexin II antibody to neutralize the COM crystal-binding activity of annexin II prior to COM binding. Nonspecific goat IgG served as the treatment control to demonstrate the specificity of neutralization of annexin II activity. N=3 independent experiments.

To identify these COM crystal-binding proteins, the preparative gel derived from 6×10^7 cells was produced. From a total of 40 gel slices (Figure 4D), a total of 96 proteins were identified Q-TOF MS and MS/MS analyses. Their identities, identification numbers, peptide mass fingerprinting and/or MS/MS ions scores, sequence coverage, number of matched peptides, homologues, and other detailed information are summarized in Table 1. The sequences of the identified hypothetical proteins, putative proteins, unnamed protein products, or unknown proteins were also submitted to BLAST search for defining their similarities or homologues, and only proteins with >80% identities are included in Table 1. The actual (experimental) molecular masses of some identified proteins shown in SDS-PAGE gel were not exactly their theoretical (calculated) molecular masses. This is not unexpected as some proteins were the fragmented products of their full lengths, whereas some other might form a tight complex with other proteins in the apical membrane and resisted to reducing agents. All of these identified proteins were classified into various functional categories based on their molecular/ cellular functions provided in the UniProt Knowledgebase (UniProtKB) protein database (Table 2). These included calcium-dependent phospholipid-binding, calcium ion-binding, cell cycle, cellular structure, immune response, ion transporter, metabolism, mRNA processing, protein and vesicular transport, protein folding and protein biosynthesis, receptor, signal transduction, stress response, and miscellaneous. Among these identified proteins, many of them were well-known or typical membrane proteins, as well as calcium-binding proteins, convincing that they play important roles in COM crystal binding.

One of the COM crystal-binding proteins identified from apical membrane of renal tubular epithelial cells in our present study is annexin A2 or annexin II (band #23; at approximately 35 kDa), which was also identified as a COM crystal-binding protein in previous study. Western blot analysis was performed to confirm the mass spectrometric identification of annexin II. The data confirmed that annexin II is an apical membrane protein that can bind tightly with COM crystals (Figure 5A). We also performed immunofluorescence staining of annexin II

followed by laser-scanning confocal microscopic examination to further confirm our proteomic data. The immunofluorescence data confirmed the expression of annexin II at apical membrane surface (Figure 5B). These consistent data strengthen the role of this well-known calcium-binding protein as the COM crystal-binding protein.

Finally, functional validation of annexin II as the COM crystal-binding protein was performed. The data revealed that preincubation of MDCK cells with antiannexin II antibody significantly reduced (approximately 40%) the number of adherent COM crystals on the apical surface of MDCK cells, whereas preincubation with nonspecific IgG did not affect the number of adherent COM crystals, indicating the specificity of this neutralization by antiannexin II (Figure 6). It should be noted that preincubation or neutralization of the polarized MDCK cells with antiannexin II could not completely abolish COM crystal adhesion on apical surface of the cells. This is not unexpected because annexin II is one among other several COM crystal-binding proteins and blocking only one binding protein definitely cannot inhibit the entire binding capacities of apical surface molecules on epithelial cells.

From the list of the identified proteins (Tables 1 and 2), many of them are able to bind with calcium ion (Ca²⁺). We found two proteins that are members of the annexin family, including annexin II (A2) and annexin VIII (A8) (band #23 and #26, respectively). Annexins have a conserved COOH-terminal "core" that mediates their membrane localization and calciumbinding properties.²⁷ Thus, it is not surprising that they were identified as COM crystal-binding proteins in our present study. Several other identified proteins are known to normally express at the apical membrane of renal tubular epithelial cells, for example, plasma membrane calcium ATPase 2 isoform b (PMCA2b) (band #5). This protein is highly enriched in the apical plasma membrane²⁸ and interacts preferentially with Na⁺/H⁺ exchanger regulatory factor 2 (NHERF2) to perform the functional assembly of PMCA2b in a multiprotein Ca2+ signaling complex and facilitate the integrated cross-talk between local Ca²⁺ influx and efflux.²⁹ It is possible that PMCA2b binds COM crystals via its Ca²⁺-binding activity.

We also found some surface receptors that were able to bind with COM crystals, including glutamate receptor 3 isoform flip (band #4) and ephrin (Eph) type-B receptor 1 (band #5). These receptors are type I transmembrane protein and their extracellular regions contain a highly conserved N-terminal domain, which is necessary for ligand binding, 30 whereas their intracellular or cytoplasmic regions contain a highly conserved kinase domain, which catalyzes tyrosine phosphorylation. In addition, the Eph-mediated signaling is restricted to specific membrane microdomains or lipid rafts. 31 Our data report for the first time that these receptors also serve for COM crystal binding.

In summary, we successfully identified several COM crystal-binding proteins from apical membrane of distal renal tubular epithelial cells by a proteomics approach using SDS-PAGE followed by Q-TOF MS and MS/MS analyses. Expression and localization of annexin II on apical surface of MDCK cells were confirmed by Western blot analysis, immunofluorescence staining and laser-scanning confocal microscopic examination. Moreover, its function as the COM crystal-binding protein was validated by a functional study. This large data set offers many opportunities for further investigations of kidney stone disease and may lead to the development of new therapeutic targets.

AUTHOR INFORMATION

Corresponding Author

*Visith Thongboonkerd, MD, FRCPT Professor and Head of Medical Proteomics Unit, Director of Center for Research in Complex Systems Science (CRCSS), Siriraj Hospital, Mahidol University, 12th Floor Adulyadej Vikrom Building, 2 Prannok Road, Bangkoknoi, Bangkok 10700, Thailand. Phone/Fax: +66-2-4184793. E-mail: thongboonkerd@dr.com or vthongbo@yahoo.com.

ACKNOWLEDGMENT

This study was supported by Office of the Higher Education Commission and Mahidol University under the National Research Universities Initiative, and The Thailand Research Fund (RTAS380005) to V.T. K.F. and P.P. are supported by the Royal Golden Jubilee PhD Program of The Thailand Research Fund, whereas V.T. is also supported by "Chalermphrakiat" Grant, Faculty of Medicine Siriraj Hospital.

■ ABBREVIATIONS:

ACN, acetonitrile; COM, calcium oxalate monohydrate; EDTA, *N,N,N',N'*-Ethylenediaminetetraacetic acid; Eph, ephrin; gp135, glycoprotein 135; HSP, heat shock protein; MDCK, Madin-Darby Canine Kidney; MS, mass spectrometry; MS/MS, tandem mass spectrometry; NHERF2, Na⁺/H⁺ exchanger regulatory factor 2; PMCA2b, plasma membrane calcium ATPase 2 isoform b; Q-TOF, quadrupole time-of-flight; TFA, trifluoroacetic acid; ZO-1, Zonula occludens-1

■ REFERENCES

- (1) Trinchieri, A.; Ostini, F.; Nespoli, R.; Rovera, F.; Montanari, E.; Zanetti, G. A prospective study of recurrence rate and risk factors for recurrence after a first renal stone. *J. Urol.* **1999**, *162*, 27–30.
- (2) Strauss, A. L.; Coe, F. L.; Deutsch, L.; Parks, J. H. Factors that predict relapse of calcium nephrolithiasis during treatment: a prospective study. *Am. J. Med.* **1982**, *72*, 17–24.
- (3) Tsujihata, M. Mechanism of calcium oxalate renal stone formation and renal tubular cell injury. *Int. J. Urol.* **2008**, *15*, 115–120.
- (4) Habibzadegah-Tari, P.; Byer, K. G.; Khan, S. R. Reactive oxygen species mediated calcium oxalate crystal-induced expression of MCP-1 in HK-2 cells. *Urol. Res.* **2006**, *34*, 26–36.
- (5) Koul, H. K.; Menon, M.; Chaturvedi, L. S.; Koul, S.; Sekhon, A.; Bhandari, A.; Huang, M. COM crystals activate the p38 mitogenactivated protein kinase signal transduction pathway in renal epithelial cells. *J. Biol. Chem.* **2002**, *277*, 36845–36852.
- (6) Khan, S. R. Crystal-induced inflammation of the kidneys: results from human studies, animal models, and tissue-culture studies. *Clin. Exp. Nephrol.* **2004**, *8*, 75–88.
- (7) Lieske, J. C.; Norris, R.; Swift, H.; Toback, F. G. Adhesion, internalization and metabolism of calcium oxalate monohydrate crystals by renal epithelial cells. *Kidney Int.* **1997**, *52*, 1291–1301.
- (8) Kramer, G.; Steiner, G. E.; Prinz-Kashani, M.; Bursa, B.; Marberger, M. Cell-surface matrix proteins and sialic acids in cell-crystal adhesion; the effect of crystal binding on the viability of human CAKI-1 renal epithelial cells. *Br. J. Urol. Int.* **2003**, *91*, 554–559.
- (9) Ebisuno, S.; Kohjimoto, Y.; Tamura, M.; Inagaki, T.; Ohkawa, T. Histological observations of the adhesion and endocytosis of calcium oxalate crystals in MDCK cells and in rat and human kidney. *Urol. Int.* **1997**, *58*, 227–231.
- (10) Khan, S. R. Calcium oxalate crystal interaction with renal tubular epithelium, mechanism of crystal adhesion and its impact on stone development. *Urol. Res.* **1995**, 23, 71–79.

- (11) Lieske, J. C.; Leonard, R.; Swift, H.; Toback, F. G. Adhesion of calcium oxalate monohydrate crystals to anionic sites on the surface of renal epithelial cells. *Am. J. Physiol.* **1996**, *270*, F192–F199.
- (12) Fullekrug, J.; Simons, K. Lipid rafts and apical membrane traffic. *Ann. N.Y. Acad. Sci.* **2004**, *1014*, 164–169.
- (13) Kumar, V.; Farell, G.; Deganello, S.; Lieske, J. C. Annexin II is present on renal epithelial cells and binds calcium oxalate monohydrate crystals. *J Am. Soc. Nephrol.* **2003**, *14*, 289–297.
- (14) Sorokina, E. A.; Kleinman, J. G. Cloning and preliminary characterization of a calcium-binding protein closely related to nucleolin on the apical surface of inner medullary collecting duct cells. *J. Biol. Chem.* **1999**, 274, 27491–27496.
- (15) Sorokina, E. A.; Wesson, J. A.; Kleinman, J. G. An acidic peptide sequence of nucleolin-related protein can mediate the attachment of calcium oxalate to renal tubule cells. *J. Am. Soc. Nephrol.* **2004**, *15*, 2057–2065.
- (16) Asselman, M.; Verhulst, A.; De Broe, M. E.; Verkoelen, C. F. Calcium oxalate crystal adherence to hyaluronan-, osteopontin-, and CD44-expressing injured/regenerating tubular epithelial cells in rat kidneys. *J. Am. Soc. Nephrol.* **2003**, *14*, 3155–3166.
- (17) Verhulst, A.; Asselman, M.; Persy, V. P.; Schepers, M. S.; Helbert, M. F.; Verkoelen, C. F.; De Broe, M. E. Crystal retention capacity of cells in the human nephron: involvement of CD44 and its ligands hyaluronic acid and osteopontin in the transition of a crystal binding- into a nonadherent epithelium. *J. Am. Soc. Nephrol.* **2003**, *14*, 107–115.
- (18) Fong-ngern, K.; Chiangjong, W.; Thongboonkerd, V. Peeling as a novel, simple, and effective method for isolation of apical membrane from intact polarized epithelial cells. *Anal. Biochem.* **2009**, 395, 25–32.
- (19) Thongboonkerd, V.; Semangoen, T.; Chutipongtanate, S. Factors determining types and morphologies of calcium oxalate crystals: Molar concentrations, buffering, pH, stirring and temperature. *Clin. Chim. Acta* **2006**, 367, 120–131.
- (20) Chutipongtanate, S.; Thongboonkerd, V. Systematic comparisons of artificial urine formulas for in vitro cellular study. *Anal. Biochem.* **2010**, *402*, 110–112.
- (21) Rindler, M. J.; Chuman, L. M.; Shaffer, L.; Saier, M. H., Jr. Retention of differentiated properties in an established dog kidney epithelial cell line (MDCK). *J. Cell Biol.* **1979**, *81*, 635–648.
- (22) Saier, M. H., Jr. Growth and differentiated properties of a kidney epithelial cell line (MDCK). Am. J. Physiol. 1981, 240, C106–C109.
- (23) Rabinovich, Y. I.; Daosukho, S.; Byer, K. J.; El Shall, H. E.; Khan, S. R. Direct AFM measurements of adhesion forces between calcium oxalate monohydrate and kidney epithelial cells in the presence of Ca2+ and Mg2+ ions. *J. Colloid Interface Sci.* **2008**, 325, 594–601.
- (24) Lieske, J. C.; Deganello, S. Nucleation, adhesion, and internalization of calcium-containing urinary crystals by renal cells. *J Am. Soc. Nephrol.* **1999**, *10* (Suppl 14), S422–S429.
- (25) Meder, D.; Shevchenko, A.; Simons, K.; Fullekrug, J. Gp135/podocalyxin and NHERF-2 participate in the formation of a preapical domain during polarization of MDCK cells. *J. Cell Biol.* **2005**, *168*, 303–313.
- (26) Hammerton, R. W.; Krzeminski, K. A.; Mays, R. W.; Ryan, T. A.; Wollner, D. A.; Nelson, W. J. Mechanism for regulating cell surface distribution of Na+,K(+)-ATPase in polarized epithelial cells. *Science* **1991**, 254, 847–850.
- (27) Gerke, V.; Moss, S. E. Annexins: from structure to function. *Physiol Rev.* **2002**, 82, 331–371.
- (28) Xiong, Y.; Antalffy, G.; Enyedi, A.; Strehler, E. E. Apical localization of PMCA2w/b is lipid raft-dependent. *Biochem. Biophys. Res. Commun.* **2009**, 384, 32–36.
- (29) DeMarco, S. J.; Chicka, M. C.; Strehler, E. E. Plasma membrane Ca2+ ATPase isoform 2b interacts preferentially with Na+/H+ exchanger regulatory factor 2 in apical plasma membranes. *J. Biol. Chem.* **2002**, 277, 10506–10511.
- (30) Himanen, J. P.; Nikolov, D. B. Eph receptors and ephrins. *Int. J. Biochem. Cell Biol.* **2003**, 35, 130–134.
- (31) Gauthier, L. R.; Robbins, S. M. Ephrin signaling: One raft to rule them all? One raft to sort them? One raft to spread their call and in signaling bind them? *Life Sci.* **2003**, *74*, 207–216.

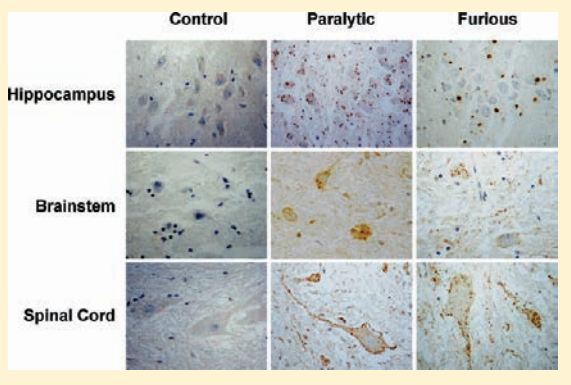


Comprehensive Proteome Analysis of Hippocampus, Brainstem, and Spinal Cord from Paralytic and Furious Dogs Naturally Infected with Rabies

Natthapaninee Thanomsridetchai, Nilubon Singhto, Veera Tepsumethanon, Shanop Shuangshoti, Supaporn Wacharapluesadee, Supachok Sinchaikul, Shui-Tein Chen, Thiravat Hemachudha, and Visith Thongboonkerd, and

Supporting Information

ABSTRACT: Paralytic and furious forms are unique clinical entities of rabies in humans and dogs. However, molecular mechanisms underlying these disorders remained unclear. We investigated changes in proteomes of the hippocampus, brainstem and spinal cord of paralytic and furious dogs naturally infected with rabies compared to noninfected controls. Proteins were extracted from these tissues and analyzed by two-dimensional gel electrophoresis (2-DE) (n = 6 gels/region in each group, a total of 54 gels were analyzed). From >1000 protein spots visualized in each gel, spot matching, quantitative intensity analysis, and ANOVA with Tukey's posthoc multiple comparisons revealed 32, 49, and 67 protein spots that were differentially expressed among the three clinical groups in the hippocampus, brainstem and spinal cord, respectively. These proteins were then identified by quadrupole time-of-flight mass spectrometry and



tandem mass spectrometry (Q-TOF MS and MS/MS), including antioxidants, apoptosis-related proteins, cytoskeletal proteins, heat shock proteins/chaperones, immune regulatory proteins, metabolic enzymes, neuron-specific proteins, transcription/translation regulators, ubiquitination/proteasome-related proteins, vesicular transport proteins, and hypothetical proteins. Among these, 13, 17, and 41 proteins in the hippocampus, brainstem and spinal cord, respectively, significantly differed between paralytic and furious forms and thus may potentially be biomarkers to differentiate these two distinct forms of rabies. In summary, we report herein for the first time a large data set of changes in proteomes of the hippocampus, brainstem and spinal cord in dogs naturally infected with rabies. These data will be useful for better understanding of molecular mechanisms of rabies and for differentiation of its paralytic and furious forms.

KEYWORDS: brainstem, furious, hippocampus, paralytic, proteomics, rabies, spinal cord

■ INTRODUCTION

Rabies remains an important public health problem in some regions as a fatal outcome is expected in almost all cases once symptoms and signs develop. Only three survivors with no or nonsignificant complications have been reported, all of which were associated with bat variants. Comparing between dogand bat-related rabies, patients who are associated with dog variants exhibit more unique clinical manifestations, including paralytic and furious forms. Also, a lesser degree of immune response to rabies virus has been shown in dog-associated cases.

None of the patients with dog-associated rabies in Thailand, Cambodia and Africa had a positive test for rabies antibody in cerebrospinal fluid (CSF). Additionally, the detection of an antibody against the rabies virus in serum is also unpredictable in dog-associated cases. In contrast, CSF and serum levels of the antirabies antibody appear to be correlated with duration of survival in bat-associated cases.

Received: March 26, 2011 **Published:** September 26, 2011

[†]Inter-Department Program of Biomedical Sciences, Faculty of Graduate School, Chulalongkorn University, Bangkok, Thailand

[‡]Medical Proteomics Unit, Office for Research and Development, Faculty of Medicine Siriraj Hospital, Mahidol University, Bangkok, Thailand

[§]Queen Saovabha Memorial Institute, Bangkok, Thailand

Faculty of Medicine, Chulalongkorn University and WHO Collaborating Center for Research and Training on Viral Zoonoses, Bangkok, Thailand

[⊥]Institute of Biological Chemistry and Genomic Research Center, Academia Sinica, Taipei, Taiwan

[£]Center for Research in Complex Systems Science, Mahidol University, Bangkok, Thailand

Comparing the two unique forms of rabies, different anatomical involvements of the nervous system have been shown in patients with paralytic versus furious rabies. In the paralytic form, peripheral nerve axonopathy or myelinopathy, not the defect of the motor neuron in the spinal cord, is responsible for muscle weakness.8 In furious form, although anterior horn cells of spinal cord are affected, clinical deficits from these defective cells are not found and their defects can be detected only by electrophysiological investigations.8 Innate immune response in the brain of paralytic dogs have been detected with a greater degree as compared to that of furious dogs and is inversely correlated with the viral amount in the brain. Also, disturbance of magnetic resonance imaging (MRI) signals of the brain in the paralytic form is greater than that of furious rabies-infected patients and dogs. The faster time to death is another characteristic of furious rabies. Despite dissimilarity of clinical manifestations, imaging features, clinical courses and the amount of viral load in the brain, they share similar pathologies of the central nervous system (CNS), including scant inflammation. 4,8,10

Lack of apoptosis in the CNS has been shown to be a marker for virulence of wild-type or street rabies virus in order to escape immune recognition and to facilitate spreading. ^{11–16} In contrast, fixed virus, such as the challenged virus standard (CVS) strain, induces marked degree of apoptosis in the infected neurons. ^{17–20} Intriguingly, neurons of different regions display diverse degrees of resistance to cell death. It has been demonstrated that motor neurons of spinal cord resist to apoptosis and cytolysis, and remain functioning several days after CVS infection. ²¹ However, hippocampal neurons become apoptotic shortly after the infection. ²¹ Midline CNS structures, that is, thalamus, brainstem, basal ganglia and spinal cord, have been shown to be preferentially infected with rabies in both humans and dogs. ^{9,10,22} Therefore, the survival of neurons may depend not only on the viral strain but also on differential site-specific responses.

Despite the aforementioned knowledge on rabies, its molecular mechanisms remained unclear. We therefore performed a proteomic study of three regions of the CNS, including the hippocampus, brainstem and spinal cord, of dogs naturally infected with rabies. Proteins were extracted from CNS tissues obtained from paralytic and furious dogs and then subjected to proteomic analysis using two-dimensional gel electrophoresis (2-DE) compared to the noninfected controls.

■ MATERIALS AND METHODS

Sample Collection

The CNS tissues were taken from paralytic (n = 3) and furious (n = 3) dogs naturally infected with rabies (street strain of genotype 1; sites of the bite were mainly head and face), as well as noninfected controls (n = 6). Each animal was observed at the Quarantine and Rabies Diagnostic Unit of the Queen Saovabha Memorial Institute (QSMI). All of the animals were in late-stage of rabies, and clinical diagnosis of furious and paralytic rabies was achieved using the criteria reported previously. The animals died naturally without receiving any treatment. From each animal, three locales of the CNS tissues, including the hippocampus, brainstem (midbrain, pons and medulla) and spinal cord, were taken and were saved at -70 °C until used.

Immunoperoxidase Staining of Rabies Antigen

The diagnosis of rabies was confirmed by the presence of rabies antigen in the CNS tissues. Paraffin-embedded sections of formalin-fixed tissues (3- μ m-thick) were stained with antirabies nucleocapsid polyclonal antibody (Bio-Rad; Marnes-la-Coquette, France) at a dilution of 1:80. After rinsing with PBS, the sections were incubated with a respective secondary antibody conjugated with horseradish peroxidase in the DAKO EnVision-System kit (DAKO Corporation; CA) for 30 min. The slides were then washed with PBS and incubated for 10 min with a peroxidase substrate containing 0.5 mg/mL diaminobenzidine (Sigma; St. Louis, MO), 30% H_2O_2 and 1 M imidazole in Tris-HCl buffer. After rinsing by tap water, the tissues were counterstained with hematoxylin.

Protein Extraction

The tissues were briskly frozen in liquid nitrogen, ground to powder, resuspended in a buffer containing 7 M urea, 2 M thiourea, 4% 3-[(3-cholamidopropyl) dimethyl-ammonio]-1-propanesulfonate (CHAPS), 120 mM dithiothreitol (DTT), 2% (v/v) ampholytes (pH 3–10) and 40 mM Tris-base, and incubated at 4 $^{\circ}$ C for 30 min. Unsolubilized nuclei, cell debris, and particulate matters were removed by a centrifugation at 10 000 rpm, 4 $^{\circ}$ C for 5 min. Protein concentrations were determined by the Bradford method using Bio-Rad protein assay (Bio-Rad Laboratories; Hercules, CA).

Two-Dimensional Gel Electrophoresis (2-DE)

For the controlled group, each gel was derived from each sample (n = 6 gels/region). For the paralytic and furious groups, duplicated 2-D gels were derived from each sample to have 6 gels/ region in each group. Overall, a total of 54 gels were analyzed in this study. For each 2-D gel, Immobiline DryStrip (nonlinear pH gradient of 3-10, 7 cm long; GE Healthcare, Uppsala, Sweden) was rehydrated overnight with an equal amount of 150 μ g of total protein that was premixed with a rehydration buffer containing 7 M urea, 2 M thiourea, 2% CHAPS, 2% (v/v) ampholytes (pH 3-10), 120 mM DTT, 40 mM Tris-base, and bromophenol blue (to make the final volume of 150 μ L per strip). The first dimensional separation or isoelectric focusing (IEF) was performed in Ettan IPGphor III System (GE Healthcare) at 20 °C, using a stepwise mode to reach 9083 Vh with limiting current of 50 mA/strip. After completion of the IEF, the strips were first equilibrated for 15 min in an equilibration buffer containing 6 M urea, 130 mM DTT, 112 mM Tris-base, 4% SDS, 30% glycerol and 0.002% bromophenol blue, and then in another similar buffer that replaced DTT with 135 mM iodoacetamide, for a further 15 min. The second dimensional separation was performed in 12% polyacrylamide gel using SE260 mini-Vertical Electrophoresis Unit (GE Healthcare) at 150 V for approximately 2 h. The resolved protein spots were stained with SYPRO Ruby fluorescence dye (Invitrogen/Molecular Probes; Eugene, OR) overnight and then visualized using Typhoon 9200 laser scanner (GE Healthcare).

Spot Matching and Quantitative Intensity Analysis

Image Master 2D Platinum software (GE Healthcare) was used for matching and analysis of protein spots in 2-D gels. Parameters used for spot detection were (i) minimal area = 10 pixels; (ii) smooth factor = 2.0; and (iii) saliency = 2.0. A reference gel was created from an artificial gel combining all of the spots presenting in different gels into one image. The reference gel was then used for determination of existence and difference of protein expression between gels. Background subtraction was performed, and the intensity volume of each spot was normalized with total intensity volume (summation of the

Journal of Proteome Research

intensity volumes obtained from all spots within the same 2-D gel).

Statistical Analysis

All the quantitative data are reported as mean \pm SEM. Intensity volumes of individual spots matched across different gels were compared among groups by multiple comparisons using one-way analysis of variance (ANOVA) with Tukey's posthoc test (SPSS; version 13.0). P values less than 0.05 were considered as statistical significant. Significantly different protein spots were subjected to in-gel tryptic digestion and identification by mass spectrometry.

In-Gel Tryptic Digestion

All of the protein spots whose intensity levels significantly differed among groups were excised from 2-D gels, washed twice with 200 μL of 50% acetonitrile (ACN)/25 mM NH₄HCO₃ buffer (pH 8.0) at room temperature for 15 min, and then washed once with 200 μ L of 100% ACN. After washing, the solvent was removed, and the gel pieces were dried by a SpeedVac concentrator (Savant; Holbrook, NY) and rehydrated with 10 µL of 1% (w/v) trypsin (Promega; Madison, WI) in 25 mM NH₄HCO₃. After rehydration, the gel pieces were crushed and incubated at 37 °C for at least 16 h. Peptides were subsequently extracted twice with 50 μ L of 50% ACN/5% trifluoroacetic acid (TFA); the extracted solutions were then combined and dried with the SpeedVac concentrator. The peptide pellets were resuspended with 10 μ L of 0.1% TFA and purified using ZipTip_{C18} (Millipore; Bedford, MA). The peptide solution was drawn up and down in the ZipTip_{C18} 10 times and then washed with 10 μ L of 0.1% formic acid by drawing up and expelling the washing solution 3 times. The peptides were finally eluted with 5 μ L of 75% ACN/0.1% formic acid.

Protein Identification by Q-TOF MS and MS/MS Analyses

The trypsinized samples were premixed 1:1 with the matrix solution containing 5 mg/mL α -cyano-4-hydroxycinnamic acid (CHCA) in 50% ACN, 0.1% (v/v) TFA and 2% (w/v) ammonium citrate, and deposited onto the 96-well MALDI target plate. The samples were analyzed by Q-TOF Ultima mass spectrometer (Micromass; Manchester, U.K.), which was fully automated with predefined probe motion pattern and the peak intensity threshold for switching over from MS survey scanning to MS/MS, and from one MS/MS to another. Within each sample well, parent ions that met the predefined criteria (any peak within the m/z 800-3000 range with intensity above 10 count \pm include/exclude list) were selected for CID MS/MS using argon as the collision gas and a mass dependent $\pm 5~\mathrm{V}$ rolling collision energy until the end of the probe pattern was reached. The MS and MS/MS data were extracted and outputted as the searchable .txt and .pkl files, respectively, for independent searches using the MASCOT search engine (http://www. matrixscience.com), assuming that peptides were monoisotopic. Fixed modification was carbamidomethylation at cysteine residues, whereas variable modification was oxidation at methionine residues. Only one missed trypsin cleavage was allowed, and peptide mass tolerances of 100 and 50 ppm were allowed for peptide mass fingerprinting and MS/MS ions search, respectively.

Western Blot Analysis

Proteins derived from CNS tissues (with an equal amount of $20 \mu g$) were resolved in 12% SDS-PAGE and then transferred onto a nitrocellulose membrane (Whatman; Dassel, Germany)

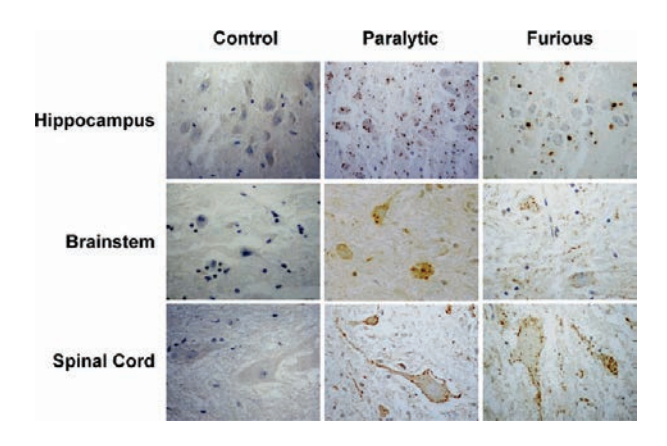


Figure 1. Immunoperoxidase staining of rabies antigen. Hippocampus, brainstem and spinal cord from noninfected dogs and those naturally infected with rabies (both paralytic and furious forms) were subjected to immunohistochemical study for rabies antigen using polyclonal antibody against rabies nucleocapsid as the primary antibody and hematoxylin as the counterstain. Immunoreactive locales of rabies nucleocapsid are shown in brown, whereas nuclei are illustrated in blue.

using a semidry transfer apparatus (Bio-Rad; Milano, Italy) at 75 mA for 1 h. Nonspecific bindings were blocked with 5% skim milk in PBS at room temperature for 1 h. The membrane was then incubated with mouse monoclonal antitubulin $\alpha 1$ or anti-HSP90 (Santa Cruz Biotechnology; Santa Cruz, CA) (1:1000 in 5% skim milk/PBS) at 4 °C overnight. Thereafter, the membrane was washed three times with PBS and further incubated with rabbit antimouse IgG conjugated with horseradish peroxidase (DAKO; Glostrup, Denmark) (1:2000 in 5% skim milk/PBS) at room temperature for 1 h. The immunoreactive bands were then visualized by SuperSignal West Pico chemiluminescence substrate (Pierce Biotechnology, Inc.; Rockford, IL) and autoradiography.

Global Protein Network Analysis

All of the significantly altered proteins in individual CNS regions of dogs naturally infected with rabies were subjected to global protein network analysis using Ingenuity Pathways Analysis (IPA) tool by Ingenuity Systems (http://www.ingenuity.com) to query each identified protein to other identified proteins and scientific findings curated from the literature relating to genes, cells, diseases, drugs and other biological entities, as described previously.²³ Finally, relevant network(s) or pathway(s) of interacting proteins are reported.

RESULTS

We investigated changes in tissue proteomes of the hippocampus, brainstem and spinal cord of paralytic (n = 3) and furious (n = 3) dogs naturally infected with rabies compared to the noninfected controls (n = 6). Rabies infection was confirmed in paralytic and furious dogs by positive immunoperoxidase staining of rabies nucleocapsid protein in their CNS tissues (as illustrated in brown in Figure 1). Proteins were extracted from these tissues and analyzed by 2-DE (n = 6 gels/region for each group, with or without replication of individual samples; a total of 54 gels were analyzed). From >1000 protein spots visualized in each gel, spot matching, quantitative intensity analysis, and ANOVA with Tukey's posthoc multiple comparisons revealed 32, 49, and 67 protein spots that were differentially expressed among the three clinical groups in the hippocampus (Figure 2),

Hippocampus

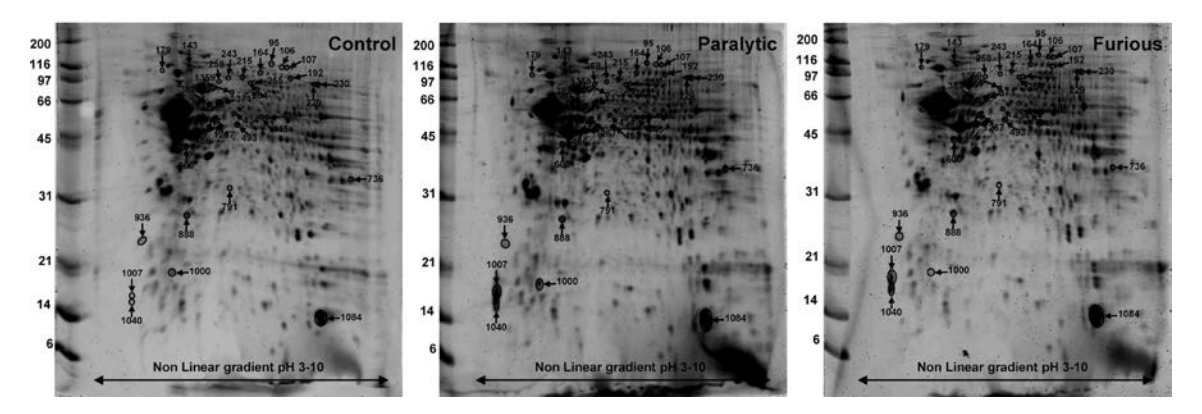


Figure 2. 2-D proteome maps of differentially expressed proteins in hippocampus of dogs naturally infected with rabies. Proteins that significantly differed among groups, including noninfected control, paralytic form of rabies and furious form of rabies, are labeled with numbers that correspond to those reported in Tables 1 and 2, and Supplementary Table S1 (Supporting Information).

Brainstem

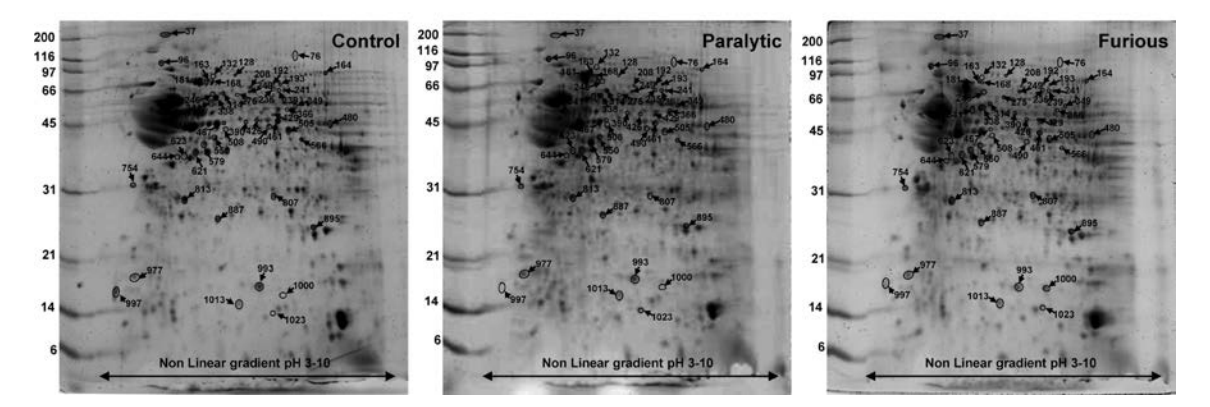


Figure 3. 2-D proteome maps of differentially expressed proteins in brainstem of dogs naturally infected with rabies. Proteins that significantly differed among groups, including noninfected control, paralytic form of rabies and furious form of rabies, are labeled with numbers that correspond to those reported in Tables 1 and 2, and Supplementary Table S2 (Supporting Information).

brainstem (Figure 3) and spinal cord (Figure 4), respectively. These differentially expressed proteins were then identified by Q-TOF MS and/or MS/MS analyses. Their mass spectrometric data (identities, identification scores, sequence coverage, number of matched peptides, isoelectric point or pI, molecular weight or MW, etc.), quantitative intensity data, and p values obtained from ANOVA as well as Tukey's posthoc multiple comparisons are summarized in Supplementary Tables S1—S3 (Supporting Information), respectively.

These identified proteins were classified into 11 main categories, namely antioxidants, apoptosis-related proteins, cytoskeletal proteins, heat shock proteins/chaperones, immune regulatory proteins, metabolic enzymes, neuron-specific proteins, transcription/translation regulators, ubiquitination/proteasome-related proteins, vesicular transport proteins, and hypothetical proteins (Figure 5). Among these, the top three of most changes (in terms of number of differentially expressed proteins in each functional category) were metabolic enzymes (32%), vesicular transport (20%) and cytoskeletal proteins (15%), respectively (Figure 5). Some proteins were identified as more than one form of the same protein. For example, annexin A2 was identified from spots #1215 and #1408 derived from

the spinal cord with a slight difference of their molecular masses in the 2-D proteome map (spot #1215 had a slightly greater molecular mass) (Figure 4). Similarly, annexin A6 was identified from both the hippocampus (spot #258) and brainstem (spot #246) with a slight difference of their molecular masses in the 2-D proteome map (spot #258 had a slightly greater molecular mass) (Figures 2 and 3). These were most likely due to post-translational modifications (PTMs) or cleavage that could alter molecular masses, isoelectric points and cellular function of different forms of the same protein. ²⁴

Some of differentially expressed proteins identified by proteomic study were validated by Western blot analysis, including significant increase of tubulin $\alpha 1$ in the brainstem of paralytic dogs (Figure 6A), significant increase of heat shock protein 90 (HSP90) in the brainstem of paralytic dogs (Figure 6B), and significant decrease of HSP90 in the spinal cord of furious dogs (Figure 6C). Moreover, all of the significantly altered proteins were subjected to global protein network analysis. Using the Ingenuity Pathway Analysis (IPA) tool, there were four important functional networks detected in differentially expressed proteins in CNS tissues of dogs naturally infected with rabies. These include Network I, Gene expression, cellular development,

Spinal Cord

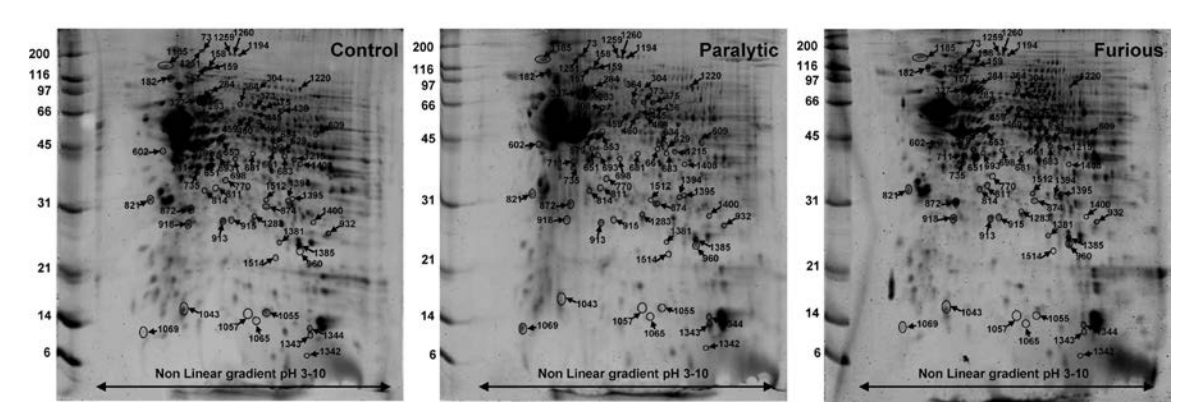


Figure 4. 2-D proteome maps of differentially expressed proteins in spinal cord of dogs naturally infected with rabies. Proteins that significantly differed among groups, including noninfected control, paralytic form of rabies and furious form of rabies, are labeled with numbers that correspond to those reported in Tables 1 and 2, and Supplementary Table S3 (Supporting Information).

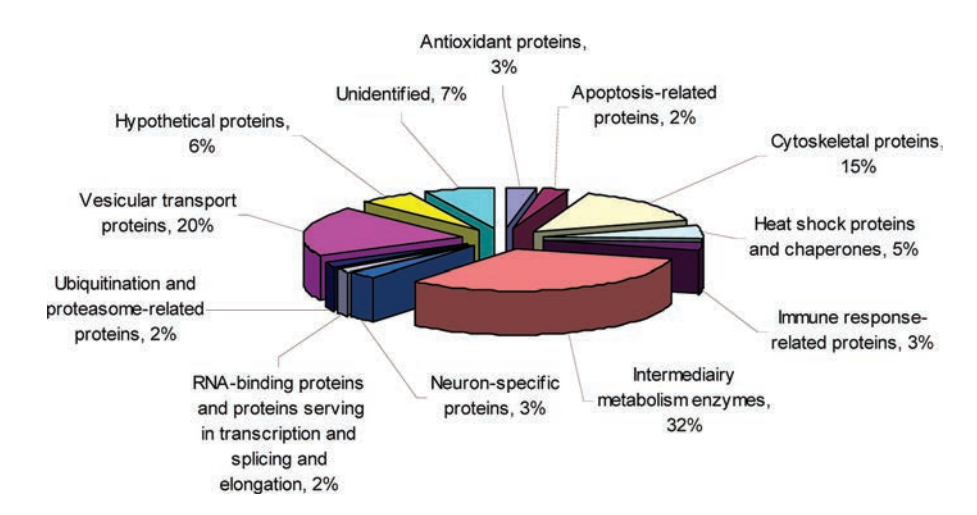


Figure 5. Summary of all differentially expressed proteins in the hippocampus, brainstem and spinal cord of dogs naturally infected with rabies. These significantly differed proteins were classified based on their molecular functions. More details of individual proteins, including mass spectrometric data (identities, identification scores, sequence coverage, number of matched peptides, isoelectric point or pI, molecular weight or MW, etc.), quantitative intensity data, and *p* values obtained from ANOVA as well as Tukey's posthoc multiple comparisons are summarized in Supplementary Tables S1—S3 (Supporting Information).

growth and proliferation (in hippocampus) (Figure 7A); Network II, Drug and lipid metabolism (in brainstem) (Figure 7B); Network III, Genetic disorder and small molecule biochemistry (in spinal cord) (Figure 7C); and Network IV, Neurological disease, energy production and nucleic acid metabolism (in spinal cord) (Figure 7D).

DISCUSSION

Natural infection of rabies virus in dog is an ideal animal model for studying the pathogenesis of rabies. Paralytic and furious manifestations can be found in rabies-infected dogs, resembling those of humans. Our results indicate that paralytic and furious rabies had a marked degree of alterations in their proteome profiles of three different locales of the CNS, including the hippocampus, brainstem and spinal cord, as compared to the noninfected controls. The differentially expressed proteins were involved in many biological processes in response to stress and to the process of rabies viral infection (Figure 5).

Among 11 main functional categories of significantly altered proteins affected by rabies, some functional groups drew our attention as they might be directed to better understanding of the molecular mechanisms of rabies (both paralytic and furious forms). These included: (i) antioxidants, (ii) apoptosis-related proteins; (iii) cytoskeletal proteins; (iv) heat shock proteins/chaperones; (v) immune regulatory proteins; and (vi) neuron-specific proteins (Table 1). Functional significance and potential roles of these proteins are highlighted as follows.

(i). Antioxidants

Oxidative stress has been reported in rabies. ^{25–27} Jackson and colleagues ²⁸ have demonstrated that rabies virus infection in cultured DRG neurons derived from adult mice caused axonal injury through oxidative stress. Protective proteins (i.e., antioxidants) have been shown to be up-regulated to counteract the oxidative stress induced by rabies infection. ²⁹ *In vivo*, oxidative stress may explain previous observations of the neuronal degeneration processes in the study of transgenic mice. ³⁰ In our present

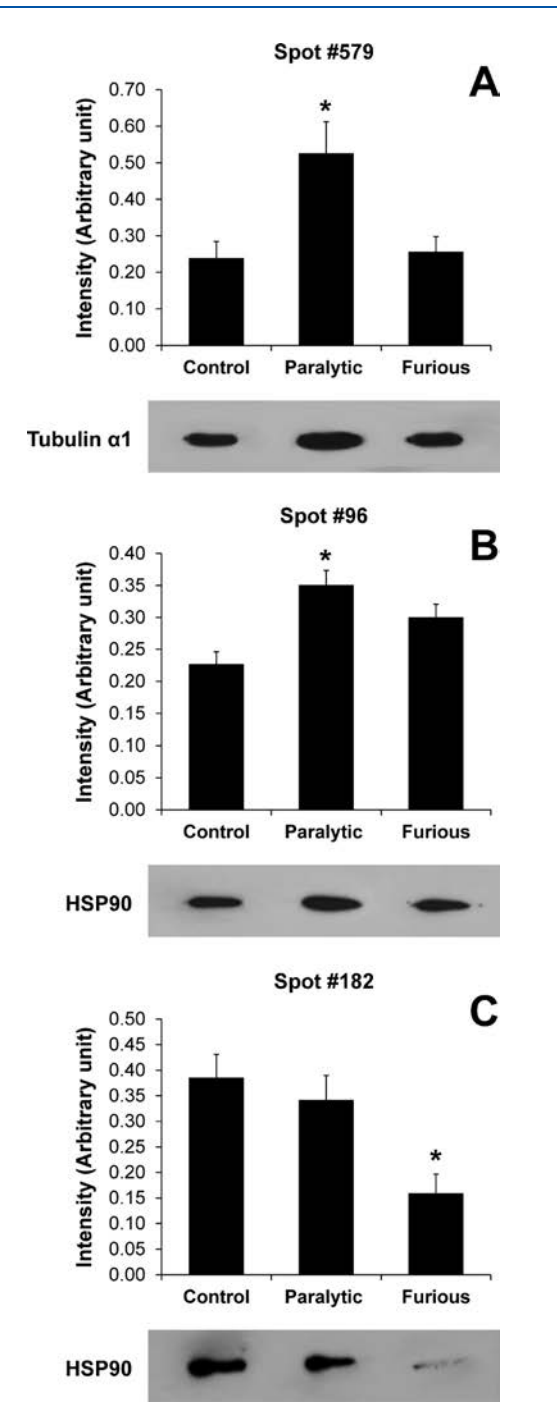


Figure 6. Western blot analysis. Some of the proteomic data were validated by Western blot analysis, including (A) significant increase of tubulin $\alpha 1$ in brainstem of paralytic dogs, (B) significant increase of heat shock protein 90 (HSP90) in brainstem of paralytic dogs, and (C) significant decrease of HSP90 in spinal cord of furious dogs. * = p < 0.05 compared to controls. See also Table 1 and Supplementary Tables S1–S3 (Supporting Information).

study, we found both up- and down-regulations of antioxidants in the brainstem and spinal cord of paralytic dogs and downregulation of one antioxidant protein in the spinal cord of furious dogs (Table 1). These data implicate that the disease process might be at the later stage than antioxidants could handle to protect the CNS from oxidative stress (i.e., irreversible deterioration stage). Analysis of the brains at an earlier stage will be helpful to address this hypothesis.

(ii). Apoptosis-related Proteins

Even with severe clinical entities of both paralytic and furious dogs, there were only 1-2 apoptosis-related proteins that were significantly altered in each region of the CNS, including two forms of annexin A2, two forms of annexin A6, and cytochrome P450 2B12 (CYPIIB12) (Table 1). These data were consistent with previous findings, demonstrating that apoptosis was almost undetectable in wild-type rabies virus infection. 11-15 Interestingly, one form of annexin A2 (spot #1215; full-length) was upregulated in the spinal cord of paralytic dogs, whereas another form (spot #1408; cleavage or fragmented) was down-regulated in the spinal cord of furious dogs. Similarly, one form of annexin A6 (spot #258; full-length) was up-regulated in the hippocampus of furious dogs, whereas another form (spot #246; cleavage or fragmented) was down-regulated in the brainstem of furious dogs. These disparate results underscore the important role of PTMs and/or cleavage on the functional roles of differential forms of the same protein.³¹

(iii). Cytoskeletal Proteins

Most of cytoskeletal proteins were down-regulated in the CNS of paralytic and furious dogs (Table 1). The decreased amount of cytoskeletal proteins is likely the result of CNS damage by rabies virus infection. These data were consistent with those reported in our previous studies on magnetic resonance imaging of the brains of furious and paralytic dogs during an early stage, which showed tract integrity and macro-structural damage in the brainstem of paralytic rabies and in the cerebral cortex of furious rabies.³² This process undoubtedly led the animals to further stage with widespread extent of CNS damage, thereby coma and death. In contrast, two forms of glial fibrillary acidic protein (GFAP), tubulin alpha-1 isoform 9, vinculin and xin actin-binding repeat containing 2 isoform 1 were up-regulated. These increases might be due to reorganization of cytoskeletal assembly in the CNS as a part of host response to the CNS infection. However, as there were much fewer up-regulated proteins, this compensatory mechanism failed to cope with the deterioration of CNS damage by rabies virus.

(iv). Heat Shock Proteins/Chaperones

Heat shock proteins or chaperones play important roles in cellular stress responses, protein folding (to ensure the proper protein conformation), and presentation of antigens for the immune system. ^{33,34} In rabies, heat shock proteins, especially heat shock protein 70 kDa (Hsp70), are known as the functional molecules for replication found in Negri body, working in concert with Toll-like receptor 3 (TLR3) and ubiquitylated proteins. ^{35–37} Our data showed up-regulation of Hsp70 in spinal cord of paralytic dogs. In addition to Hsp70, there were many heat shock proteins or chaperones that were significantly altered in the CNS tissues of both paralytic and furious dogs. However, their levels were either increased or decreased (Table 1). These disparate results might be due to the balance between deteriorated effects of virus infection and their counter-balances as the compensatory mechanisms of the host to cope with diseases/disorders.

(v). Immune Regulatory Proteins

There were concordant changes in immune regulatory proteins in CNS tissues of both paralytic and furious dogs. These included up-regulation of immunoglobulin heavy chain in the

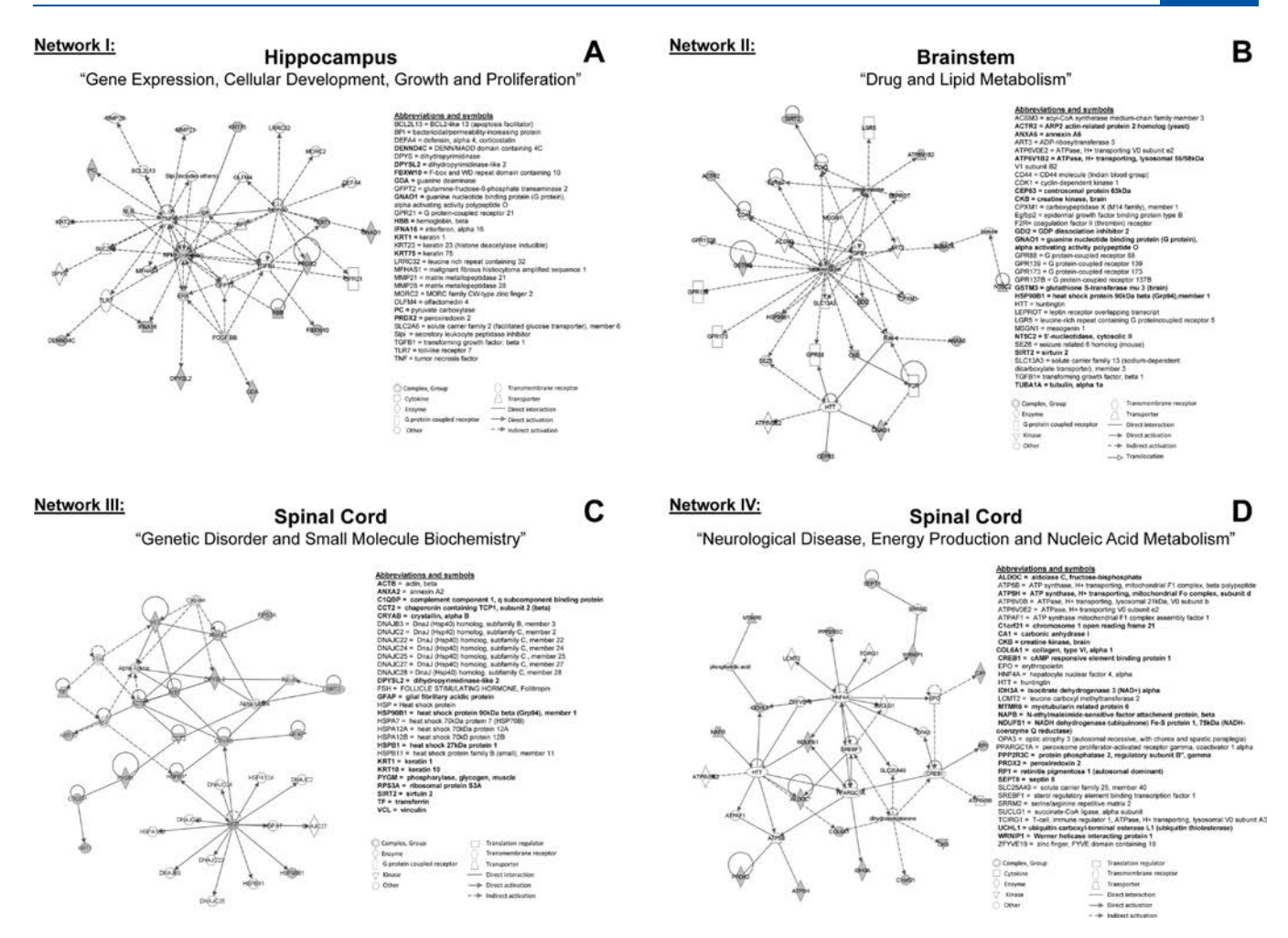


Figure 7. Global protein network analysis. Using the Ingenuity Pathways Analysis (IPA) tool, there were four important functional networks detected in differentially expressed proteins in CNS tissues of dogs naturally infected with rabies. These include (A) Network I, Gene expression, cellular development, growth and proliferation (in hippocampus); (B) Network II, Drug and lipid metabolism (in brainstem); (C) Network III, Genetic disorder and small molecule biochemistry (in spinal cord); and (D) Network IV, Neurological disease, energy production and nucleic acid metabolism (in spinal cord).

brainstem of paralytic dogs and up-regulations of interferon alpha-4 and SARM1 protein in the hippocampus of furious dogs (Table 1). Our data were consistent with the previous findings, indicating the involvement of innate immune response in the brain of rabies-infected dogs.⁹

(vi). Neuron-specific Proteins

Collapsin response mediator proteins (CRMPs) are members of the family of cytosolic phosphoproteins. They are strongly expressed throughout the developing nervous system. RRMP-2 has been shown to bind with tubulin heterodimers and promote microtubule assembly, thereby enhancing axonal growth and branching. RRMP-2 can induce neuronal differentiation in hippocampal cultures. In addition, CRMP-2 is also expressed in immune cells and plays a crucial role in T lymphocyte migration as the increased expression of CRMP-2 is associated with the increase in migratory rate of peripheral T lymphocytes. Therefore, CRMP2 expression may serve as an indicator for neuroinflamation. Interestingly, we found that CRMP-2 was down-regulated in the spinal cord of both paralytic and furious forms of rabies but was up-regulated in the brainstem of paralytic dogs (Table 1). These data might be evidence of

ingression of activated T cells in the brainstem, consistent with our observation that inflammatory T cells could be demonstrated only in the brainstem of paralytic rabies (Shuangshoti et al., unpublished data).

Global protein network analysis of all differentially expressed proteins in CNS tissues of dogs naturally infected with rabies using the IPA tool revealed four important functional networks detected in these affected tissues. In the hippocampus, Network I associated with gene expression, cellular development, growth and proliferation was observed (Figure 7A), consistent with the data reported in previous studies indicating that several genes involved in cell growth and proliferation are altered in the hippocampus upon rabies virus infection. 43,44 In the brainstem, Network II associated with drug and lipid metabolism was found (Figure 7B). Although a few proteins (e.g., annexin, HSP90, H⁺ ATPase) in this network have been found to be altered in rabies-infected CNS tissues in previous genomic/proteomic studies, 44,45 other altered proteins in this network are novel and deserve further investigations to address their functional significance in drug and lipid metabolism upon rabies virus infection. In the spinal cord, two protein networks involved in rabies were identified, including Network III associated with

 ${\bf Table~1.~~Some~Interesting~Changes~in~Furious~and~Paralytic~Dogs~Compared~to~Noninfected~Controls}^a$

				alterations	(vs control)
protein name	spot no.	NCBI ID	region	paralytic (P)	furious (1
	Ant	ioxidants			
150 kDa oxygen-regulated protein precursor	73	gi 73955046	Spinal cord	\uparrow^b	NS
(Orp150) (Hypoxia up-regulated 1)					
Glutathione S-transferase Mu 3 (GSTM3-3)	807	gi 57088159	Brainstem	\uparrow^b	NS
(GST class-mu 3) (hGSTM3-3) isoform 1					
Oxygen-regulated protein 1; AltName: Full=Retinitis	157	gi 62900882	Spinal cord	\downarrow^b	NS
pigmentosa RP1 protein homologue					
Peroxiredoxin 1	932	gi 4505591	Spinal cord	\downarrow^b	\downarrow^b
	Apoptosis-	related proteins			
Annexin A2	1215	gi 18645167	Spinal cord	NS	\downarrow^b
Annexin A2	1408	gi 50950177	Spinal cord	\uparrow^b	NS
Annexin A6 (Annexin VI) (Lipocortin VI) (P68) (P70)	246	gi 73953627	Brainstem	NS	\downarrow^b
(Protein III) (Chromobindin 20) (67 kDa calelectrin)					
(Calphobindin-II) (CPB-II) isoform 2					
Annexin A6 (Annexin VI) (Lipocortin VI) (P68) (P70)	258	gi 73953627	Hippocampus	NS	\uparrow^b
(Protein III) (Chromobindin 20) (67 kDa calelectrin)		- '			
(Calphobindin-II) (CPB-II) isoform 2					
Cytochrome P450 2B12 (CYPIIB12)	192	gi 62639273	Hippocampus	\downarrow^b	NS
	Cystocko	letal proteins			
Drynamia	•	•	Llimmaaammua	\downarrow^b	NS
Dynamin	164	gi 181849	Hippocampus Brainstem	\downarrow^b	
Fascin 1	366	gi 4507115		·	NS ↑ ^b
Glial fibrillary acidic protein, astrocyte (GFAP) isoform 1	459	gi 73965500	Spinal cord	NS	I
Glial fibrillary acidic protein, astrocyte (GFAP) isoform 1	602	gi 73965500	Spinal cord	NS	\uparrow^b
Myosin, heavy chain 2, skeletal muscle, adult	208	gi 115947178	Brainstem	\downarrow^b	NS
Nebulin-related anchoring protein isoform 2	132	gi 114632883	Brainstem	\downarrow^b	$\downarrow b$
NEFM protein	1185	gi 148342538	Spinal cord	\downarrow^b	\uparrow^b
Neurofilament, heavy polypeptide 200 kDa	37	gi 50979202	Brainstem	\downarrow^b	\downarrow^b
Septin-8	460	gi 73971156	Spinal cord	\downarrow^b	\downarrow^b
TUBB2B protein	1000	gi 133778299	Hippocampus	NS	\downarrow^b
Tubulin, alpha-1 isoform 9	579	gi 73996547	Brainstem	↑ ^b	NS
Tubulin, alpha-2 chain (Alpha-tubulin 2) isoform 7	623	gi 73996522	Brainstem	\downarrow^b	NS
Vinculin (Metavinculin)	1259	gi 73953587	Spinal cord	↑ ^b	↑ ^b
Xin actin-binding repeat containing 2 isoform 1	1260	gi 66841385	Spinal cord	↑ ^b	NS
8			-F		
		roteins/chaperones	0 . 1 . 1	1 <i>h</i>	Ab
Alpha-Crystallin B chain (Alpha(B)-Crystallin)	960	gi 149716488	Spinal cord	↓ <i>b</i>	↑ ^b
Alpha Crystallin B chain (Alpha(B)-Crystallin)	895	gi 57085977	Brainstem	NS	\uparrow^b
(Rosenthal fiber component) (Heat-shock					
protein beta-5) (HspB5) isoform 1				∆ h	≜ h
Alpha Crystallin B chain (Alpha(B)-Crystallin)	1385	gi 57085977	Spinal cord	\uparrow^b	\uparrow^b
(Rosenthal fiber component)					
(Heat-shock protein beta-5) (HspB5) isoform 1				1.6	1.6
DnaJ (Hsp40) homologue, subfamily C, member	1055	gi 149050007	Spinal cord	\downarrow^b	\downarrow^b
15 (predicted), isoform CRA_b				₂ 1.	
Heat shock cognate 71 kDa protein	327	gi 123647	Spinal cord	\uparrow^b	NS
(Heat shock 70 kDa protein 8)				. 1.	
Heat shock protein 90 kDa beta, member 1	96	gi 50979166	Brainstem	\uparrow^b	NS
Heat shock protein 90 kDa beta, member 1	182	gi 50979166	Spinal cord	NS	\downarrow^b
Heat shock protein beta-1	874	gi 50979116	Spinal cord	NS	\uparrow^b
Heat shock protein beta-1	1512	gi 50979116	Spinal cord	\uparrow^b	NS

Table 1. Continued

				alterations	(vs control)
protein name	spot no.	NCBI ID	region	paralytic (P)	furious (F)
	Immune re	gulatory proteins			
Immunoglobulin heavy chain variable region	1023	gi 112700066	Brainstem	\uparrow^b	NS
Interferon alpha 4	107	gi 18767673	Hippocampus	NS	\uparrow^b
SARM1 protein	1359	gi 114325428	Hippocampus	NS	\uparrow^b
	Neuron-s	pecific proteins			
Dihydropyrimidinase related protein-2	364	gi 73993705	Spinal cord	NS	\downarrow^b
(DRP-2) (CRMP-2) isoform 6 (Turned on after					
division, 64 kDa protein) (TOAD-64) (Collapsin response mediator protein 2)					
Dihydropyrimidinase related protein-2 (DRP-2)	314	gi 73993705	Brainstem	\uparrow^b	NS
(Turned on after division, 64 kDa protein)	314	g1 /3993/03	Dramstem	ı	113
(TOAD-64) (Collapsin response					
mediator protein 2) (CRMP-2) isoform 6					
Dihydropyrimidinase related protein-2 (DRP-2)	373	gi 73993699	Spinal cord	\downarrow^b	\downarrow^b
(Turned on after division, 64 kDa protein)		81	1		
(TOAD-64) (Collapsin response mediator protein 2)					
(CRMP-2) isoform 4					
Dihydropyrimidinase related protein-2 (DRP-2)	375	gi 73993705	Spinal cord	\downarrow^b	\downarrow^b
(Turned on after division, 64 kDa protein)		- '			
(TOAD-64) (Collapsin response					
mediator protein 2) (CRMP-2) isoform 6					
Dihydropyrimidinase related protein-2 (DRP-2)	382	gi 73993705	Hippocampus	NS	\uparrow^b
(Turned on after division, 64 kDa protein)					
(TOAD-64) (Collapsin response					
mediator protein 2) (CRMP-2) isoform 6					

^a NCBI = National Center for Biotechnology Information. ↑ = Increased levels as compared to the control (non-infected). ↓ = Decreased levels as compared to the control (non-infected). b p < 0.05 vs control.

genetic disorder and small molecule biochemistry (Figure 7C) and Network IV associated with neurological disease, energy production and nucleic acid metabolism (Figure 7D). Similar to the findings for Network II, most of the altered proteins in Network III and Network IV are novel and their roles in rabies should be further elucidated.

Interestingly, there were five proteins that were undetectable in spinal cord of the controlled animals, but were detectable in spinal cord of both paralytic and furious forms of rabies, including one form of vinculin (spot #1259), thymopoietin II (spot #1283), hypothetical protein (spot #1342), a form of beta globin (spot #1344), and heat shock protein beta-1 (spot #1512) (Figure 4 and Supplementary Table S3, Supporting Information). These proteins might be involved in the pathogenesis and neurological manifestations of rabies. Furthermore, this phenomenon (the presence of newly expressed proteins in CNS tissues of rabies-infected animals) was observed only in the spinal cord, not in the hippocampus or brainstem.

In addition, we also focused our attention to significant differences between the two forms of rabies in individual CNS tissues, as these data may lead to further identification of tissue biomarkers for differentiation of these two distinct clinical entities of rabies and may also facilitate understanding of factors determining clinical manifestations of rabies. All of these significant differences are summarized in Table 2. A total of 13, 17, and 41 proteins in the hippocampus, brainstem and spinal cord,

respectively, significantly differed between paralytic and furious forms. Among these, the most obvious differences were the absence of one form of carbonic anhydrase I (spot #1395), astrocytic GFAP isoform 2 (spot #445), NADH dehydrogenase (ubiquinone) Fe-S protein 1 (75 kDa precursor, isoform 1) (spot #283), and N-ethylmaleimide sensitive fusion protein attachment protein beta (spot #735) in the spinal cord of furious dogs and, vice versa, the absence of oxygen-regulated protein 1 (spot #157) and rCG47063 (spot #158) in the spinal cord of paralytic dogs (Figure 4 and Table 2). Again, this phenomenon (the absence of some proteins in CNS tissues of one form of rabies compared to the other form) was observed only in the spinal cord, not in the hippocampus or brainstem. These proteins may potentially be "tissue biomarkers" to differentiate the two distinct forms of rabies. However, for clinical diagnostics, further investigations are needed to validate these "tissue biomarkers" in body fluids (i.e., plasma/serum and cerebrospinal fluid, which are easier to access and obtain from patients) to find the "more practical" biomarkers that can really be used in routine clinical practice.46

There is a previous proteomics study on CVS rabies virus infection in mammalian kidney cells.²⁹ In this previous study, a baby hamster kidney cell line (BHK-21) was infected with CVS rabies virus and alterations in the cellular proteome were identified by 2-DE followed by liquid chromatography (LC) coupled to MS/MS. Limited but significant changes were found

Journal of Proteome Research

Table 2. Summary of Significant Differences between Furious and Paralytic Rabies a

				intensity (mean \pm SEM)	()		mult	multiple comparisons	ons
protein name	NCBI ID	spot no.	control [C]	paralytic [P]	furious [F]	ANOVA p value	P vs C	F vs C	P vs F
Beta globin	gi 57113367	1084	Hippocampus 3.2760 ± 0.6120	3.1782 ± 0.2172	5.6296 ± 0.0810	0.0004	NS	0.0014	0.0010
Cytochrome P450 2B12 (CYPIIB12)	gi 62639273	192	0.1120 ± 0.0081	0.0798 ± 0.0014	0.1251 ± 0.0082	0.0008	0.0111	NS	0.0007
Cytokeratin type II	gi 73996498	255	0.0253 ± 0.0055	0.0357 ± 0.0022	0.0173 ± 0.0056	0.0480	NS	NS	0.0390
Dihydropyrimidinase related protein-2 (DRP-2)	gi 73993697	371	0.4072 ± 0.1000	0.2610 ± 0.0174	0.5731 ± 0.0446	0.0126	NS	NS	0.0095
(Turned on after division, 64 kDa protein)									
(TOAD-64) (Collapsin response mediator protein 2)									
(CRMP-2) isoform 3									
FBXW10 protein	gi 20306882	736	0.2409 ± 0.0428	0.2500 ± 0.0288	0.1221 ± 0.0148	0.0182	NS	0.0406	0.0271
Guanine deaminase	gi 73946803	1267	0.0424 ± 0.0139	0.0456 ± 0.0102	0.1045 ± 0.0042	0.0009	NS	0.0018	0.0028
Guanine nucleotide-binding protein G(o),	gi 73949832	009	0.1778 ± 0.0254	0.1457 ± 0.0104	0.2802 ± 0.0271	0.0018	NS	0.0141	0.0019
alpha subunit 2 isoform 1									
Interferon alpha 4	gi 18767673	107	0.1034 ± 0.0076	0.1106 ± 0.0066	0.1439 ± 0.0101	0.0078	NS	0.0092	0.0313
Keratin 1	gi 160961491	264	0.0330 ± 0.0027	0.0358 ± 0.0050	0.0625 ± 0.0049	0.0004	NS	0.0007	0.0016
Peroxiredoxin 2 (Thioredoxin peroxidase 1)	gi 73986497	888	0.2700 ± 0.0363	0.2982 ± 0.0272	0.4202 ± 0.0262	0.0073	NS	0.0084	0.0311
(Thioredoxin-dependent peroxide reductase 1)									
(Thiol-specific antioxidant protein) (TSA) (PRP)									
(Natural killer cell enhancing factor B)									
(NKEF-B) isoform 1									
Protein C9orf55 isoform 1	gi 73971036	106	0.0696 ± 0.0106	0.0623 ± 0.0055	0.0964 ± 0.0097	0.0395	NS	SN	0.0410
Pyruvate carboxylase, mitochondrial precursor	gi 73982897	95	0.0881 ± 0.0107	0.0907 ± 0.0041	0.0410 ± 0.0185	0.0225	NS	0.0456	0.0346
(Pyruvic carboxylase) (PCB) isoform 1									
SARM1 protein	gi 114325428	1359	0.0231 ± 0.0118	0.0180 ± 0.0030	0.0535 ± 0.0116	0.0440	NS	0.0308	0.0204
			Brainstem						
Actin-related protein 2 isoform 4	gi 73969820	490	0.1348 ± 0.0067	0.1785 ± 0.0249	0.1128 ± 0.0063	0.0250	NS	NS	0.0216
Annexin A6 (Annexin VI) (Lipocortin VI) (P68)	gi 73953627	246	0.0739 ± 0.0071	0.0722 ± 0.0074	0.0456 ± 0.0023	0.0078	NS	0.0127	0.0193
(P70) (Protein III) (Chromobindin 20)									
(6/ KDa caletectrin) (Calphobindin-II) (CPB-II) isotorm 2	0.0000000	o c	70000	00000	100000	0000	OI.V	OIX	2000
A1 Fase, r1+ transporting, v1 subunit b, isotorm 2 isotorm 2	gl/3993820	238	0.3890 ± 0.0343	0.2400 ± 0.0090	0.5255 ± 0.0595	0.0008	NS	N	0.0003
ATPase, H+ transporting, V1 subunit B, isoform 2 isoform 2	gi 73993820	341	0.2130 ± 0.0295	0.0973 ± 0.0214	0.2944 ± 0.0141	0.0001	0.0066	NS	0.0001
Centrosomal protein 63 kDa isoform 2	gi 194221623	754	0.1721 ± 0.0061	0.3377 ± 0.0335	0.2202 ± 0.0244	0.0007	0.0006	NS	0.0098
Chain A, Solution Structure Of The Twelfth Cysteine-Rich	gi 159164645	128	0.0365 ± 0.0077	0.0699 ± 0.0118	0.0339 ± 0.0044	0.0160	0.0363	SN	0.0241
Ligand- Binding Repeat In Rat Megalin									
Creatine kinase B-type (Creatine kinase, B chain)	gi 73964131	808	0.0802 ± 0.0087	0.1289 ± 0.0137	0.0846 ± 0.0072	0.0076	0.0115	NS	0.0209
(B-CK) isotorm 1									

Table 2. Continued

			·ii	intensity (mean \pm SEM)	(1		mult	multiple comparisons	ons
protein name	NCBI ID	spot no.	control [C]	paralytic [P]	furious [F]	ANOVA p value	P vs C	F vs C	P vs F
Cytosolic purine 5-nucleotidase	gi 73998435	993	0.3931 ± 0.0260	0.6284 ± 0.0636	0.4158 ± 0.0390	0.0041	0.0063	NS	0.0128
(3-nucleoudase cytosone 11) isotorm o GDP dissociation inhibitor 2	91 50978926	429	0.1042 ± 0.0063	0.0839 ± 0.0096	0.0335 ± 0.0150	0.0011	NS	0.0010	0.0135
Glutathione S-transferase Mu 3 (GSTM3-3)	gi 57088159	807	0.1705 ± 0.0128	0.2736 ± 0.0398	0.1591 ± 0.0229	0.0186	0.0452	NS	0.0257
(GST class-mu 3) (hGSTM3-3) isoform 1									
GTP-binding protein alpha o	gi 8394152	550	0.1927 ± 0.0220	0.3018 ± 0.0375	0.1850 ± 0.0118	0.0104	0.0164	SN	0.0248
Immunoglobulin heavy chain variable region	gi 112700066	1023	0.2323 ± 0.0192	0.4159 ± 0.0349	0.2525 ± 0.0302	0.0007	0.0012	NS	0.0031
Silent information regulator 2	gi 73697550	999	0.1672 ± 0.0204	0.1711 ± 0.0177	0.0590 ± 0.0072	0.0002	NS	0.0007	0.0005
Tubulin, alpha 1 isoform 9	gi 73996547	879	0.2392 ± 0.0452	0.5260 ± 0.0861	0.2565 ± 0.0414	0.0074	0.0122	NS	0.0018
Unidentified	NA	275	0.0747 ± 0.0070	0.0338 ± 0.0020	0.0627 ± 0.0023	0.0000	0.0000	NS	0.0009
Unidentified	NA	813	0.4906 ± 0.0173	0.3973 ± 0.0308	0.5654 ± 0.0213	0.0006	0.0360	NS	0.0004
Unidentified	NA	1000	0.0931 ± 0.0101	0.1017 ± 0.0117	0.2252 ± 0.0550	0.0216	NS	0.0321	0.0457
			Spinal cord						
40S ribosomal protein S3a (V-fos transformation	gi 73977917	1394	0.1508 ± 0.0410	0.0887 ± 0.0187	0.2208 ± 0.0126	0.0152	NS	NS	0.0116
effector protein) isoform 11									
Alpha-Crystallin B chain (Alpha(B)-Crystallin)	gi 149716488	096	0.5524 ± 0.0525	0.2190 ± 0.0289	0.7896 ± 0.0898	0.0001	0.0054	0.0452	0.0000
Alpha Crystallin B chain (Alpha(B)-Crystallin)	gi 57085977	1385	0.0076 ± 0.0076	0.4507 ± 0.0203	0.1978 ± 0.0448	0.0000	0.0000	0.0011	0.0001
(Rosenthal fiber component) (Heat-shock protein beta-5)									
(HspB5) isoform 1									
ATP synthase, H+ transporting, mitochondrial F0	gi 57108097	913	0.3123 ± 0.0156	0.2056 ± 0.0114	0.2918 ± 0.0095	0.0001	0.0001	NS	0.0009
complex, subunit d isoform a									
Carbonic anhydrase I (Carbonate dehydratase I) (CA-I)	gi 57108007	1395	0.1720 ± 0.0571	0.1475 ± 0.0069	0.0000 ± 0.0000	0.0048	NS	0.0063	0.0178
(Carbonic anhydrase B)									
Chaperonin containing TCP1, subunit 2 isoform 1	gi 73968673	469	0.1049 ± 0.0087	0.0837 ± 0.0081	0.1453 ± 0.0194	0.0173	SN	SN	0.0146
Chromosome 1 open reading frame 27	gi 126306536	711	0.1848 ± 0.0194	0.2134 ± 0.0278	0.3747 ± 0.0224	0.0002	SN	0.0003	0.0013
Collagen, type VI, alpha 1 isoform 1	gi 119887130	1251	0.0041 ± 0.0041	0.0881 ± 0.0190	0.0050 ± 0.0050	0.0006	0.0014	SN	0.0016
Complement component 1, q subcomponent	gi 73955331	821	0.3736 ± 0.0209	0.2669 ± 0.0160	0.4236 ± 0.0577	0.0270	NS	NS	0.0238
binding protein precursor									
Creatine kinase B-type (Creatine kinase, B chain)	gi 73964131	553	0.6536 ± 0.0330	0.6194 ± 0.0661	0.8821 ± 0.0517	0.0110	SN	0.0330	0.0144
(B-CK) isoform 1									
Creatine kinase B-type (Creatine kinase, B chain) (B-CK) isoform 1	gi 73964131	829	0.4507 ± 0.0290	0.4179 ± 0.0323	0.6666 ± 0.0596	0.0023	NS	0.0093	0.0033
Cytoplasmic beta-actin isoform 2	gi 73958067	814	0.0935 ± 0.0197	0.1495 ± 0.0279	0.0139 ± 0.0139	0.0037	NS	NS	0.0028
Dihydropyrimidinase-like 2	gi 40254595	408	0.2805 ± 0.0384	0.1761 ± 0.0329	0.3310 ± 0.0298	0.0244	NS	NS	0.0212
Dihydrouridine synthase 1-like (S. cerevisiae)	gi 123288584	1065	0.1881 ± 0.0199	0.1801 ± 0.0299	0.2720 ± 0.0120	0.0329	NS	NS	0.0449
Fructose-bisphosphate aldolase C	gi 57091277	679	0.4337 ± 0.0392	0.2344 ± 0.0208	0.3765 ± 0.0454	0.0055	0.0050	NS	0.0425
(Brain-type aldolase) isoform 1									

Table 2. Continued

			i	intensity (mean \pm SEM)	(J)		mul	multiple comparisons	sons
protein name	NCBI ID	spot no.	control [C]	paralytic [P]	furious [F]	ANOVA p value	P vs C	F vs C	P vs F
Fructose-bisphosphate aldolase C	gi 73966974	634	0.0640 ± 0.0110	0.0090 ± 0.0076	0.0703 ± 0.0200	0.0149	0.0381	NS	0.0207
(Brain-type aldolase) isoform 2									
Glial fibrillary acidic protein, astrocyte (GFAP) isoform 1	gi 73965500	459	0.0620 ± 0.0050	0.0517 ± 0.0032	0.1421 ± 0.0210	0.0003	NS	0.0013	0.0004
Glial fibrillary acidic protein, astrocyte (GFAP) isoform 1	gi 73965500	602	0.0585 ± 0.0379	0.1897 ± 0.1438	4.3635 ± 0.4024	0.0000	NS	0.0000	0.0000
Glial fibrillary acidic protein, astrocyte (GFAP) isoform 2	gi 73965502	445	0.0174 ± 0.0059	0.0371 ± 0.0069	0.0000 ± 0.0000	0.0017	NS	NS	0.0012
Glycogen phosphorylase, muscle form (Myophosphorylase)	gi 1730556	1514	0.0906 ± 0.0323	0.0644 ± 0.0049	0.1619 ± 0.0258	0.0319	NS	SN	0.0304
Heat shock protein 90 kDa beta, member 1	gi 50979166	182	0.3857 ± 0.0451	0.3422 ± 0.0475	0.1595 ± 0.0373	0.0000	NS	0.0101	0.0370
Heat shock protein beta-1	gi 50979116	1512	0.0000 ± 0.0000	0.1178 ± 0.0105	0.0191 ± 0.0191	0.0000	0.0000	SN	0.0003
Hypothetical rhabdomyosarcoma antigen Mu-ms-40.6c	gi 48476968	159	0.0630 ± 0.0070	0.0087 ± 0.0048	0.0411 ± 0.0100	0.0007	0.0005	SN	0.0266
Isocitrate dehydrogenase 3 (NAD+) alpha isoform 2	gi 73951310	651	0.1590 ± 0.0061	0.1092 ± 0.0059	0.2230 ± 0.0127	0.0000	0.0041	0.0005	0.0000
Keratin 1	gi 160961491	869	0.1207 ± 0.0148	0.0849 ± 0.0108	0.1658 ± 0.0247	0.0222	NS	NS	0.0173
Keratin 10 isoform 2	gi 114667513	1381	0.0176 ± 0.0176	0.0756 ± 0.0227	0.3540 ± 0.1066	0.0047	NS	0.0057	0.0205
Heat shock protein beta-1	gi 50979116	874	0.3965 ± 0.0214	0.3070 ± 0.0141	0.6276 ± 0.0376	0.0000	NS	0.0001	0.0000
Myotubularin related protein 6	gi 194672062	811	0.1762 ± 0.0133	0.0835 ± 0.0066	0.1628 ± 0.0140	0.0001	0.0002	NS	0.0000
NADH dehydrogenase (ubiquinone) Fe—S protein	gi 57110953	283	0.0410 ± 0.0095	0.0402 ± 0.0048	0.0000 ± 0.0000	0.0005	NS	0.0011	0.0013
1, 75 kDa precursor isoform 1									
N-ethylmaleimide sensitive fusion protein	gi 62645998	735	0.0988 ± 0.0099	0.1470 ± 0.0457	0.0000 ± 0.0000	0.0155	SN	NS	0.0134
attachment protein beta									
Oxygen-regulated protein 1; AltName: Full=Retinitis	gi 62900882	157	0.0231 ± 0.0035	0.0000 ± 0.0000	0.0214 ± 0.0071	0.0047	0.0076	NS	0.0130
pigmentosa RP1 protein homologue									
Peroxiredoxin 2 (Thioredoxin peroxidase 1)	gi 73986497	816	0.3579 ± 0.0243	0.2140 ± 0.0242	0.4055 ± 0.0460	0.0035	0.0247	NS	0.0035
(Thioredoxin-dependent									
peroxide reductase 1) (Thiol-specific antioxidant protein)									
(TSA) (PRP) (Natural killer cell enhancing factor B)									
(NKEF-B) isoform 1									
rCG47063	gi 149028757	158	0.0375 ± 0.0045	0.0000 ± 0.0000	0.0332 ± 0.0095	0.0010	0.0015	NS	0.0042
Septin-8	gi 73971156	460	0.0907 ± 0.0047	0.0126 ± 0.0106	0.0516 ± 0.0047	0.0000	0.0000	0.0118	0.0118
Serotransferrin precursor (Transferrin) (Siderophilin)	gi 73990142	1220	0.0647 ± 0.0102	0.1730 ± 0.0231	0.0849 ± 0.0173	0.0033	0.0039	NS	0.0166
(Beta-1-metal binding globulin) isoform 1									
Silent information regulator 2	gi 73697550	199	0.1419 ± 0.0139	0.1653 ± 0.0132	0.0792 ± 0.0254	0.0167	NS	NS	0.0158
Thymopoietin II	gi 229542	1283	0.0000 ± 0.0000	0.1248 ± 0.0057	0.1722 ± 0.0153	0.0000	0.0000	0.0000	0.0091
Ubiquitin carboxy-terminal hydrolase L1	gi 73951868	872	0.5050 ± 0.0347	0.3185 ± 0.0398	0.5122 ± 0.0482	0.0105	0.0226	SN	0.0180
Unidentified	NA	436	0.0494 ± 0.0051	0.0468 ± 0.0050	0.0092 ± 0.0060	0.0002	NS	0.0005	0.0000
Werner helicase interacting protein 1,	gi 148700412	304	0.0527 ± 0.0031	0.0363 ± 0.0072	0.1077 ± 0.0110	0.0001	NS	0.0008	0.0001
isoform CRA_b									
Zinc finger protein 615	gi 197102729	693	0.1327 ± 0.0094	0.1273 ± 0.0073	0.1698 ± 0.0141	0.0316	NS	NS	0.0394
^a NCBI = National Center for Biotechnology Information. NA = Not applicable. NS = Not statistically significant.	NA = Not applic	able. NS =	Not statistically sigr	uificant.					

4922

in the expression of viral and host cellular proteins with different functions, including those involved in cytoskeletal assembly, oxidative stress and protein synthesis. Another study was done in rabies-infected mice using 2-DE followed by matrix-assisted laser desorption/ionization time-of-flight (MALDI-TOF) MS. 45 In the latter study, ICR mice were intracerebrally inoculated with attenuated CVS-B2C or wild-type silver-haired bat rabies virus (SHBRV). Animals were sacrificed when they developed severe paralysis and the brains were removed. The expression of host brain proteins, particularly those involved in ion homeostasis and docking and fusion of synaptic vesicles to presynaptic membranes in the CNS, were altered in the animals infected with SHBRV. On the other hand, attenuated rabies virus CVS-B2C up-regulated the expression of proteins involved in the induction of apoptosis. Comparing the data reported in these two aforementioned studies to ours, there were not many identical changes observed. This was not surprising as there were many differences in the study design and models of rabies infection as well as the affected tissues/cells for proteome analysis. Integrative analysis of several models of rabies virus infection at different stages and in different affected organs/tissues or their locales would be very helpful to obtain a larger and clearer picture of the pathophysiology or pathogenic mechanisms of rabies in humans.

In summary, we report herein for the first time a large data set of changes in proteomes of the hippocampus, brainstem and spinal cord in dogs naturally infected with rabies. These data will be useful for better understanding of molecular mechanisms of rabies and for differentiation of its paralytic and furious forms.

ASSOCIATED CONTENT

Supporting Information

Table S1. Summary of differentially expressed proteins in hippocampus identified by Q-TOF MS and/or MS/MS analyses. Table S2. Summary of differentially expressed proteins in brainstem identified by Q-TOF MS and/or MS/MS analyses. Table S3. Summary of differentially expressed proteins in spinal cord identified by Q-TOF MS and/or MS/MS analyses. This material is available free of charge via the Internet at http://pubs.acs.org.

AUTHOR INFORMATION

Corresponding Author

*Thiravat Hemachudha, Faculty of Medicine, Chulalongkorn University and WHO Collaborating Centre for Research and Training on Viral Zoonoses, Rama 4 Road, Bangkok 10330, Thailand. Phone: +66-2-6523122. Fax: +66-2-6523122. E-mail: fmedthm@gmail.com or th-cu@usa.net. Visith Thongboonkerd, Head of Medical Proteomics Unit, Office for Research and Development, Faculty of Medicine Siriraj Hospital, Mahidol University, 12th Floor Adulyadejvikrom Building, 2 Prannok Rd., Bangkoknoi, Bangkok 10700, Thailand. Phone/Fax: +66-2-4184793. E-mail: thongboonkerd@dr.com or vthongbo@yahoo.com.

■ ACKNOWLEDGMENT

We are grateful to the technical assistance of Phattara-orn Havanapan and Siriwan Mungdee. This work was supported by the National Center for Genetic Engineering and Biotechnology (BIOTEC), the National Science and Technology Development Agency (Thailand); The Thailand Research Fund (DBG5180026 & RTA5380005); The National Research University Project of CHE

and the Ratchadaphiseksomphot Endowment Fund (HR1160A); Office of the Higher Education Commission and Mahidol University under the National Research Universities Initiative. V. Thongboonkerd is also supported by "Chalermphrakiat" Grant, Faculty of Medicine Siriraj Hospital.

REFERENCES

- (1) Hattwick, M. A.; Weis, T. T.; Stechschulte, C. J.; Baer, G. M.; Gregg, M. B. Recovery from rabies. A case report. *Ann. Intern. Med.* **1972**, 76, 931–942.
- (2) Willoughby, R. E., Jr.; Tieves, K. S.; Hoffman, G. M.; Ghanayem, N. S.; Amlie-Lefond, C. M.; Schwabe, M. J.; Chusid, M. J.; Rupprecht, C. E. Survival after treatment of rabies with induction of coma. *N. Engl. J Med.* **2005**, 352, 2508–2514.
- (3) Presumptive abortive human rabies Texas, 2009. *Morb. Mortal. Wkly. Rep.* **2010**, *59*, 185–190.
- (4) Ĥemachudha, T.; Laothamatas, J.; Rupprecht, C. E. Human rabies: a disease of complex neuropathogenetic mechanisms and diagnostic challenges. *Lancet Neurol.* **2002**, *1*, 101–109.
- (5) Hemachudha, T., Mitrabhakdi, E. Rabies. In *Infectious diseases of the nervous*; Davis, L., Kennedy, P. G. E., Eds.; Butterworth-Heinemann: Oxford, 2000; pp 401–444.
- (6) Dacheux, L.; Reynes, J. M.; Buchy, P.; Sivuth, O.; Diop, B. M.; Rousset, D.; Rathat, C.; Jolly, N.; Dufourcq, J. B.; Nareth, C.; Diop, S.; Iehle, C.; Rajerison, R.; Sadorge, C.; Bourhy, H. A reliable diagnosis of human rabies based on analysis of skin biopsy specimens. *Clin. Infect. Dis* **2008**, *47*, 1410–1417.
- (7) Hemachudha, T. Human rabies: clinical aspects, pathogenesis, and potential therapy. *Curr. Top. Microbiol. Immunol.* **1994**, *187*, 121–143.
- (8) Mitrabhakdi, E.; Shuangshoti, S.; Wannakrairot, P.; Lewis, R. A.; Susuki, K.; Laothamatas, J.; Hemachudha, T. Difference in neuropathogenetic mechanisms in human furious and paralytic rabies. *J, Neurol. Sci,* **2005**, 238, 3–10.
- (9) Laothamatas, J.; Wacharapluesadee, S.; Lumlertdacha, B.; Ampawong, S.; Tepsumethanon, V.; Shuangshoti, S.; Phumesin, P.; Asavaphatiboon, S.; Worapruekjaru, L.; Avihingsanon, Y.; Israsena, N.; Lafon, M.; Wilde, H.; Hemachudha, T. Furious and paralytic rabies of canine origin: neuroimaging with virological and cytokine studies. *J. Neurovirol.* **2008**, *14*, 119–129.
- (10) Laothamatas, J.; Hemachudha, T.; Mitrabhakdi, E.; Wannakrairot, P.; Tulayadaechanont, S. MR imaging in human rabies. *Am. J Neuroradiol.* **2003**, *24*, 1102–1109.
- (11) Yan, X.; Prosniak, M.; Curtis, M. T.; Weiss, M. L.; Faber, M.; Dietzschold, B.; Fu, Z. F. Silver-haired bat rabies virus variant does not induce apoptosis in the brain of experimentally infected mice. *J. Neurovirol.* **2001**, *7*, 518–527.
- (12) Sarmento, L.; Li, X. Q.; Howerth, E.; Jackson, A. C.; Fu, Z. F. Glycoprotein-mediated induction of apoptosis limits the spread of attenuated rabies viruses in the central nervous system of mice. *J. Neurovirol.* **2005**, *11*, 571–581.
- (13) Suja, M. S.; Mahadevan, A.; Madhusudhana, S. N.; Vijayasarathi, S. K.; Shankar, S. K. Neuroanatomical mapping of rabies nucleocapsid viral antigen distribution and apoptosis in pathogenesis in street dog rabies--an immunohistochemical study. *Clin. Neuropathol.* **2009**, *28*, 113–124.
- (14) Jackson, A. C.; Randle, E.; Lawrance, G.; Rossiter, J. P. Neuronal apoptosis does not play an important role in human rabies encephalitis. *J. Neurovirol.* **2008**, *14*, 368–375.
- (15) Schnell, M. J.; McGettigan, J. P.; Wirblich, C.; Papaneri, A. The cell biology of rabies virus: using stealth to reach the brain. *Nat. Rev. Microbiol.* **2010**, *8*, 51–61.
- (16) Prehaud, C.; Wolff, N.; Terrien, E.; Lafage, M.; Megret, F.; Babault, N.; Cordier, F.; Tan, G. S.; Maitrepierre, E.; Menager, P.; Chopy, D.; Hoos, S.; England, P.; Delepierre, M.; Schnell, M. J.; Buc, H.; Lafon, M. Attenuation of rabies virulence: takeover by the cytoplasmic domain of its envelope protein. *Sci. Signal.* **2010**, *3*, ra5.
- (17) Jackson, A. C.; Rossiter, J. P. Apoptosis plays an important role in experimental rabies virus infection. *J. Virol.* **1997**, *71*, 5603–5607.

(18) Jackson, A. C.; Park, H. Apoptotic cell death in experimental rabies in suckling mice. *Acta Neuropathol.* **1998**, *95*, 159–164.

- (19) Morimoto, K.; Hooper, D. C.; Spitsin, S.; Koprowski, H.; Dietzschold, B. Pathogenicity of different rabies virus variants inversely correlates with apoptosis and rabies virus glycoprotein expression in infected primary neuron cultures. *J. Virol.* **1999**, *73*, 510–518.
- (20) Weli, S. C.; Scott, C. A.; Ward, C. A.; Jackson, A. C. Rabies virus infection of primary neuronal cultures and adult mice: failure to demonstrate evidence of excitotoxicity. *J. Virol.* **2006**, *80*, 10270–10273.
- (21) Guigoni, C.; Coulon, P. Rabies virus is not cytolytic for rat spinal motoneurons in vitro. *J. Neurovirol.* **2002**, *8*, 306–317.
- (22) Tirawatnpong, S.; Hemachudha, T.; Manutsathit, S.; Shuangshoti, S.; Phanthumchinda, K.; Phanuphak, P. Regional distribution of rabies viral antigen in central nervous system of human encephalitic and paralytic rabies. *J. Neurol. Sci.* 1989, 92, 91–99.
- (23) Rajagopalan, D.; Agarwal, P. Inferring pathways from gene lists using a literature-derived network of biological relationships. *Bioinformatics* **2005**, *21*, 788–793.
- (24) Jensen, O. N. Modification-specific proteomics: characterization of post-translational modifications by mass spectrometry. *Curr. Opin. Chem. Biol.* **2004**, *8*, 33–41.
- (25) Koprowski, H.; Zheng, Y. M.; Heber-Katz, E.; Fraser, N.; Rorke, L.; Fu, Z. F.; Hanlon, C.; Dietzschold, B. In vivo expression of inducible nitric oxide synthase in experimentally induced neurologic diseases. *Proc. Natl. Acad. Sci. U.S.A.* **1993**, *90*, 3024–3027.
- (26) Hooper, D. C.; Ohnishi, S. T.; Kean, R.; Numagami, Y.; Dietzschold, B.; Koprowski, H. Local nitric oxide production in viral and autoimmune diseases of the central nervous system. *Proc. Natl. Acad. Sci. U.S.A.* 1995, 92, 5312–5316.
- (27) Shin, T.; Weinstock, D.; Castro, M. D.; Hamir, A. N.; Wampler, T.; Walter, M.; Kim, H. Y.; Acland, H. Immunohistochemical localization of endothelial and inducible nitric oxide synthase within neurons of cattle with rabies. *J. Vet. Med. Sci.* **2004**, *66*, 539–541.
- (28) Jackson, A. C.; Kammouni, W.; Zherebitskaya, E.; Fernyhough, P. Role of oxidative stress in rabies virus infection of adult mouse dorsal root ganglion neurons. *J. Virol.* **2010**, *84*, 4697–4705.
- (29) Zandi, F.; Eslami, N.; Soheili, M.; Fayaz, A.; Gholami, A.; Vaziri, B. Proteomics analysis of BHK-21 cells infected with a fixed strain of rabies virus. *Proteomics* **2009**, *9*, 2399–2407.
- (30) Scott, C. A.; Rossiter, J. P.; Andrew, R. D.; Jackson, A. C. Structural abnormalities in neurons are sufficient to explain the clinical disease and fatal outcome of experimental rabies in yellow fluorescent protein-expressing transgenic mice. *J. Virol.* **2008**, 82, 513–521.
- (31) Oueslati, A.; Fournier, M.; Lashuel, H. A. Role of post-translational modifications in modulating the structure, function and toxicity of alpha-synuclein: implications for Parkinson's disease pathogenesis and therapies. *Prog. Brain Res.* **2010**, *183*, 115–145.
- (32) Laothamatas, J.; Sungkarat, W.; Hemachudha, T. Neuroimaging in human rabies. In *Advances in virus research*; Jackson, A. C., Ed.; Academic Press/Elsevier: New York, 2011; Vol. 79, 309–327.
- (33) Latchman, D. S. Protective effect of heat shock proteins in the nervous system. *Curr. Neurovasc. Res.* **2004**, *1*, 21–27.
- (34) Pockley, A. G. Heat shock proteins as regulators of the immune response. *Lancet* **2003**, 362, 469–476.
- (35) Sagara, J.; Kawai, A. Identification of heat shock protein 70 in the rabies virion. *Virology* **1992**, *190*, 845–848.
- (36) Lahaye, X.; Vidy, A.; Pomier, C.; Obiang, L.; Harper, F.; Gaudin, Y.; Blondel, D. Functional characterization of Negri bodies (NBs) in rabies virus-infected cells: Evidence that NBs are sites of viral transcription and replication. *J. Virol.* **2009**, *83*, 7948–7958.
- (37) Menager, P.; Roux, P.; Megret, F.; Bourgeois, J. P.; Le Sourd, A. M.; Danckaert, A.; Lafage, M.; Prehaud, C.; Lafon, M. Toll-like receptor 3 (TLR3) plays a major role in the formation of rabies virus Negri Bodies. *PLoS Pathog.* **2009**, *5*, e1000315.
- (38) Charrier, E.; Reibel, S.; Rogemond, V.; Aguera, M.; Thomasset, N.; Honnorat, J. Collapsin response mediator proteins (CRMPs): involvement in nervous system development and adult neurodegenerative disorders. *Mol. Neurobiol.* **2003**, *28*, 51–64.

- (39) Fukata, Y.; Itoh, T. J.; Kimura, T.; Menager, C.; Nishimura, T.; Shiromizu, T.; Watanabe, H.; Inagaki, N.; Iwamatsu, A.; Hotani, H.; Kaibuchi, K. CRMP-2 binds to tubulin heterodimers to promote microtubule assembly. *Nat. Cell Biol.* **2002**, *4*, 583–591.
- (40) Inagaki, N.; Chihara, K.; Arimura, N.; Menager, C.; Kawano, Y.; Matsuo, N.; Nishimura, T.; Amano, M.; Kaibuchi, K. CRMP-2 induces axons in cultured hippocampal neurons. *Nat. Neurosci.* **2001**, *4*, 781–782
- (41) Vincent, P.; Collette, Y.; Marignier, R.; Vuaillat, C.; Rogemond, V.; Davoust, N.; Malcus, C.; Cavagna, S.; Gessain, A.; Machuca-Gayet, I.; Belin, M. F.; Quach, T.; Giraudon, P. A role for the neuronal protein collapsin response mediator protein 2 in T lymphocyte polarization and migration. *J. Immunol.* 2005, 175, 7650–7660.
- (42) Vuaillat, C.; Varrin-Doyer, M.; Bernard, A.; Sagardoy, I.; Cavagna, S.; Chounlamountri, I.; Lafon, M.; Giraudon, P. High CRMP2 expression in peripheral T lymphocytes is associated with recruitment to the brain during virus-induced neuroinflammation. *J. Neuroimmunol.* **2008**, *193*, 38–51.
- (43) Fu, Z. F.; Weihe, E.; Zheng, Y. M.; Schafer, M. K.; Sheng, H.; Corisdeo, S.; Rauscher, F. J.; Koprowski, I. I. I.; Dietzschold, H. B. Differential effects of rabies and borna disease viruses on immediate-early- and late-response gene expression in brain tissues. *J. Virol.* 1993, 67, 6674–6681.
- (44) Prosniak, M.; Hooper, D. C.; Dietzschold, B.; Koprowski, H. Effect of rabies virus infection on gene expression in mouse brain. *Proc. Natl. Acad. Sci. U.S.A.* **2001**, *98*, 2758–2763.
- (45) Dhingra, V.; Li, X.; Liu, Y.; Fu, Z. F. Proteomic profiling reveals that rabies virus infection results in differential expression of host proteins involved in ion homeostasis and synaptic physiology in the central nervous system. *J. Neurovirol.* **2007**, *13*, 107–117.
- (46) Thongboonkerd, V. Urinary proteomics: towards biomarker discovery, diagnostics and prognostics. *Mol. Biosyst.* **2008**, *4*, 810–815.